Prepared for:

Rijkswaterstaat Rijksinstituut voor Kust en Zee/RIKZ

Morphological modelling of the Western Scheldt.

Validation of DELFT3D.

Report

Prepared for:

Rijkswaterstaat Rijksinstituut voor Kust en Zee/RIKZ

Morphological modelling of the Western Scheldt

C. Kuijper
R. Steijn
D. Roelvink
T. van der Kaaij
P. Olijslagers

Report

Z3648 / A1198

Contents

List of Figures

List of Figures

Figure numbers marked with • refer to figures at the end of the text. All other figures are included in the text.

Summary

Morphological changes of the Scheldt estuary are extensively monitored by the Dutch and Belgian authorities. To predict effects of long-term natural changes (sea level rise) and the consequences of various human interventions, such as dredging/dumping/sand mining and deepening of the navigation channel, there is an urgent need for adequate and reliable tools in these matters. As part of the projects MOVE, ZEEKENNIS and K2005*WSMOND the Ministry of Transport and Public Works of The Netherlands (Rijkswaterstaat/RIKZ) has commissioned WL| DELFT HYDRAULICS and ALKYON to investigate the capability of the DELFT3D morphological model to simulate the morphodynamics of the Western Scheldt on the short term (years) as well as on the mid term (decades).

The present model is based on the KUSTZUID hydrodynamic model from Rijkswaterstaat denoted as. The model employs a depth-averaged approach, although three-dimensional effects have also been investigated. Dredging is computed by the model and the dredged sediment is dumped in the locations that were actually used during dredge operations. The extraction of sand due to mining operations is also accounted for. Furthermore the thickness of the erodible sand layer, as based on available field data, was incorporated in the model schematisation. Finally, bank protection measures have been included in the model.

Following the calibration and verification of the hydrodynamic model the morphodynamic model was set-up. Sensitivity simulations for the year 2001 showed the effect of various model parameters on the results in terms of yearly-averaged changes of: (i) bed levels, (ii) volumes of the ebb and flood channels of six sub areas (macro cells), (iii) areas for a number of bed level classes, (iv) dredge volumes and (v) the residual sediment transport. An optimum set of model parameters was derived and two calibration simulations were carried out: for the period 1998-2002, i.e. during and following the second deepening of the navigation channel, and for the period 1960-1966, which is prior to the first deepening of the navigation channel in the 1970's. Comparison with field data necessitated a further optimisation of one of the model parameters, resulting in a final calibration run for 1998-2002. For the confrontation of model results with observations it is a prerequisite to take into account 'uncertainties' in both data sets. This has lead to so-called broad ranges, representing sets of possible outcomes for the studied quantities. The broad ranges for the observations reflect natural fluctuations as well as measurement inaccuracies. For the model simulations uncertainties in the exact values of the model parameters determine these ranges. The magnitude of the broad ranges for the various quantities have been estimated and used for comparison of computational results with measurements.

For the verification period 1970-1985 model parameters were kept similar to those as applied during the final calibration. The results of this hindcast show, with additional information of the sensitivity and calibration runs, that:

- Net volume changes of the macro cells can be reproduced by the model;
- The uncertainties with respect to changes of areas per depth class, as computed by the model, are large; the model shows a gradual steepening of the bathymetry whereas observations do not.
- Total annual dredge volumes are simulated by the model with differences in the order of a few million cubic metres between measurements and simulation results.

- Residual sediment transports in the estuary, following from sand balance studies, are reproduced for the period 1960-1966 and for the period 1970-1985 with differences in the order of 2 million cubic metres/year or less. For the period 1998-2002 a small net import is predicted, whereas observations show an export of sediment.
- The sedimentation-erosion pattern gives the most detailed information (with the resolution of the computational grid) on the morphological changes. For some of the simulation periods the large-scale erosion and sedimentation (i.e. on the scale of the main channels) could be more or less reproduced, although both sedimentation and erosion appear to be overestimated by the model. Further improvement seems to be possible. Presently, the model does not allow for predictions of bed level changes on small spatial scales (i.e. on the scale of the smaller connecting channels and single intertidal flats).

These findings result in the following assessment of the applicability of the model to managerial issues. A ranking is applied on a scale from 1 (low applicability) to 5 (high applicability).

Type of problems/aspects	**Applicability ranking**
Effects on overall hydrodynamic parameters (e.g. asymmetry).	5
Dredging volumes, effects of management, support of conceptual models.	4
Behaviour of large-scale system and effects of strategies. Behaviour of sills. Spatial and temporal variations in transport patterns.	3
Overall import/export: effects of management strategies.	2-3
Tidal flats: effects of deepening, dumping.	2
Salt marshes and effects on them.	1-2

1 Introduction

1.1 Research framework

Within the study *Lange Termijn Visie Schelde-estuarium* (Winterwerp et al., 2000, RWS & MVG, 2001) the following three main functions of the Scheldt-estuary have been distinguished:

⇒ Accessibility of ports ('Toegankelijkheid')
⇒ Safety against flooding ('Veiligheid')
⇒ Ecological status ('Natuurlijkheid')

Preservation of the physical characteristics of the Scheldt-estuary, especially the presence of the multiple channel system, is hereby the governing condition. Large-scale interventions, such as sand mining, dredging and dumping and deepening of the navigation channel, can have major impacts on the physical characteristics of the estuary in general and morphological changes of the channels and shallow (intertidal) areas in particular. These changes may offer 'gains' or result in 'losses' with respect to the above-mentioned functions. With the identification of these gains and losses adequate measures can be undertaken as part of an optimal strategy on water management. This strategy requires a sound knowledge of the physical and ecological processes in the estuary. For this reason the Directorate Zeeland of Rijkswaterstaat has initiated three projects to further develop specific knowledge as well as adequate tools with respect to hydrodynamics, morphology and ecology: (i) project MOVE (to establish physical and ecological changes in the Western Scheldt in order to advise on effects of the 48'/43' deepening of the navigation channel), (ii) project ZEEKENNIS (to supply knowledge regarding hydrodynamics, morphology and ecology as well as their interrelation to advise on accessibility, safety and ecological status of the Western Scheldt) and (iii) project K2005*WSMOND (to investigate the effects of natural processes and human interventions on the morphology of the sub-tidal delta and adjacent areas regarding the sustainable management of the sand volume of The Netherlands).

1.2 Issues on policy and management

The following issues addressed in the three projects MOVE, ZEEKENNIS and K2005*WSMOND, are of major importance for an optimum management of the Scheldt estuary:

A. Optimum sand mining strategy:	• What is the effect of sand mining activities on sediment import into or sediment export out of the estuary?

B. Optimum dredging and dumping strategy:	• Can the Western Scheldt and the sub-tidal delta be considered as one overall system, sharing the total amount of available sand? • What is the effect of the dumping strategy on the tidal asymmetry? • To what extent can the Western Scheldt be considered as a closed (sand conserving) system? • What is the natural fluctuation of the various components of the sand balance of the estuary? <u>Following dumping of sediment:</u> • How long should the dumping capacity of a channel be exceeded, to transfer a two-channel system into a single channel system? • Along which trajectories net transport of sediment occurs? • Under which conditions is this transport initiated? • What is the variation in time? • And to what extent do these aspects differ from the situation without dumping?
C. Effects of the deepening/widening of the navigation channel on the morphology:	• How can the sand export from the Western Scheldt be related to the deepening/widening of the navigation channel in the 1970's and 1990's • What will be the consequences of a sand-exporting system on the physical and ecological characteristics? • Is the decrease of the maintenance dredging volume since the 48'/43' widening caused by either the widening or the deepening or is it the result of the increased sand export from the Western Scheldt? • What mechanisms govern the development of sills and how can it be modelled morphologically? How is it affected by dredging and dumping? • What can be the explanation that the total intertidal and shallow water area has developed differently from what was predicted in the MOVE-project after the 48'/43' widening and deepening?

D. Effects of future large-scale interventions on the morphology:	• How can the relations between the physical processes and an intervention be described in a conceptual model? • Can sand, originating from a further deepening, be dumped in the sub-tidal delta (Voordelta), so that it will remain available for the Western Scheldt? • What will be the effect of a further deepening of the Wielingen/Scheur on the morphology of the Voordelta and the adjacent coastal areas of South-west Walcheren and Zeeuws Vlaanderen? • What (innovative) large-scale morphological measures can be undertaken to mitigate the steepening of the coast of South-west Walcheren?
E. Effects of future large-scale interventions on the ecology:	• What are the effects of dredging and dumping on the intertidal and shallow water areas (of importance for the ecosystem), such as level, duration of drying, hydrodynamics, morphodynamics and sediment composition? • What are the effects of deepening of the navigation channel on the development of the intertidal and shallow water areas? • How will the steepness of the tidal flats be affected after morphological interventions? • Which interventions influence the development of salt marshes?

1.3 Objectives of the study

Numerical modelling forms one of the options to assist in the set-up of an optimal management strategy for the Scheldt-estuary. However, numerical models can only be relied on if they are thoroughly validated against measurements. The set-up and development of a sound morphological model for the Scheldt-estuary is a target for all three aforementioned projects (MOVE, ZEEKENNIS and K2005*WSMOND). The objective of the present study is to construct a widely applicable and well validated morphological model for the Western Scheldt with known ranges as a measure for the accuracy of morphological predictions. The model should be capable to perform morphological simulations for periods of 3 to 15 years. Furthermore, it should be robust and flexible, so that it can be used in addressing various managerial questions as described in Section 1.2.

1.4 Modelling strategy and set-up of the study

Presently, various types of models are available to simulate the morphological behaviour of coastal areas, estuaries, tidal basins and rivers. Distinction can be made between idealised models, hybrid models and process-based models (Winterwerp and Kuijper, 2002). Idealised models are based on schematisations of the governing equations. They are intended to give explanations of and acquire insight in specific phenomena by means of an analytical

approach; however they are less suitable to reproduce in detail realistic, complicated cases. Hybrid models (such as ESTMORF and ASMITA) combine process-based equations (such as continuity and momentum equations for the hydrodynamics and advection-diffusion equations for the sediment) with empirical (often equilibrium) relationships. Aggregation is on a relatively high level so that computational elements are large and the computational effort is limited. Simulation periods may be as long as decades to centuries. Process-based morphological models, such as DELFT3D, compute on a high-resolution grid various local quantities (suspended sediment concentrations, suspended and bed load transport and bed level changes) as induced by the hydrodynamic forcing (tidal flow, waves). From this the morphological changes on larger, aggregated scales can be inferred (bottom-up approach). The computational effort is large, especially if three-dimensional simulations are performed over long periods.

In this study morphological changes of the Western Scheldt are simulated with the DELFT3D software package. The so-called online version of DELFT3D is employed, which implies that at each time step simultaneously the hydrodynamics and the sediment dynamics are computed. Bed level changes are immediately fed back to the hydrodynamic computation. Simulations are done in 2D mode (depth-averaged approach) apart from some sensitivity runs with a full three-dimensional functionality. Three-dimensional morphological simulations over a long period are presently not feasible, because of the excessive computation times involved. A morphological acceleration factor can be used to assist in dealing with the difference in time-scales between hydrodynamic and morphological developments. A detailed description of the DELFT3D morphological model (online) is given by Lesser et al. (2004).

As a first step in the calibration process the hydrodynamics is calibrated, because this is a necessary condition for an adequate reproduction of the morphological processes. The morphological model requires quantitative input of several model parameters. These parameters may be directly related to physical quantities (such as the sediment grain size) or to specific coefficients in process formulations (such as in sediment transport formula). During calibration of the model the parameters are tuned by means of sensitivity simulations, in such a way that an optimum agreement between observations and model results is found. Verification of the model is generally considered as the subsequent comparison between observations and model results for a data set different from that used for calibration (other simulation period, stations or physical quantities) without modifying the numerical input of the model parameters. However, because these parameters are seldom exactly known, or may vary in space and time, multiple simulations should be performed with different values of the input parameters, resulting in a range of the quantities utilised as model output. This range is then compared with observations and the extent to which model predictions agree with observations is established. In the latter case also the accuracy of the observations should be taken into account. The assessment of the so-called broad ranges of the model predictions is also carried out by means of sensitivity computations, using the final calibration result as a reference. The overall result of the calibration and verification is generally denoted as validation, i.e. the establishment to what extent the model is capable to reproduce the characteristics of the physical system. The procedure, as described above, is schematically depicted hereafter:

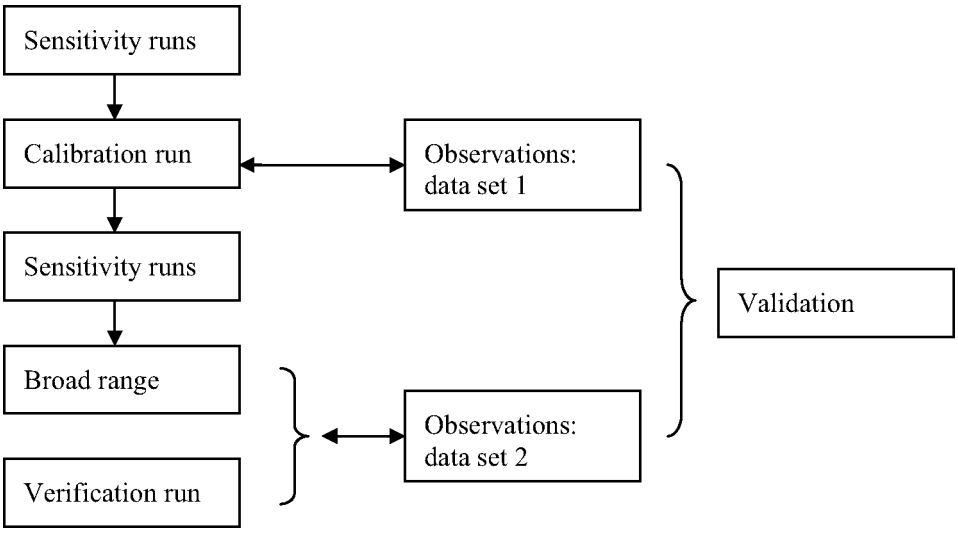

Activities as part of the validation of the morphological model.

1.5 Contents of the report

The contents of this report is based on intermediate reports produced during the project:

1. Morphological modelling of the Western Scheldt, Intermediate report Phase I: Part I: Hydrodynamic model set-up, calibration and verification; Part II: Wave model set-up, Theo van der Kaaij, Dano Roelvink, Kees Kuijper, February 2004, WL | Delft Hydraulics / Alkyon.
2. Morphological modelling of the Western Scheldt, Intermediate report Phase II: Calibration of the morphological model (2 volumes: text and figures), Theo van der Kaaij, Dano Roelvink, Kees Kuijper, May 2004, WL | Delft Hydraulics / Alkyon.
3. Morfologisch model van de Westerschelde, Tussenrapport fase III: Bandbreedte-onderzoek en morfologische verificatie, Paul Olijslagers, juni 2004, WL | Delft Hydraulics / Alkyon.

The present report summarises the major results of the morphological modelling of the Western Scheldt and can be read independently from the aforementioned intermediate reports. For more background information and supplementary results reference is made to these intermediate reports.

Chapter 2 gives a description of the Scheldt estuary with respect to hydrodynamic and morphodynamic processes.

The calibration and verification of the hydrodynamic model is discussed in *Chapter 3*.

The calibration of the morphodynamic model is extensively treated in *Chapter 4*. The activity firstly consists of sensitivity runs for the year 2001 to investigate the effect of various model parameters on the results. With the optimum combination of these parameters two calibration simulations are carried out: for 1998-2002 and for 1960-1966. This results in a final calibration run for 1998-2002, after a modification of one of the parameters, to

further improve the results. The chapter also describes the results of a number of three-dimensional simulations for the year 1998.

Observations as well as model results have their uncertainties. *Chapter 5* presents the methodology to establish these uncertainties in terms of 'broad ranges'. They are further quantified on the basis of field data and the results from sensitivity simulations with the model.

The verification of the model is carried out for a 15 year period (1970-1985) with the model parameters kept similar to those of the final calibration run. Observations and model results are compared, taking into account the derived broad ranges in Chapter 5. Results of this comparison are presented in *Chapter 6*.

As the purpose of the model will be to assist in answering various managerial questions, the applicability of the model in these matters is discussed in *Chapter 7*.

Recommendations for further improvement of the morphological model are finally given in *Chapter 8*.

2 The Scheldt estuary

2.1 Topography

The Scheldt river originates in France near Gouy at an altitude of 100 m and discharges into the North Sea near Vlissingen at a distance of 350 km from its origin. Sub regions of the Scheldt river are given in Table 2.1.

km				
0 – 160	Gouy – Gent	Upper Scheldt	non-tidal	fresh water zone
160 – 250	Gent - Rupelmonde	Upper Sea Scheldt	tidal	fresh water zone
250 – 290	Rupelmonde – Belgian/Dutch border	Lower Sea Scheldt	tidal	mixing zone
290 – 350	Belgian/Dutch border – Vlissingen/Breskens	Western Scheldt	tidal	mixing zone
> 350	Vlissingen/Breskens – NAP-20 m depth contours	Voordelta	tidal	transition mixing zone - salt water zone

Table 2.1: Sub regions in the Scheldt river.

The Scheldt *estuary* is defined as that part of the river basin with a tidal influence. It consists of a freshwater zone between Gent and Rupelmonde and a mixing zone between Rupelmonde and Vlissingen/Breskens. The sub tidal delta, seaward of Vlissingen and Breskens, forms the transition between the Western Scheldt and the North Sea and is generally denoted as the Voordelta. This study focuses on the morphological modelling of the Western Scheldt (see Figure 2.1).

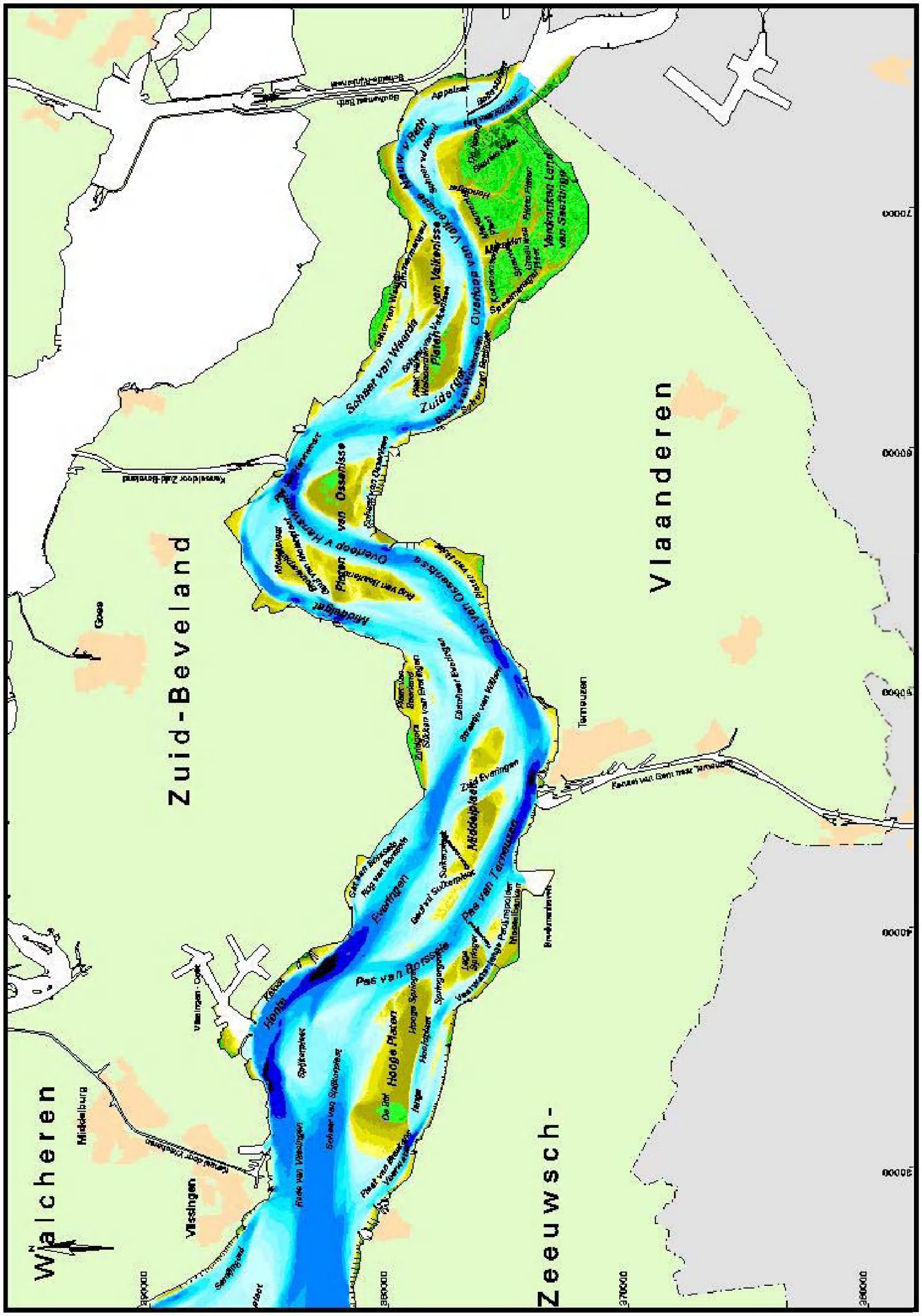

Figure 2.1: Western Scheldt estuary.

2.2 Hydrodynamic characteristics

The annual-averaged river discharge of the Scheldt River near Schelle, at the confluence of the Rupel and the Scheldt, amounts to 110 m^3/s with approximately equal contributions from both tributaries. However, variations from year to year can be large, ranging between 50 and 200 m^3/s. Also seasonal fluctuations are significant with highest discharges (> 600 m^3/s) between January and April.

The tidal wave is semi-diurnal with a mean tidal range of 3.8 m at Vlissingen, 5.2 m at Rupelmonde and 1.9 m at Gent. The estuary can thus be classified as mesotidal to macrotidal (Dyer, 1997). The propagating tide is blocked by weirs at Gent and, in the Dender, near Dendermonde. In the lower reaches of the Dijle, Zenne and the Grote and Kleine Nete the tidal influence is still noticeable. The ratio between the rise and fall time of the tidal wave decreases from 0.88 at Vlissingen to 0.75 at Rupelmonde and 0.39 at Gent (Claessens and Belmans, 1984), showing the asymmetry of the vertical tide. Maximum flow velocities in the main channels are between 1 and 1.5 m/s and can be locally 2 m/s during spring tide conditions.

The tidal volume (= ebb + flood volume) is in the order of 2.2 10^9 m^3 near Vlissingen, 0.2 10^9 m^3 at the Belgian-Dutch border and 0.1 10^9 m^3 at Antwerp (Verlaan, 1998, and the SchkeldeAtlas, 1999). Based on the ratio of the freshwater discharge and the tidal volume the estuary can be classified as partially mixed between Rupelmonde and Hansweert (only during high river discharges) and well-mixed downstream of Hansweert (Verlaan, 1998). However, the meandering of the river can cause lateral salinity differences giving rise to stratification, while also during slack water stratified conditions occur. The limit of salt intrusion can shift over a distance of 40 km, i.e. between Antwerp and 10-20 km upstream of Rupelmonde, due to variations of the river discharge.

2.3 Morphodynamics of the Western Scheldt

2.3.1 Morphological description

Multiple channel system

The Scheldt estuary consists of a meandering channel system with an increasing geometrical scale in seaward direction. Its lateral boundaries are formed by man-made dikes and bank protection measures. Within these constraints the channel system shows a regular, repetitive pattern of main ebb and flood channels. The larger main ebb channels are part of a more or less continuously meandering channel between Belgium and the estuary mouth. The main flood channels originate in the bends of the ebb channels and are generally shallower than the ebb channels. Shallow areas (sills) are found at the seaward side of the ebb channels and at the landward side of the flood channels. Furthermore, some smaller, former main channels can be observed along the embankments of the estuary, see Jeuken (2000). The major transport takes place through the present main ebb and flood channels, while the transport function of the former main channels has become limited.

In addition to the main ebb and flood channels, smaller channels, denoted as connecting channels, can be present in the estuarine cross-section. They are subdivided into (Jeuken, 2000): (i) bar channels, cutting through the shallow areas of the flood channel and linking two large main channels, (ii) cross channels, cutting through the elongated intertidal shoals between the main ebb and flood channels and (iii) margin channels, connecting large and small main channels along the estuarine boundaries. The connecting channels induce a redistribution of the tidal flow, while there transport function is limited. Presently, the morphodynamics are mainly determined by the quasi-cyclic behaviour of these channels.

Winterwerp et al. (2000) have schematised the channel system by means of a chain of so-called macro and meso cells, see the lower panel of Figure 2.2. Macro cells are formed by the main ebb and flood channels while most of the meso cells represent the connecting channels.

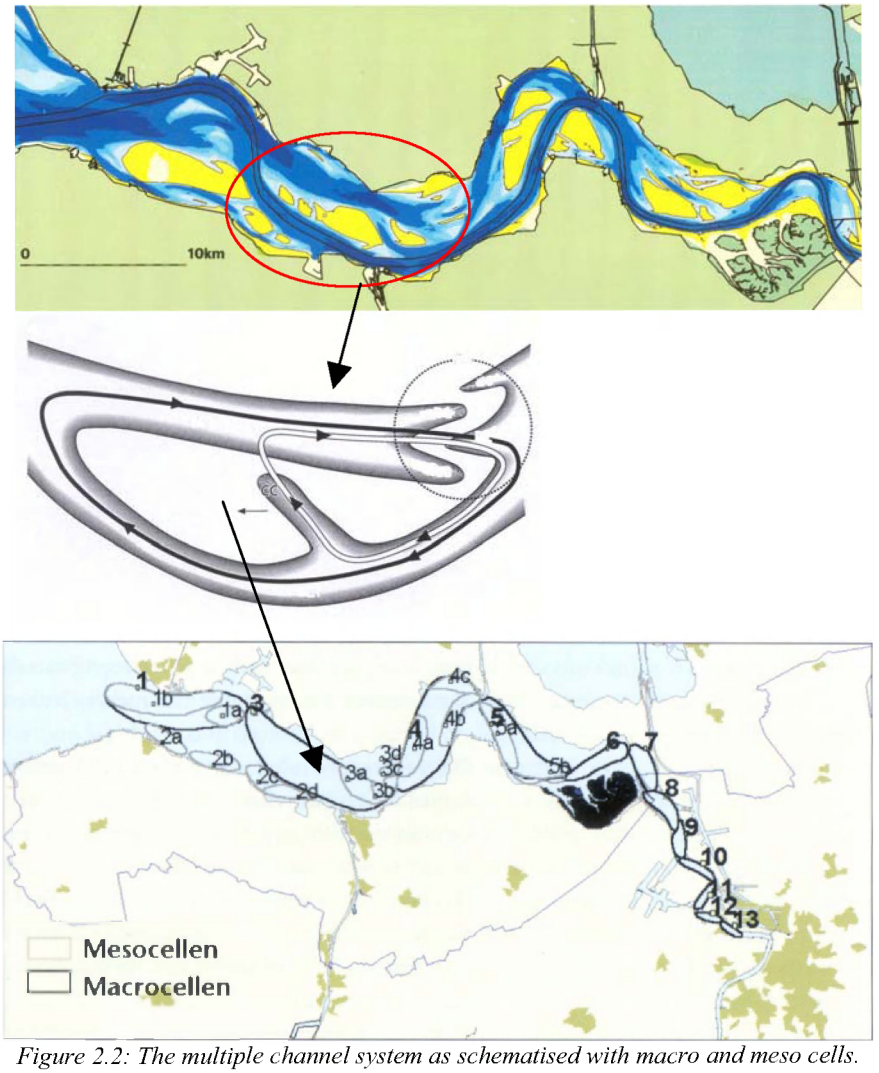

Figure 2.2: The multiple channel system as schematised with macro and meso cells.

In the Western Scheldt six macro cells are distinguished, see Table 2.2.

Macro cell	Ebb channel	Flood channel
1	Honte	Schaar van de Spijkerplaat
3	Pas van Terneuzen	Everingen
4	Middelgat	Gat van Ossenisse
5	Zuidergat / Overloop van Valkenisse	Schaar van Valkenisse / Waarde
6	Nauw van Bath	Schaar van de Noord
7	Vaarwater boven Bath	Appelzak

Table 2.2: Macro cells in the Western Scheldt

Sub tidal and intertidal areas and salt marshes

In the Western Scheldt various morphological features can be distinguished with respect to their elevation relative to the vertical tide: sub tidal areas (Dutch: "ondiepwatergebieden"), intertidal areas ("intergetijdengebieden") and salt marshes ("schorren"). The presence of these morphological features is considered to be of major importance for the ecological functioning of the area.

The lower boundary of the *sub tidal area* is generally defined at NAP-5 m. The upper boundary is taken at the bed level for which the time of exposure amounts to 1% of the total time (as based on actual water levels). Because water levels vary in the Western Scheldt, the level of the upper boundary relative to NAP depends on the actual location under consideration. The sub tidal area forms part of the channels and acts as a breeding place for fish and shrimp.

The *intertidal area* consists of *shoals* and *'slikken'*. The bed is above the level with an exposure time of 1%. The upper level of the intertidal area is roughly around high water during neap tide. Especially the area for which exposure is less than 75% and more than 25% is of major ecological importance. During drying, i.e. exposure of the bed to the open air, shoals are completely surrounded by water. "Slikken" are found along the estuarine margins and as such they remain connected to the shore during drying.

The lower level of the *salt marshes* coincides with the upper level of the intertidal areas. The upper limit is defined as the level with a flooding frequency of five times per year. Salt marshes are found along the estuarine margins, but have also recently been found on shoals. Salt marshes are covered with vegetation.

Bed composition

The sediment in the Western Scheldt mainly consists of sand with less than 10% mud in the channels and on the shoals (Dutch: platen), see van Eck (1999). However, alongside the estuarine margins, at the intertidal areas (Dutch: slikken) and salt marshes (Dutch: schorren), the percentage of mud can be much larger. Characteristic values for the median diameter (d_{50}), as given by (van Eck, 1999), are:

- channels: $d_{50} > 150$ μm;
- shoals: $d_{50} = 50\text{-}150$ μm;
- estuarine margin (intertidal areas and salt marshes): $d_{50} < 125$ μm.

In the upstream estuarine sections the grain size diameter in the channels is somewhat finer than in the downstream sections.

Figure 2.3 gives the spatial distribution of the median grain size (d_{50}) and the percentage of mud (% < 50 μm) in the upper few decimetres of the bed as measured in 1993 (McLaren data set). These figures show that in the western part the median grain size can be larger than 300 μm. Relatively coarse sediment is found in the channels, whereas the fine sediments are found at the intertidal areas. High percentages of mud are present along the margins of the estuary as well as on some shoals.

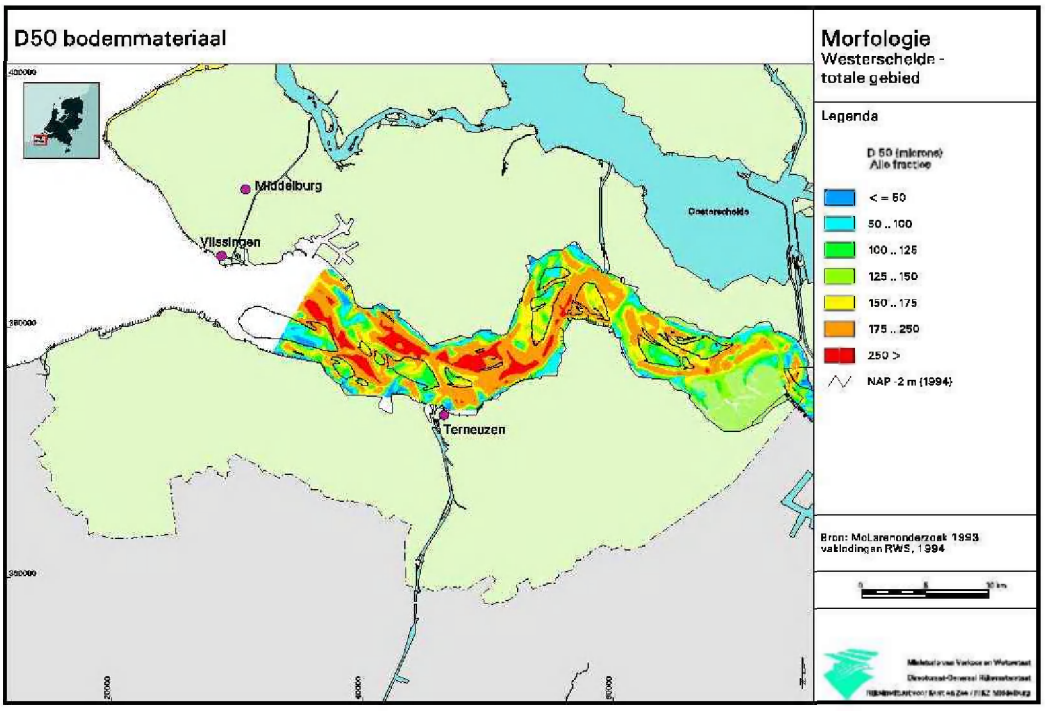

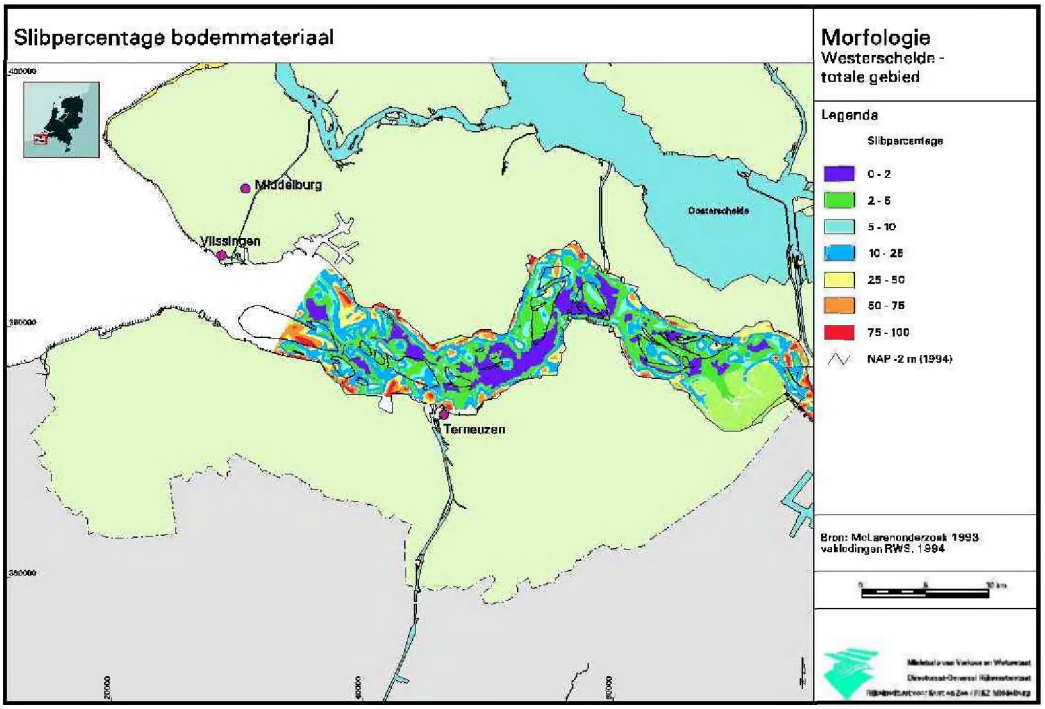

Figure 2.3: Median grain size (d_{50}) (upper panel) and percentage of mud (lower panel) in the Western Scheldt as measured during 1993.

The subsoil consists of alternating erosive and non-erosive layers, see Gruijters et al. (2004). The upper level of the topmost erosion resistant layer and the bed level determine the thickness of the sand layer, which is available for sediment transport. The thickness of this sand layer is given in Figure 2.4, showing that sand layer thicknesses of less than one metre are found in the Voordelta and some channels in the Western Scheldt (Schaar van Spijkerplaat, Pas van Terneuzen, Gat van Ossenisse).

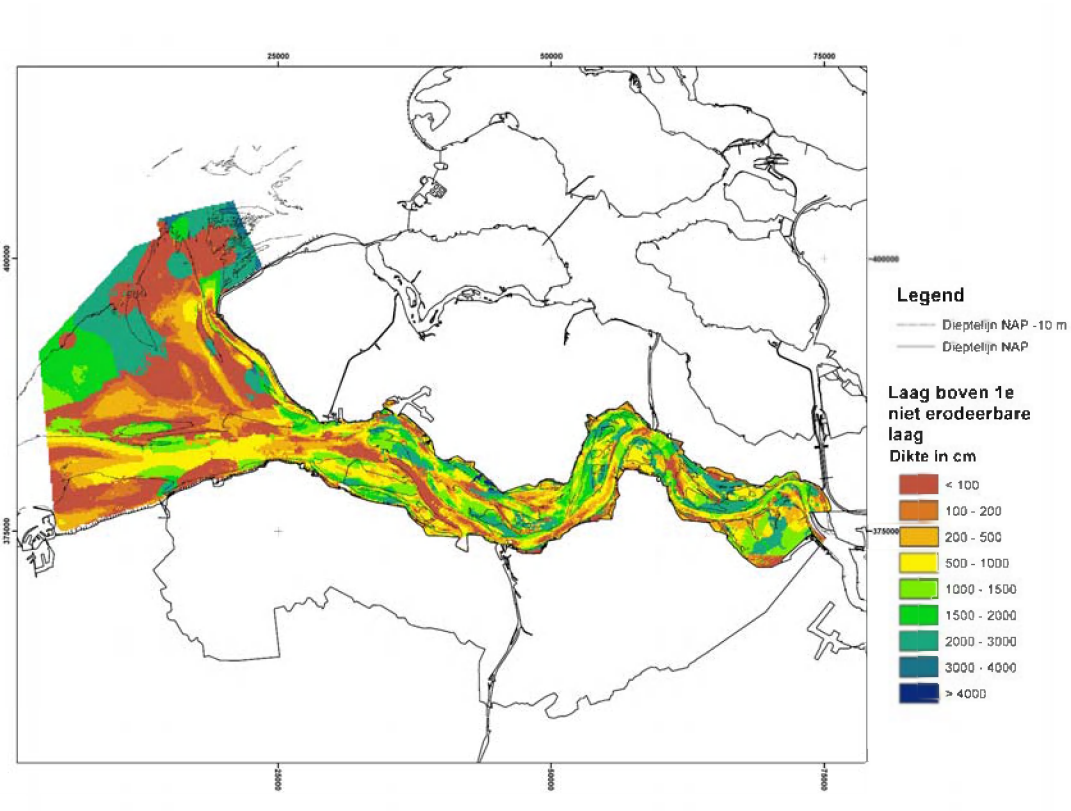

Figure 2.4: Thickness of the upper erodible sand layer.

2.3.2 Morphological changes

Channels

From hydrographic maps since 1800 it follows that the regular pattern of channels and intertidal areas has taken its present shape between 1800 and 1905 (Jeuken, 2000). This process was accompanied with a meandering of the ebb channels and a shift of these channels towards the river banks, a deepening and enlargement of the flood channels, a building up of the intertidal areas and the development of connecting channels between the main ebb and flood channels. Since approximately 1930 the configuration of the main ebb and flood channels remains unaltered in most locations.

The stability of the macro cells can be described by means of the (spatially-averaged) depth ratio of ebb channel to flood channel, hereafter denoted by a. Major changes in a on a time scale of decennia (1955-2002) can be observed for macro cells 1, 4, 5 and 6 (see Figure 2.2

for locations). A decrease in *a* for macro cells 1 and 4 is caused by the deepening of the flood channels (Schaar van de Spijkerplaat and Gat van Ossenisse). In macro cell 4 the depth of the ebb channel (Middelgat) simultaneously decreases, which enhances the decrease in *a*. This process seems to be accelerated between 1997 and 2002, when significant amounts of sediment were dumped in the ebb channel. In the eastern part, in macro cells 5, 6 and 7, the general trend is that of a deepening of the ebb channels (Overloop van Valkenisse, Nauw van Bath and Vaargeul van Bath respectively). For macro cell 5 this results in an increase of *a*, because the flood channel remains stable, whereas for macro cell 6 *a* decreases due to simultaneous erosion of the flood channel (Schaar van de Noord). Fluctuations on a shorter time scale (10 years) occur, especially for macro cells 6 and 7. In the latter case this is probably caused by the construction of a local dam in 1970 (Jeuken et al., 2004).

The change in depth ratio of the ebb and flood channels over the years does not necessarily imply that degeneration of the macro cells occurs; it does show that the morphodynamic equilibrium changes. However, if the tendency of an increasing or decreasing *a* continues and accelerates on the long-term, the two-channel system may degenerate into a single-channel system (Jeuken et al., 2004).

Sub tidal and intertidal areas and salt marshes

The development of the intertidal areas (shoals and 'slikken') and sub tidal areas has been investigated and reported in the project MOVE (Peters et al., 2003). The morphological changes for these areas have been described on the aggregation level of the eastern (macro cells 5-7), central (macro cell 4) and western part of the Western Scheldt (macro cells 1 and 3) and with a fixed reference level. Between 1955 and 1980, i.e. prior to and during the first deepening of the navigation channel, the total area of shoals in the Western Scheldt has increased by 800 10^4 m^2 (800 ha), i.e. approximately 20%, see Figure 2.5.

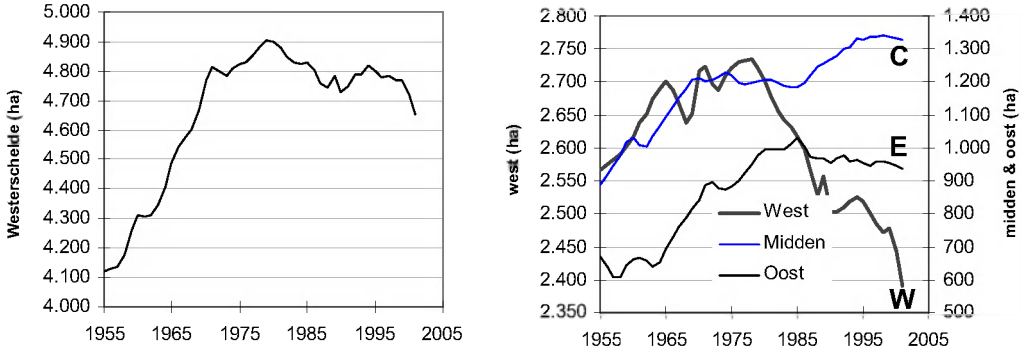

Figure 2.5: Area of shoals in the Western Scheldt in the western, central and eastern part (Peters et al., 2003). W = west; C = central; E = east.

During the subsequent period (1980-2002) there is a minor decrease of shoal area. The increase concerns the western, central as well as the eastern areas, although the phasing in time is somewhat different. This increase in shoal area is most likely associated with changes in the behaviour of the connecting channels (Jeuken et al., 2004). The decrease in shoal area since 1980 has mainly taken place in the western part of the Western Scheldt,

which is also associated with the origination, migration and degeneration of the connecting channels (Jeuken, 2000).

Changes in the sub tidal area are closely related to the morphological changes of the channels (in the macro and meso cells) and the intertidal areas. Historical observations show that between 1955 and 2002 the total sub tidal area in the Western Scheldt has significantly decreased (35%), see Figure 2.6. This decrease is most pronounced during the period between 1960 and 1980. The timing of the reduction in the sub tidal area is different for the western, central and eastern part. There is some resemblance between the sand volume extracted from the Western Scheldt due to sand mining since 1955 (see Figure 2.8) and the decrease of sub tidal areas. It is not known whether there is a causal relationship between both observations. The increase of the areas of shoals and the decrease of the sub tidal areas indicate a general steepening of the bathymetry since 1955.

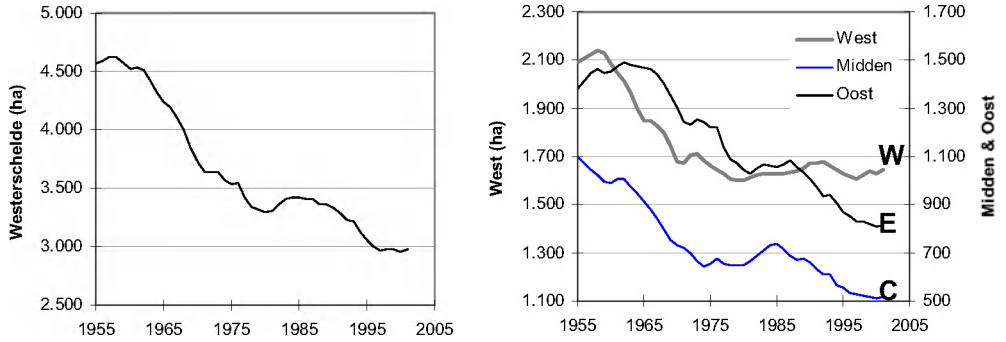

Figure 2.6: Sub tidal areas in the Western Scheldt in the western, central and eastern part (Peters et al., 2003 and Jeuken et al., 2004). W = west; C = central; E = east.

Data regarding the area of salt marshes and 'slikken' are limited. Between 1959 and 2001 the total area of salt marshes in the Western Scheldt has decreased from 3500 10^4 m^2 (3500 ha) to 2350 10^4 m^2 (2350 ha), i.e. 30-35%, see Figure 2.7.

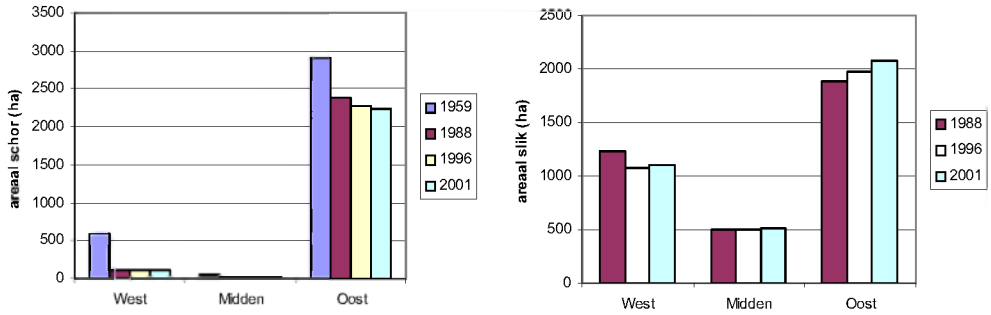

Figure 2.7: Areas of salt marshes (left panel) and 'slikken' (right panel) in the western, central and eastern part of the Western Scheldt (Jeuken et al., 2004).

The major part of this reduction has taken place between 1959 and 1988. Since 1988, only the eastern part shows a limited on-going reduction of the area covered by salt marshes. The total area of 'slikken' has remained (more or less) constant since 1988.

Dredging, dumping and sand mining

In addition to the natural sediment fluxes, sand is redistributed within and extracted from the Western Scheldt by means of dredging, dumping and sand mining. Annual dredge volumes have increased over the last decades from 4-5 Mm^3 in the 1960's to 8-14 Mm^3 between 1997 and 2002 (the latter figures include capital dredging resulting from the 2nd deepening of the navigation channel). Furthermore, apart from the maintenance dredging in the channels dredged material from the harbours in the Western Scheldt is dumped in the estuary (approximately 2 Mm^3/year of sand for the period 1998-2002). Sediment volumes associated with sand mining amount to approximately 2 Mm^3/year. The figures on dredging, dumping and sand mining are of the same magnitude as the residual sediment fluxes in the estuary.

Sand balance

The sand balance of the Western Scheldt is determined by natural erosion and sedimentation processes and human interventions (dredging, dumping and sand mining). During the period 1878–1952 the Western Scheldt was a sand importing system (from sea) with an annual-averaged import of 1.3 Mm^3 (Haring, 1949 and 1955). This import was accompanied with sedimentation on the intertidal areas and erosion of the channels below average low water. More recent studies, see Figure 2.8 (Jeuken et al., 2003a and 2003b, Nederbragt and Liek, 2004), conclude that since 1955 there are alternating periods with sand import (positive slope for natural erosion/sedimentation) and sand export (negative slope). Between 1955 and 1970 large variations regarding the sediment exchange between the estuary and the sub tidal delta occur. Natural sedimentation/erosion (V_{nat}) follows from net sedimentation and erosion (V_{net}) and human interferences (dredging/dumping and sand mining (V_{hi})) according to:

$$V_{nat} = V_{net} - V_{hi} \tag{2.1}$$

where natural sedimentation and dumping are positive and natural erosion and dredging and sand mining are negative.

Most of the dredged material is dumped in the estuary, so that the amount of sand extracted from the Western Scheldt is relatively small in comparison with the total dredge volume. Sand mining directly influences the sand balance as sand is extracted from the estuary. The sand mining volumes (1.5-2 Mm^3) and the accuracy of these figures determine, amongst others (such as bathymetry measurements), the magnitude of the natural sediment transports and thus the import or export in the estuary mouth.

From the natural erosion/sedimentation it follows that between 1971 and 1980 an average sand import of 1 Mm^3/year occurs and between 1981 and 1990 an import of 2 Mm^3/year. Since 1990 the Western Scheldt is exporting with an annual-averaged value of approximately 1-2 Mm^3.

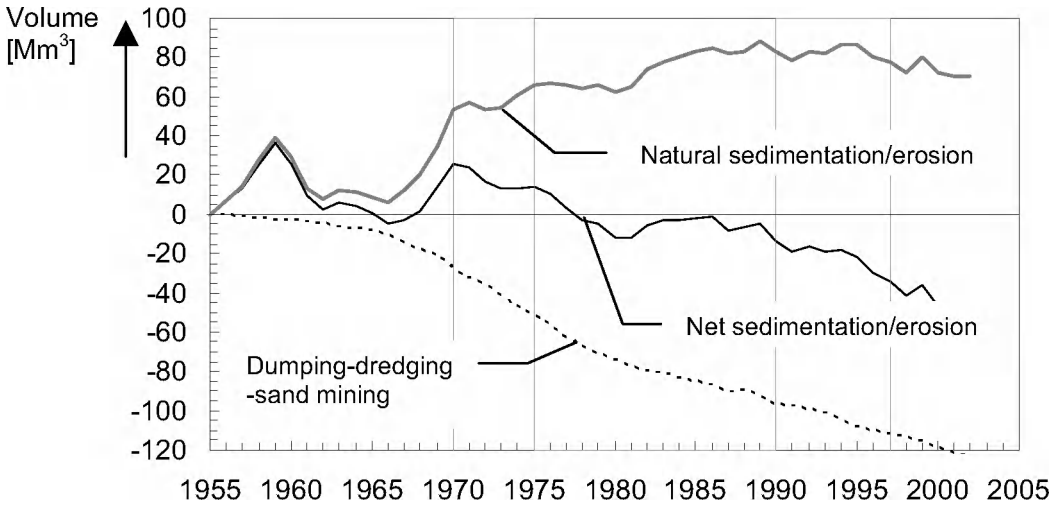

Figure 2.8: Cumulative net sedimentation (+) and erosion (-), cumulative dumping (+) and dredging (-) and sand mining (-) and 'natural' sedimentation and erosion in the Western Scheldt since 1955 (derived from Jeuken et al., 2003a).

Jeuken et al. (2003a) and Nederbragt and Liek (2004) describe in more detail the changes of the net sediment transport for the individual macro cells:

- Since 1960 a landward directed transport in the eastern part (macro cells 5-7) of approximately 1 Mm^3/year with maximum values of 3 Mm^3/year during the period following 1980.
- During the period 1960-1990 a landward directed transport at the western boundary of macro cell 4 of approximately 2 Mm^3/year. Between 1990 and 2001 this has reduced to almost nil.
- During 1960-1990 a landward directed transport at the western boundary of macro cell 3 of approximately 1 Mm^3/year. From 1990 until 2001 the transport direction changes in a seaward directed transport of slightly less than 1 Mm^3/year.
- A landward directed transport at the western boundary of macro cell 1 (import towards the Western Scheldt) of approximately 1-3 Mm^3/year during 1971-1990. Since 1990 the Western Scheldt is exporting with 1-2 Mm^3/year.

The change of a sand importing into a sand exporting system has apparently its origin in the western and central part of the Western Scheldt (Jeuken et al., 2004). An explanation for this is yet unknown, but possibly the cut-off of the channel bend in the central part has influenced this process. This may be further affected by the relocation of the sand mining activities from the western to the eastern part of the Western Scheldt and changes in the dumping strategy.

3 The hydrodynamic model

3.1 Set-up of the model

The hydrodynamic, *two-dimensional* (depth-averaged) and homogeneous model (no salinity differences), as used in the present project, is derived from an existing hydrodynamic model, denoted as KUSTZUID, which was set-up, calibrated and verified by the Dutch Ministry of Transport and Public Works. The original KUSTZUID model covers both the Eastern Scheldt and the Western Scheldt. Since the present project only focuses on the Western Scheldt, the coverage of the model was adjusted. The entire Eastern Scheldt estuary was removed from the model. In addition, the sea area of the model was stripped. In total the grid includes approximately 12,500 active computational points. Grid cell sizes vary between 800*800 m^2 at the open sea to 150*250 m^2 within the estuary. The bathymetry of the model represents the actual situation of 2001.

The open sea boundaries of the model are forced by means of Riemann boundary conditions, i.e. a combination of water levels and velocities. The boundary conditions are specified in terms of amplitudes and phases of the most important tidal components. Hence, astronomical boundary forcing allows for the simulation of any calendar period in time. Amplitudes and phases of tidal components at the open sea boundary were generated by means of a tidal analysis on time series generated by a set of larger models. At the open river boundary near Rupelmonde discharges are used as boundary conditions. The discharges originate from a computation with the SCALWEST model, which covers the period from the 17th of June 2000 to the 5th of July 2000. To allow for astronomical forcing, the time-series generated by the SCALWEST model were transformed into amplitudes and phases of the most important tidal constituents by means of a tidal analysis.

Bed friction exerted on the moving water is included in the model schematisation by means of a Manning roughness, which was taken from the SCALWEST model. Values vary between 0.02 and 0.04 $s/m^{1/3}$.

3.2 Calibration

As the original KUSTZUID model was already thoroughly calibrated by Rijkswaterstaat no extensive calibration appeared to be necessary. Results are discussed hereafter in terms of water levels (time series and astronomical components), discharges and velocities.

Water levels

In Figure 3.1 computed water levels in the stations Westkapelle, Vlissingen, Hansweert and Bath are compared with tidal predictions for the period 19-21 June 2000. The tidal range in these stations, as well as in the Belgian stations (not shown here) is predicted well. With respect to the phase of the tide it appears, that in the vicinity of the open sea boundary the phase is also well reproduced but that in the upstream region (Lower Sea Scheldt) deviations

become noticeable. This is most pronounced at Antwerpen in the vicinity of the upstream model boundary, where the model lags the tidal prediction with approximately 0.5 hr.

Tidal asymmetry

The morphological development of an estuary is often associated with the asymmetry of the tide. The asymmetry can be described using amplitudes and phases of the most important semi-diurnal and quarterly diurnal tidal components (Wang et al., 2002):

- the amplitude ratio M_4/M_2, which determines the strength of the tidal asymmetry;
- the phase difference $2\varphi_2-\varphi_4$: a positive value means a flood period of shorter duration than the ebb period. Hence, maximum flow velocities during flood are larger than during ebb.

Results for the semi-diurnal and quarterly diurnal tidal components are given in Figure 3.2 for stations Westkapelle and Cadzand (0 km), Vlissingen (13 km), Terneuzen (34 km), Hansweert (50 km) and Bath (63 km).

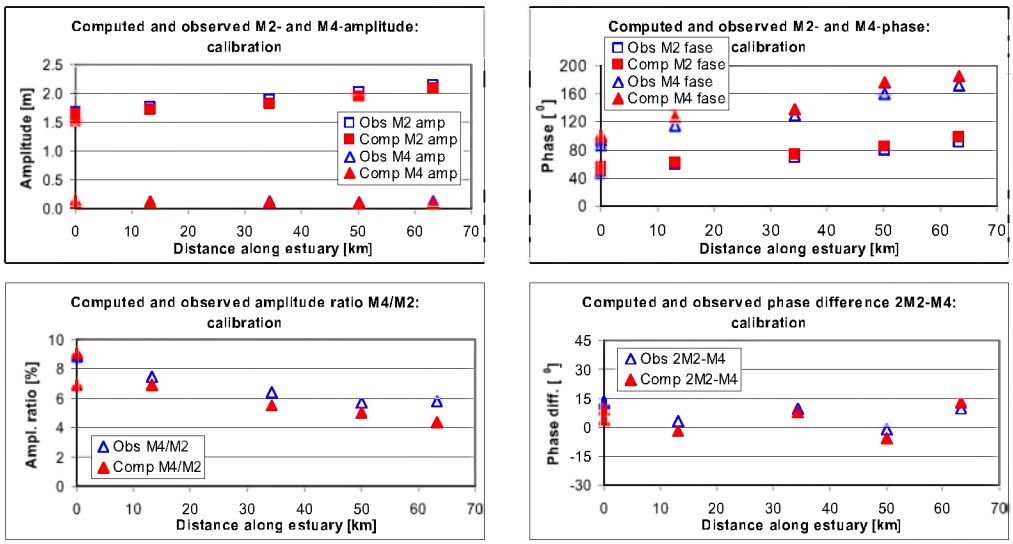

Figure 3.2: Longitudinal variation of M_2 and M_4 amplitudes and phases, M_4/M_2 and $2\varphi_2-\varphi_4$ for the calibration period. Stations: Westkapelle and Cadzand (0 km), Vlissingen (13 km), Terneuzen (34 km), Hansweert (50 km) and Bath (63 km).

The magnitudes of the M_2 and M_4 amplitudes and phases, as well as their variation in longitudinal direction are reproduced by the model. The observed magnitude of the tidal asymmetry, expressed as the amplitude ratio M_4/M_2, decreases from 10% near Vlissingen to 5% near Bath. This is adequately reproduced by the model. The (absolute) difference between measured and computed amplitude ratio is less than 1% in the entire Western Scheldt. The longitudinal variation of the phase difference as computed by the model agrees with the observations. It is noted, that rather the change of the tidal asymmetry between two stations than the tidal asymmetry itself is related to the morphological changes (Wang et al., 2002). Assuming that variation in storage area and variation in cross-sectional area can be neglected, it follows that the relation between the horizontal and vertical tide is linear. It can then be estimated, that differences between the observed and computed ratios M_4/M_2 result in differences between observed and computed net sediment transport of approximately 2%

near Vlissingen, 10-15% at the middle of the estuary and 35% near the river entrance. This is relatively small given the accuracies of present sediment transport formulae.

Discharges

Within the estuary a number of standard cross-sections is being used by Rijkswaterstaat in which on a regular basis velocities are measured. Resulting discharges are derived for both the flood channel and the ebb channel. Measurements during the period 2000-2002 are used to compare with model results following from simulations with the actual boundary conditions. Generally, computed discharges are in good agreement with observations. Ebb and flood volumes of model results versus observations, as derived from the discharges, are given in Figure 3.3. The slope of the regression line through the data amounts to 0.95, indicating that computed ebb and flood volumes are 5% smaller than observed volumes. This is consistent with the slight underestimation of the M_2-amplitude of the vertical tide by the model.

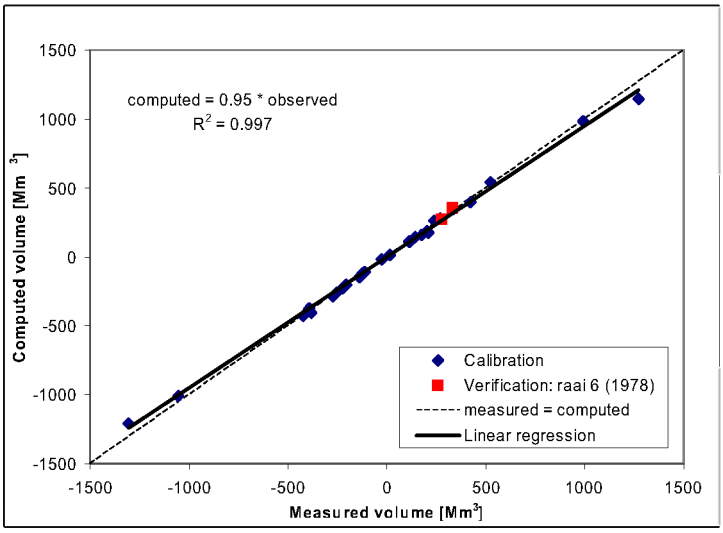

Figure 3.3: Computed versus measured flood and ebb volumes of flood and ebb channels for the calibration and verification period. The simulations employ the actual boundary conditions during the measurements.

Flow velocities

Further, flow velocities, as obtained with OSM-measurements in 17 locations at one specific depth below the water surface, are used to compare with model results. The duration of these measurements was approximately one month, allowing for an assessment of the long term residual flow and sediment transport. Because of the non-linearity between sediment transport and flow velocity a comparison has been made in terms of the so-called velocity moment, which is defined by the vector quantity $\left(\vec{u}\,(u^2+v^2), \vec{v}\,(u^2+v^2)\right)$. Measurements taken in the centre of a channel are generally reasonably reproduced by the model. However, most of the measurements are taken at the slopes of a channel, where often a transition occurs from ebb-directed to flood-directed residual transport. At these locations, the model

reproduction is poor. This is, at least partly, caused by the resolution of the model grid, which is not sufficiently high to resolve the relatively steep gradients of the bathymetry.

3.3 Verification

For the verification of the model the year 1972 was selected, i.e. during the first deepening of the navigation channel. The original model bathymetry was replaced by a bathymetry that corresponds with 1972 and the roughness schematisation remained unaltered. Amplitudes and phases of the tidal constituents at both the sea and river boundary are used to make a tidal prediction, taking into account the nodal amplification factors and astronomical arguments, resulting in time-series of the boundary signal for 1972. The application of the astronomical boundary conditions, derived for 2000, is only allowed if no significant changes between 1972 and 2000 have occurred. For the open sea boundaries of the model this assumption is most likely valid. Whether significant changes occurred at the upstream river boundary is not known.

Water levels

Figure 3.4 presents for the period 19-21 June 1972 the computed and measured time series for the water levels in Westkapelle, Vlissingen, Hansweert and Bath. It appears that, compared with the 2000 simulation, an increased phase lag between measurements and computation exists. At the seaside of the estuary already a small phase difference is present, which increases in upstream direction towards a phase difference of approximately 45 minutes near Bath. However, results improve if a different period is selected. Figure 3.5 shows observed and computed water levels in the aforementioned stations for the period 14-16 June 1972. A reason for this is, that the forcing at the model boundaries is done with a limited set of tidal constituents, resulting in phase differences between observations and computational results during certain periods of the simulation.

Tidal asymmetry

The semi-diurnal and quarterly-diurnal components as well as the parameters that represent the tidal asymmetry of the vertical tide are shown in Figure 3.6. The figure shows, that the model reproduction of the tidal asymmetry for the verification period is comparable with that for the calibration period. Particularly, the changes in the phase difference $2\varphi_2-\varphi_4$ in Hansweert and Bath are accounted for by the model.

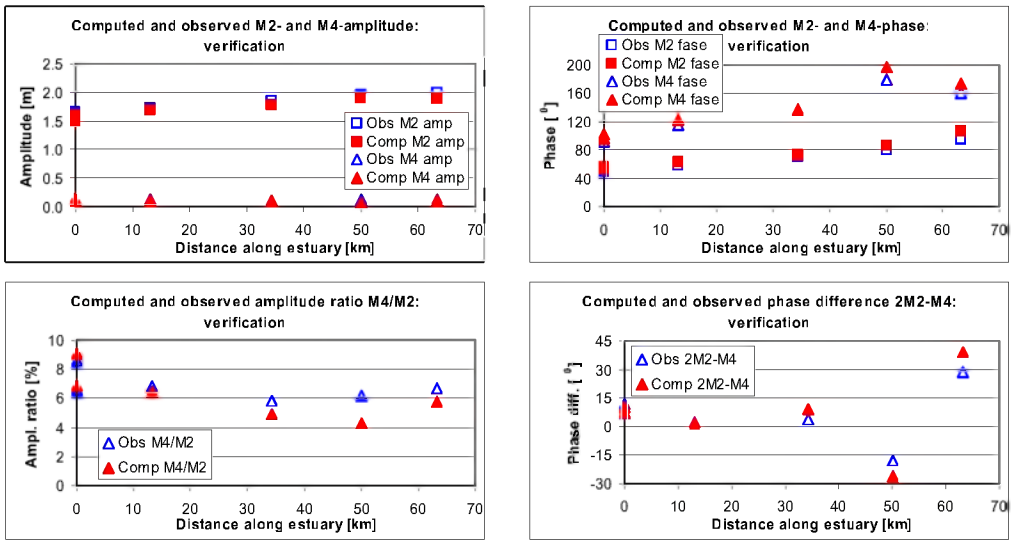

Figure 3.6: Longitudinal variation of M_2 and M_4 amplitudes and phases, M_4/M_2 and $2\varphi_2-\varphi_4$ for the verification period.

Discharges

For the verification period the measured discharge in 1978 in 'Raai 6' (Middelgat and Gat van Ossenisse) was used. Flood and ebb volumes are computed from the observed and simulated discharges and mutually compared. Results are shown in Figure 3.3 (see Section 3.2), from which it follows that these quantities are reproduced by the model.

3.4 Conclusions

Results of the calibration and verification process show, that the model is capable to reproduce the hydrodynamics with respect to water levels and discharges. In the latter case distinction has been made between the main flood and ebb channels. This implies that also the distribution of the tidal flow over these channels is properly accounted for by the model. Water levels have been analysed in terms of amplitudes and phases of some primary tidal constituents. It is shown that computed amplitude ratios and phase differences of the semi-diurnal and quarterly-diurnal components show good resemblance with observations. It is concluded, that the hydrodynamics in terms of one-dimensional quantities (water levels, discharges) is reproduced by the model and that a necessary condition is fulfilled to proceed with the calibration and verification of the morphodynamic model. However, no detailed comparison has been made with respect to the three-dimensional flow field as this would require measurements with a high spatial resolution, especially in lateral direction. With these types of measurements it can be assessed whether the model also reproduces the flow field at the sub tidal and intertidal areas and in particular the lateral water exchange between the channels and the intertidal areas.

4 Calibration of the morphodynamic model

To obtain a calibrated morphological model for the Western Scheldt the following activities are employed:

- *Set-up of the morphological model:* two-dimensional versus three-dimensional modelling, selection of the morphological tide, schematisation of the wind/wave climate, schematisation of the erodible bed with a spatial varying thickness, schematisation of dredging, dumping and sand mining as well as the inclusion of bank protection measures.
- *Sensitivity runs for 2001:* relatively short simulations to assess, as a first estimate, the model input parameters, such as the sediment grain size diameter, wave effects, the sediment transport formula, the horizontal dispersion coefficient.
- *Calibration runs:* simulations with a duration of several years for two different periods with an optimal combination of the input parameters.
- *Sensitivity runs for 1998-2002:* variations of the model input parameters, representing uncertainties in the model schematisation, and their consequences for the model results.
- *3D-effects:* assessment of three-dimensional effects on the model results including the effects of non-homogeneous flow (salt-fresh water interaction).

4.1 Set-up of the model

In Section 1.4 it has been mentioned, that the online version of DELFT3D is used for the morphological simulations. At each computational time step the hydrodynamics are computed by the model, as described in Chapter 3, and used as input for the computation of sediment transports and bed level changes in each point of the computational grid. A morphological acceleration factor is used to assist in dealing with different time scales between hydrodynamic and morphological development. At each time step the changes in bed sediment are multiplied by this factor, extending the morphological time step ("elongated tide" approach), see Lesser et al. (2004).

2D/3D

The DELFT3D model can be run in two-dimensional or in three-dimensional mode. In the latter case morphological simulations over a long period result in a huge computational effort. Roughly, the computational time increases proportional with the number of computational layers. As such, a two-dimensional (depth-averaged), approach is presently still inevitable to perform simulations over several years. The validity of a two-dimensional approach is assessed prior to the actual calibration process on the basis of three-dimensional simulations for the year 2001. These simulations are still done without dredging, dumping and sand mining, a varying thickness of the erodible bed and bank protection measures. Figure 4.1 shows the scatter plot of bed level changes in each grid point of run 005 (two-dimensional) versus run 006 (three-dimensional). It appears that the sedimentation-erosion patterns of the two-dimensional model and the three-dimensional model are very much alike. Run 006 is performed with 10 non-equidistant layers, i.e. the grid is refined near the bed.

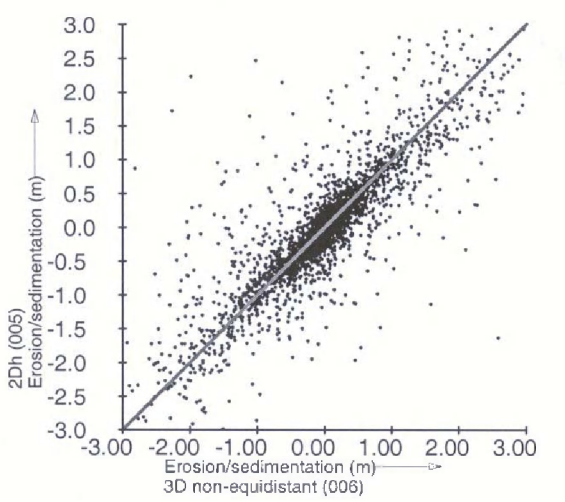

Figure 4.1: Erosion-sedimentation of run 005 (depth-averaged) versus run 006 (3D).

Morphological tide

With the application of a morphological tide, in combination with an acceleration factor, the computational time for the morphological simulations can be further reduced. The morphological tide, with a duration of 25 hours, is selected in such a way, that during ebb and during flood the computed sediment transport through a cross-section near Vlissingen is similar to the average ebb and flood transport for a complete spring-neap tidal cycle. For the morphological tide an enhancement factor of 120 is selected, which implies that one morphological year is simulated with three hydrodynamic tides, each with duration of 25 hours (run 004). The spring-neap tidal cycle is simulated in combination with an enhancement factor of 24 (run 002), resulting in a computational time which is five times larger than for run 004. From Figure 4.2 it follows, that the computed bed level changes for both runs are almost identical.

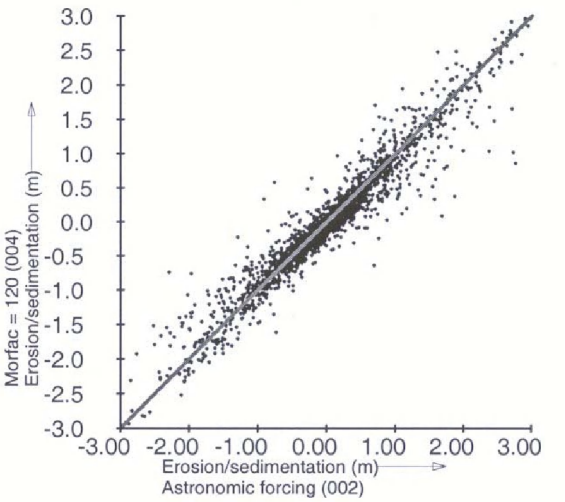

Figure 4.2: Erosion-sedimentation of run 004 (3D, morphological tide) versus run 002 (3D, spring-neap tide).

Wind/wave climate

Wind-induced waves affect the bed shear stresses, especially in the shallow areas of the Voordelta and western part of the Western Scheldt. Consequently, sand is eroded and transported by the tide-induced flow. Available wind and wave data in locations Scheur West, Euro Platform and Vlissingen are used to derive a representative wind and wave climate for the morphological simulations. In total 52 wind speed and wind direction classes are distinguished, each associated with a significant wave height, peak wave period, wave direction and frequency of occurrence. As it is impossible to apply a wave climate consisting of 52 different conditions to the full morphological model, a schematisation procedure was devised to reduce the number of conditions to a limited set of conditions. This restricted set leads to the same initial sedimentation-erosion pattern as the weighted average of the full set of conditions. It was ultimately found that even with one condition, the initial erosion-sedimentation pattern, following from all 52 conditions, could be reproduced. Table 4.1 presents the single wave condition as applied during the morphological simulations. The simulations show, that the wave energy is considerably dissipated in the Voordelta and that wave heights in the inner estuary are generally less than 0.4 m.

Wind speed [m/s]	Wind direction [deg. N]	Significant wave height [m]	Peak period [s]	Wave direction [deg. N]
6.8	258	0.90	5.0	263

Table 4.1: Single wave condition for morphological simulations.

Non-erodible layers

The bed of the Western Scheldt consists of alternating erodible sand layers and non-erodible layers of, for instance, stiff clay ("Boomse Klei"). Available data on the top level of the first non-erodible layer have been used in conjunction with the bed level to derive the thickness of the space-varying deposits, which are available for erosion (see Figure 2.4). In the outer region of the Voordelta data are lacking and a thickness of the erodible bed of 20 m is assumed. Similarly, in the Lower Sea Scheldt a thickness of 2.5 m is used.

Dredging, dumping and sand mining

Each dredging area in the Western Scheldt is defined by means of a dredging polygon and a dredging depth. If net sedimentation occurs in a dredging area, the depth in that area is kept to the pre-defined value. The volume of removed bed material is transported to one or more dumping areas. In case of more than one dumping area per dredging area, the percentage of dredged material brought to each dumping area is specified. This percentage is based on dredging data from Rijkswaterstaat. The local water depth in a dumping area decreases due to dumping of dredged material; however in the model no upper limit of the bed level is specified (in reality dumping is restricted to levels below NAP-5 m). Furthermore, for simulations over several years average polygons and dredging depths are specified. Specifically for this project, the on-line version of the DELFT3D model is extended with the dredging and dumping functionality as described above. In addition to dredging and dumping, sand mining is also included in the model as a volume of dredged material removed annually from a sand mining area (but without dumping within the estuary). Also

for sand mining an "average" scenario is applied. This scenario ensures that the correct amount of material is removed from the estuary over the entire computational period.

Bank protection measures

At many locations in the Western Scheldt banks are protected by various kinds of measures to avoid bank erosion and migration of channels. Bank protection is included in the model schematisation as non-erodible computational cells over the entire thickness of the bed.

The sensitivity runs are performed with the inclusion of the aforementioned functionality (waves, dredging and dumping, specified thickness of the erodible sand layer, bank protection measures). Sand mining is not yet included in the model during the sensitivity runs.

4.2 Sensitivity runs for 2001

In order to establish the sensitivity of the model results for changes in the input parameters a number of sensitivity runs is carried out. All runs are carried out for the year 2001, i.e. the measured bathymetry of 2001 is used in the model as the initial bed for the morphological simulations. The morphological tide (see Section 4.1) with a period of 1500 min is prescribed at the seaward boundary. The simulation is performed over three of these tidal periods and a morphological acceleration factor of 120 is applied. This effectively scales up the morphological changes equivalent to those over a period of one year. In total two morphological years are simulated of which the second year is used for model analysis; the first year is used for the spinning-up of the model to eliminate initial inaccuracies of the model bathymetry. The discharges at the upstream boundary near Rupelmonde are derived from a SCALWEST simulation for June 2000 from which the most important tidal constituents are computed (see Chapter 3). The model set up is extended with dredging and dumping (scenario 2001), the thickness of the first erodible layer and bank protection measures.

Model results are compared with observations in terms of (i) the sedimentation and erosion pattern, (ii) sediment volume changes of the macro cells, (iii) changes of the areas for seven depth classes, (iv) dredge volumes and (v) net sediment transport.

The simulation runs are described in Table 4.2; run 007 is the reference run and all modifications to the model input are relative to this run.

Simulation	Run description
007 (Reference)	Depth-averaged approach with a morphological tide (6 tidal days and an enhancement factor of 120), including (i) an erodible sand layer with specified thickness, (ii) bank protection measures and (iii) dredging and dumping.
008	Instead of a space varying roughness based upon a Manning roughness formulation, a constant Chézy value of 60 $m^{½}/s$ is applied in the entire model domain with exception of "Het verdronken land van Saeftinge", where a coefficient of 30 $m^{½}/s$ is used, to account for the dense vegetation.

009	Wave effects, see Section 4.1, are included in the model. Although the importance of waves is expected to be small in the inner estuary there may be some effects in the western part of the Western Scheldt and Voordelta.
010	The mean diameter of the bed material is decreased from 200 to 150 μm to investigate the sensitivity of the results for this parameter.
011	A space varying distribution of bed material is used. The mean diameter varies in between 150 μm and 200 μm to account for the observed spatial variability.
012	In stead of the transport formula of van Rijn the Engelund Hansen transport formula is used to investigate the effect of computed sediment transports on the morphological changes.
013	Instead of the transport formula of van Rijn, the Ackers-White transport formula is used to investigate the effect of computed sediment transports on the morphological changes.
014	The horizontal dispersion coefficient is increased from 1 m^2/s to 50 m^2/s to investigate the influence of the dispersive transport on the erosion-sedimentation pattern.
017	The horizontal dispersion coefficient is decreased from 1 m^2/s to 0 m^2/s to investigate the influence of the dispersive transport on the erosion-sedimentation pattern.
016	A local enhanced bottom shear stress in the vicinity of "Hansweert is introduced in the model in order to ensure that the deep pit in the ebb channel near "Hansweert" remains intact.
018	The ebb channel in the vicinity of "Hansweert" is defined as non-erodible in order to ensure that the deep pit in the ebb channel near "Hansweert" remains intact.
019	The horizontal viscosity is increased from 2 m^2/s to 25 m^2/s. The purpose of this computation is to examine to what extent the hydrodynamics affect the morphological development of the estuary.
020	In both horizontal directions the grid is refined by a factor 3 to investigate to what extent the spatial discretisation affects the model results..

Table 4.2: Calibration simulations for the year 2001.

Sedimentation and erosion

The morphological changes during 2001 are presented as plots of bed level changes, showing sedimentation (positive values) and erosion (negative values). Figures 4.3a and 4.3b present the observed changes for the years 1998-1999, 1999-2000, 2000-2001, 2001-2002 as well as the average changes for the period 1998-2002. It follows, that the observed changes significantly vary from year to year. This may be attributed to natural fluctuations, human interventions (dredging, dumping and sand mining) and inaccuracies of the bed level measurements. Model results are therefore compared with the observed annual-average

sedimentation and erosion for the period 1998-2002 to eliminate the contributions of these 'random' fluctuations.

Results for run 007 are presented in Figure 4.4 in comparison with the annual-average sedimentation and erosion during 1998-2002. The major conclusion that can be drawn from the comparison between observations and simulations is that quantitatively, the computed erosion and sedimentation is much larger than according to the observations. Although the patterns are rather irregular (alternating patches of erosion and sedimentation) there is some qualitative agreement on a larger spatial scale: The model shows a tendency to deepen the channels, whereas sedimentation occurs on the channel edges. Although much less pronounced, the tendency to deepen the channels is also observed in the measurements, especially in the eastern part of the estuary (Gat van Ossenisse/Overloop van Hansweert, Overloop van Valkenisse, Schaar van Valkenisse). Significant differences occur near Vlissingen, where the model computation reveals that the ebb channel is eroding. However, with the exception of sedimentation in a dumping area the measurements indicate that almost no erosion or sedimentation occurs. This may be due to the fact that the non-erodible shell layer, which is locally present, may be more extensive than present data indicate. Whereas measurements show that the Put van Hansweert remains in place, the simulation indicates that this large pit is travelling upstream.

Following run 007 only one model input quantity (parameter, process description, schematisation) is changed for each simulation and the differences with the results of run 007 are established. The main finding of all simulations is that the erosion-sedimentation pattern is almost not affected. This is especially true for run 008 (constant Chézy instead of a space-varying Manning roughness), runs 010 and 011 (variations of the grain size diameter) and run 017 (horizontal dispersion coefficient set to zero). The effect of waves (run 009) is restricted to the shallow area east of the entrance to the harbour of Vlissingen. The impact of the Engelund Hansen transport formula (run 012) on the erosion sedimentation pattern is limited; only local differences can be observed. The major effect appears to be an increase in sedimentation on the channel edges. The application of the Ackers White transport formula (run 013) has the largest impact on the computed pattern of erosion and sedimentation, i.e. the magnitude of erosion and sedimentation strongly decreases, and an improved agreement is found between observed and computed bed level changes, see Figure 4.4. This indicates that sediment transport gradients according to the Ackers-White formula are smaller than transport gradients according to the Engelund Hansen formula or the van Rijn formulae. The increase of horizontal dispersion (run 014) results in an increase of both erosion and deposition, with enhanced sedimentation on the channel edges; however the overall pattern remains unchanged. The impact of the change in erodibility of the bed near Hansweert (runs 016 and 018) is only local. If a larger (actually unrealistic) value for the eddy viscosity is used (run 019), horizontal velocity gradients, and consequently horizontal transport gradients, become smaller, resulting in a reduction of erosion and sedimentation. However, the pattern itself is not very much affected. Finally, the application of a finer computational grid (run 020[1]) gives a more detailed erosion-sedimentation pattern. The erosional behaviour of the cross channel near Terneuzen is now more clearly predicted by the simulation. The large-scale pattern is not significantly affected though.

[1] *Run 020 gave problems with respect to post processing and could not be analysed with respect to all output quantities.*

To assess the magnitude of the average difference between observed and computed erosion and sedimentation the parameters $|H_c-H_m|$ and H_c-H_m are computed:

$$|H_c - H_m| = \frac{1}{n}\sum_i^n |H_{c,i} - H_{m,i}| \quad and \quad H_{c,i} - H_{m,i} = \frac{1}{n}\sum_i^n \left(H_{c,i} - H_{m,i}\right) \qquad (4.1)$$

where $H_{c,i}$ and $H_{m,i}$ are the computed and measured erosion ($H_{c,i}$ and $H_{m,i} < 0$) and sedimentation ($H_{c,i}$ and $H_{m,i} > 0$) in grid point i during one year (2001) and n is the total number of grid points in the Western Scheldt. Both parameters are *aggregated* quantities of *local* differences between computed and measured bed level changes and are used for mutual comparison of the simulations. However, no inferences can be made with respect to the reproduction of erosion and sedimentation patterns (e.g. the migration of a channel). Figure 4.5 presents $|H_c-H_m|$ for all sensitivity runs, showing that values are in the order of 0.5 m with lowest values for run 013 (Ackers-White transport formula: 0.33 m) and run 019 (increased eddy viscosity: 0.37 m) if compared with the average observed bed level changes for the period 1998-2002. The too large sedimentation and erosion, as computed by the model, cancel each other out to a large extent. It is shown by the parameter H_c-H_m, i.e. the average over all computational points of the actual difference between the computed and measured erosion and sedimentation. The average of H_c-H_m for all runs is -0.004 m (compared with the observations for the period 1998-2002).

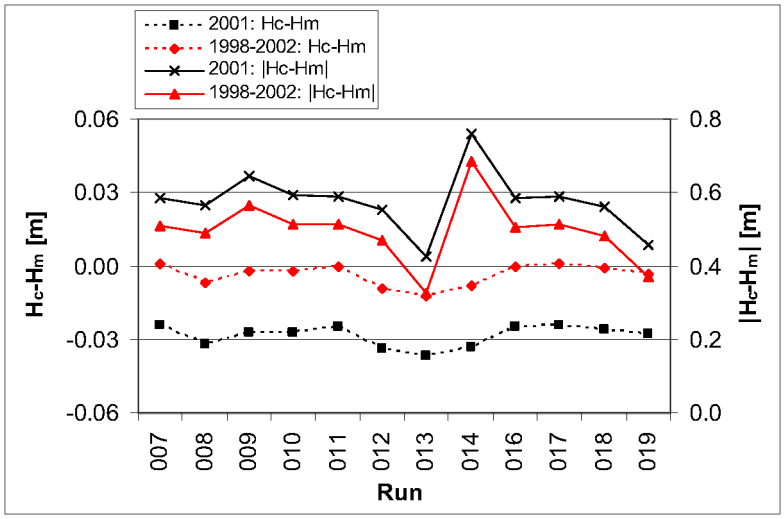

Figure 4.5: Average actual and absolute differences between computed and observed erosion (H_c and $H_m < 0$) and sedimentation (H_c and $H_m > 0$).
H_c: computed bed level changes.
H_m: measured bed level changes.

The results of the sensitivity runs are summarised as follows:

1. The erosion-sedimentation *pattern* is negligibly affected by changes of the model input parameters and model schematisation.
2. Sedimentation and erosion, as predicted by the model, are too large. However, the overestimate of sedimentation is balanced by the overestimate of erosion, so that the

computed net volume change for the Western Scheldt differs only in the order of 1 Mm^3 with observations.

3. The results thus indicate that sediment transport gradients, as computed by the model, are too large. This is illustrated by runs 013 and 019, reducing the magnitude of the sediment transport (run 013) or reducing horizontal velocity gradients and consequently horizontal transport gradients (run 019).

Net sediment volume changes

The subdivision into ebb and flood channels of the macro cells is shown in Figure 4.6 (following Jeuken et al., 2003a). The net sediment volume changes of the ebb and flood channels (below NAP+3.5 m) are computed for each of the macro cells. The average values and the standard deviations of all sensitivity runs are given in Figure 4.7. In addition, the observed net volume changes for 2001 and the average value for the period 1998-2002 are shown.

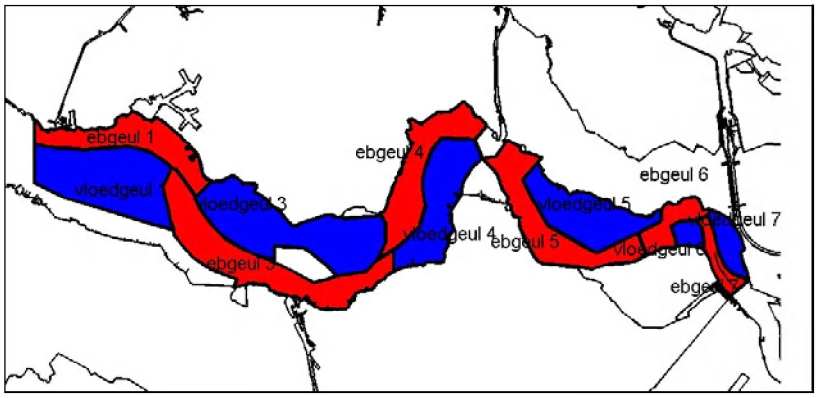

Figure 4.6: Subdivision of the Western Scheldt into macro cells, ebb (shown in red) and flood channels (blue) (Jeuken, 2003a).

The longitudinal variation of the net volume changes follows more closely the observed average changes for the period 1998-2002 than for the year 2001 only, although differences can be rather large, especially for the ebb and flood channels of macro cell 1. It is noted, that sand mining with a total of approximately 2 Mm^3 is not included in the sensitivity runs, which may explain to some extent the differences with observations.

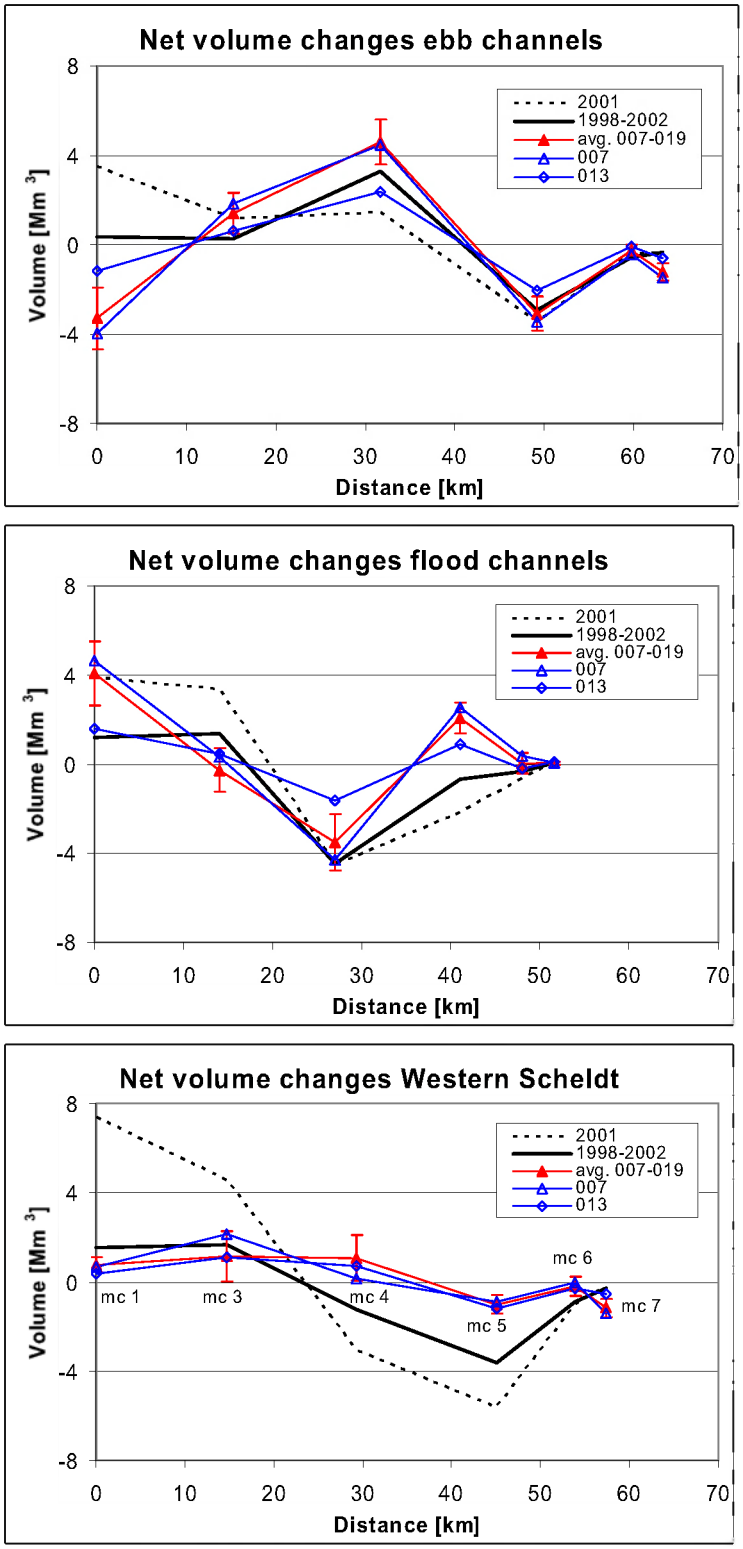

Figure 4.7: Computed (avg. run 007-019, run 007 and run 013; 2001) and observed (2001, 1998-2002) net volume changes of the ebb and flood channels of the macro cells.
mc = macro cell.

Figure 4.7 also shows the individual results for the run 007 (reference) and run 013 (Ackers-White). Run 007 follows closely the average results of all runs, whereas run 013 gives smaller net volume changes for the ebb as well as the flood channels of the macro cells, apparently due to reduced sediment transports. However, for the ebb and flood channels combined the results for run 007 and run 013 are similar.

A quantitative comparison between observed and computed net volume changes, both for the period 1998-2002, follows from a regression according to:

$$\Delta V_c = b * \Delta V_m \qquad (4.2)$$

where ΔV_c and ΔV_m [Mm^3] are the computed and measured net volume changes of the individual ebb and flood channels and b [-] is the slope of the regression line, which is one for a perfect agreement. Values for b and the regression coefficient r^2 are given in Figure 4.8: b varies between 0.52 and 1.32 and r^2 between 0.29 and 0.67. Run 013 (Ackers-White) gives the largest regression coefficient (= 0.67), however with a low value for b (= 0.52). Run 008 (uniform Chézy) and run 014 (increased horizontal dispersion) give lowest regression coefficients. If computational results are compared with observations for the year 2001 only, regression coefficients are smaller (between 0.1 and 0.3).

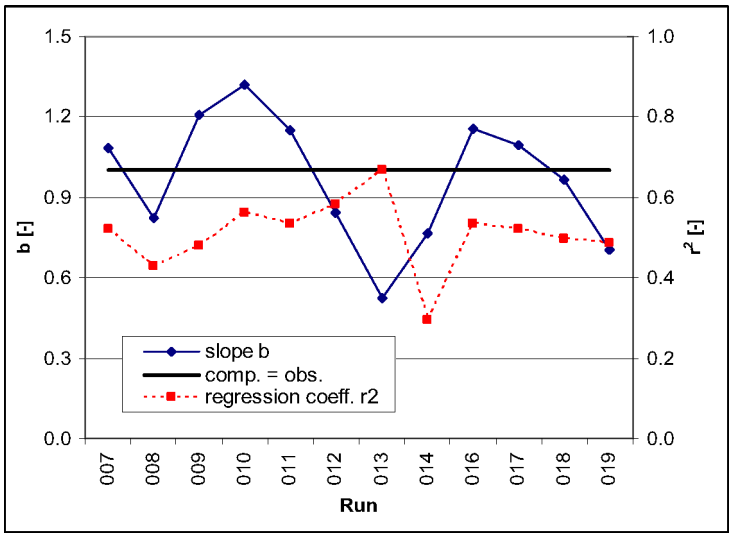

Figure 4.8: Slope b of the regression line and regression coefficient of computed (2001) versus observed net volume changes of the individual ebb and flood channels (1998-2002).

Area changes per depth class

A number of depth contour lines of the bed is defined for further analysis: 0, -2, -5, -7, -10 and -20 m NAP. This results in the following depth classes of the bed levels:

[> 0 m NAP] and [0, -2 m NAP]	representing the upper and lower intertidal areas
[-2, -5 m NAP]	representing the sub tidal areas
[-5, -7 m NAP] and [-7, -10 m NAP]	representing the shallow channels
[-10, -20 m NAP] and [< -20 m NAP]	representing the deep channels

It is noted that, for practical reasons, depths are relative to a fixed reference level (NAP) and thus differ from the definitions as given in Section 2.3.1.

In Figure 4.9 observed and computed changes of the areas per depth class are compared for the entire Western Scheldt (ebb and flood channels). Observations are given for the year 2001 and for the yearly-averaged value of the period 1998-2002. The results of the sensitivity simulations are presented as the average and the standard deviation of all simulations. The figure shows, that the model significantly overestimates the area changes for all depth classes. The area with a depth larger than -20 m NAP as well as the area above -5 m NAP increases relatively to observations. Between -5 m and -20 m NAP the computed area decreases relatively to observations. This implies that the computed morphological changes result in a gradual steepening of the bathymetry. The results of run 007 (reference) follow closely the average values of all sensitivity runs. Area changes of run 013 (Ackers-White) are less than for run 007, but they still predict changes which are larger than those observed.

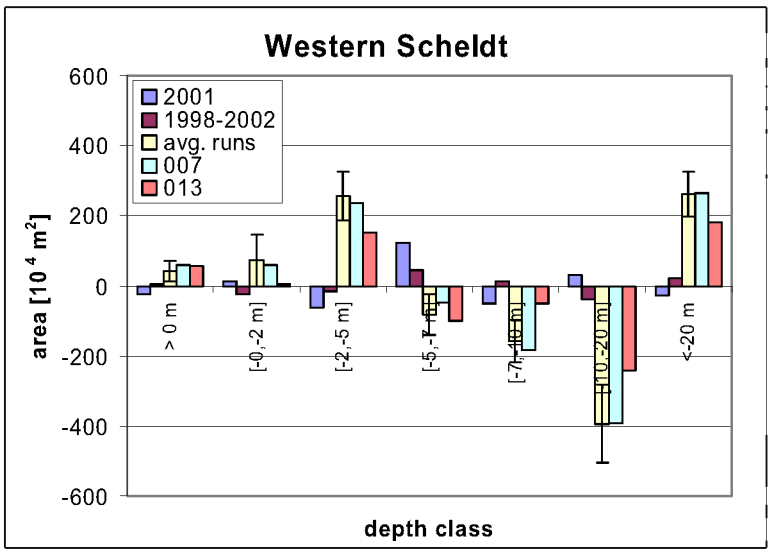

Figure 4.9: Observed and computed area changes for the Western Scheldt. A positive (negative) value indicates an increase (decrease) of the area occupied by the bed with levels as given by the class bounds.

Dredge volumes

Total annual dredge volumes for the Western Scheldt, as computed by the model, are given in Figure 4.10. Computed dredge volumes are for the year 2001, whereas the measured dredge volume is the average for the period 1998-2002 (converted to in situ m^3 by multiplication with 0.91 assuming a bulking factor of 1.1 due to dredging).

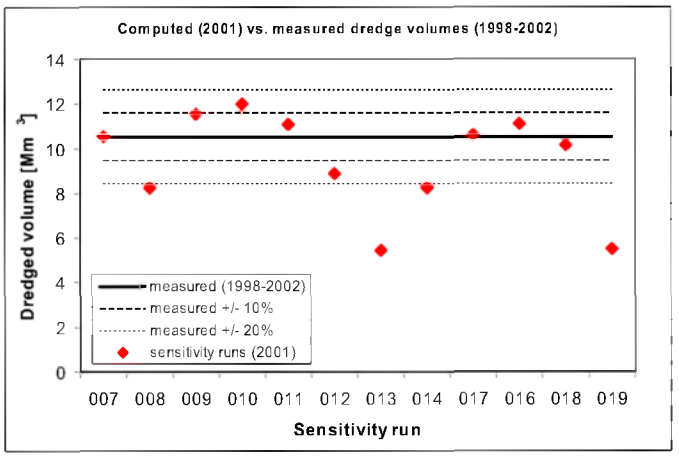

Figure 4.10: Computed dredge volumes (2001) and average measured dredge volume (1998-2002).

Apart from run 013 (Ackers-White) and run 019 (increased eddy viscosity) all sensitivity runs produce a total dredge volume equal to the observed dredge volume ± 20%. The observed dredge volumes for 2001, the yearly-average dredge volume for 1998-2002 and the average dredge volume and standard deviation for runs 007-019 are shown in Figure 4.11.

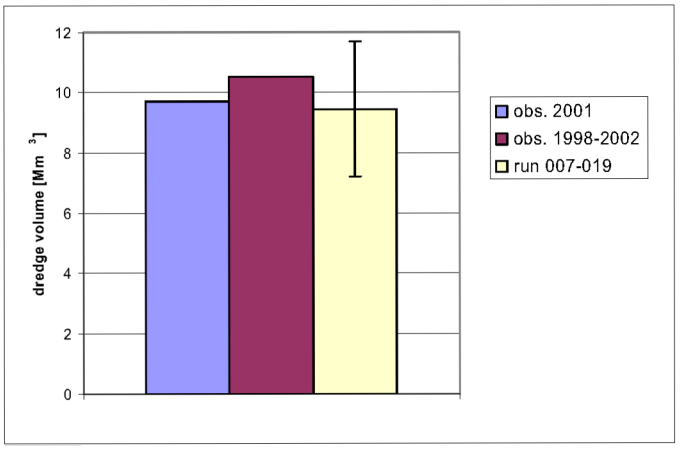

Figure 4.11: Measured dredge volumes (2001 and average for 1998-2002) and average computed dredge volume (2001).

Net sediment transport

For all sensitivity runs the residual sediment transport through cross-sections 1 and 2 is given in Figure 4.12b. Cross-section 2 (c.s. 2) is located approximately 4 km eastward of cross-section 1 (c.s. 1), see Figure 4.12a. The residual transport following from the sand balance study (Nederbragt and Like, 2004) is derived for a cross-section between c.s. 1 and c.s. 2. Computed transports are converted to volumes per unit of time including the pores (assuming a porosity of 0.4) to allow for comparison with the results of the sand balance.

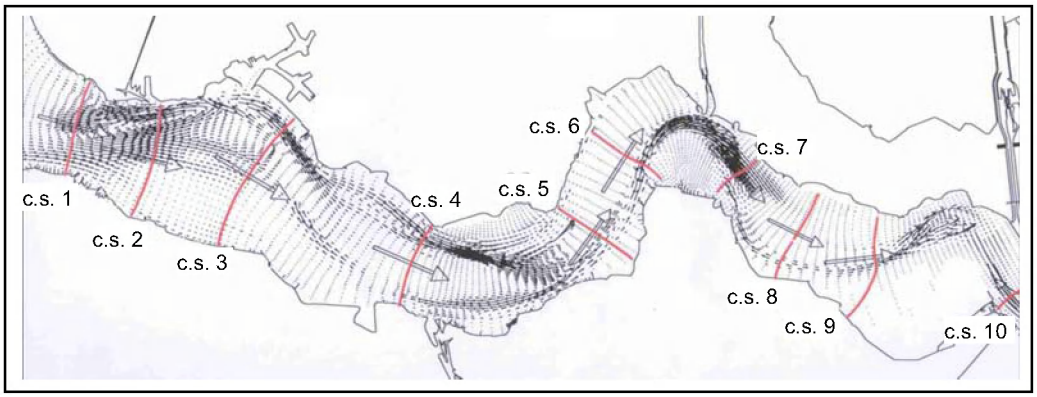

Figure 4.12a: Cross-sections for the computation of the residual sediment transport.

Run 012 (Engelund-Hansen transport formula), run 013 (Ackers-White transport formula) and run 014 (increased horizontal dispersion) produce the lowest values for the net sediment import.

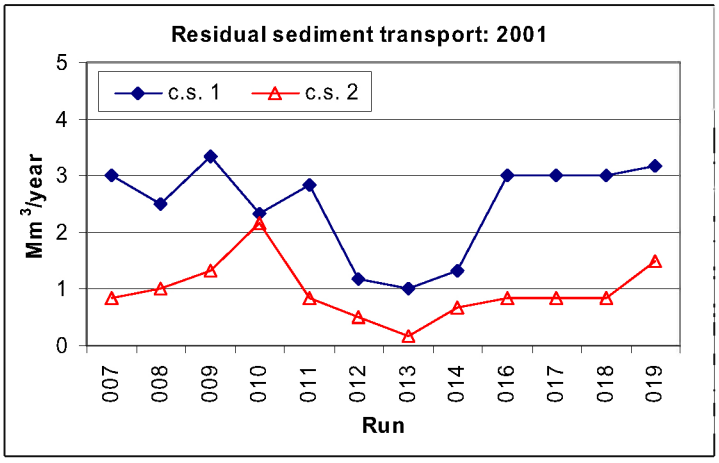

Figure 4.12b: Residual sediment transport through cross-sections 1 and 2 (as shown in Figure 4.12a) for runs 007-019. Positive = landward (from west to east). Transports are volumes per unit of time including pores (porosity: 0.4).

Figure 4.13 compares the observed and computed residual transports. Observations are given for four subsequent periods of 10 years. Model results are shown as the average and standard deviation for all sensitivity runs as well as for the individual runs 007 (reference) and 013 (Ackers-White). The model predicts a net sediment *import* of 1-3 Mm^3/year, which is comparable with the observed net import during 1960-1989 (also 1-3 Mm^3/year), but not in agreement with the observed sediment *export* of 1.5 Mm^3 during the period 1990-2001.

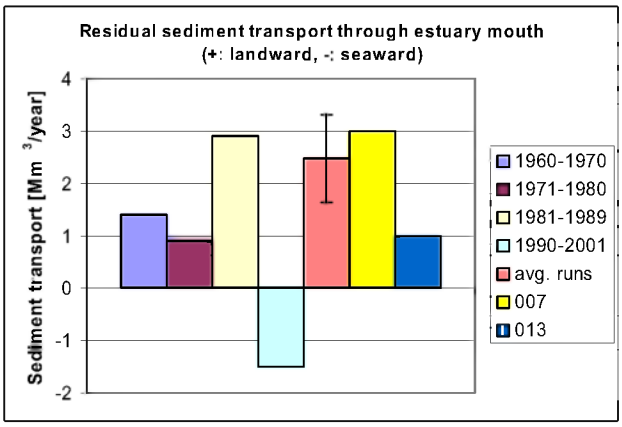

Figure 4.13: Observed and computed residual sediment transport through cross-section 1 (see Figure 4.12a).

4.3 Calibration runs

The parameter settings of reference simulation 007 are selected for the calibration runs on the basis of the following considerations:

1. The statistical parameters of the calibration runs ($|H_c-H_m|$ and H_c-H_m give no indication that other parameter settings result in a major improvement, although run 013 (Ackers-White) and run 019 (increased eddy viscosity) perform somewhat better;
2. The sedimentation and erosion patterns of the sensitivity runs, as assessed visually, do not show major differences;
3. The computed net volume changes of the individual ebb and flood channels and the Western Scheldt for run 007 correlate reasonably well with the observed net volume changes, like most of the other sensitivity runs, but with a slope of the regression line which is almost one. Run 013 shows a larger correlation coefficient, but the slope of the regression line is a factor two too small, indicating that computed net volume changes are approximately 50% of the observed changes.
4. Observed area changes at the spatial scale of the Western Scheldt are not reproduced by any of the sensitivity runs. The computed area changes for run 013 (Ackers-White) are less than for the other runs and as such closer to the observed changes.
5. Computed total dredge volumes for the Western Scheldt are in good agreement with observations.
6. Most simulations predict more or less the same sediment import in the estuary mouth and as such there is no preference for one of these runs. However, run 012 (Engelund Hansen), run 013 (Ackers-White) and run 014 (increased horizontal dispersion) give lowest values for the sediment import and are therefore more close to the observed export of sediment since 1990.
7. None of the sensitivity runs following run 007 give an improvement of all analysed output results, however for some of these results run 013 (Ackers-White) performs better.

Although waves hardly affect the large-scale morphological development of the estuary, they might be important on a local scale. This especially holds for the shallows in the western section of the Western Scheldt estuary. Since the final calibration computation will be analysed also with respect to the changes of areas of shoals and 'slikken', it was decided

to include the impact of waves in the final calibration simulation (i.e. the final calibration run is actually based on run 009 as described in the previous section).

Dredging and dumping is included by means of an "average" dredging and dumping scenario. This implies that polygons for the dredge and dump locations represent their average locations during the period 1998-2002. In addition to dredging and dumping, sand mining is also included in the model as a volume of dredged material removed annually from a sand mining area. Also for sand mining an "average" scenario for the considered period is applied.

Similar to the sensitivity runs, the calibration runs are preceded by a one year spin-up of the morphological model to eliminate inaccuracies of the initial bed. Morphological changes following this initial year are used for analysis.

In the following sections the results of two calibration periods are discussed:
- 1998-2002: during and following the second deepening of the navigation channel;
- 1960-1966: prior to the first deepening of the navigation channel.

4.3.1 1998-2002

Sedimentation and erosion

Figure 4.14 shows for run 021 the annual erosion-sedimentation pattern derived by averaging over four years. The pattern is comparable with run 007. The magnitude of erosion and sedimentation appears slightly less than for run 007 so that the reproduction of the observations improves (see e.g. near the ebb channel Everingen to the north-east of Terneuzen).

Net sediment volume changes

Figure 4.15 presents the net volume changes of sediment per macro cell (ebb and flood channel) for the period 1998-2002 (4 years). A positive volume change results from net deposition, whereas a negative volume change results from net erosion. In addition, distinction has been made between the flood and ebb channel. In Figure 4.15 the total volume change over four years has been averaged, to arrive at an annual-averaged change. The bars around the data points represent the standard deviation of the yearly variation for the considered four-year period.

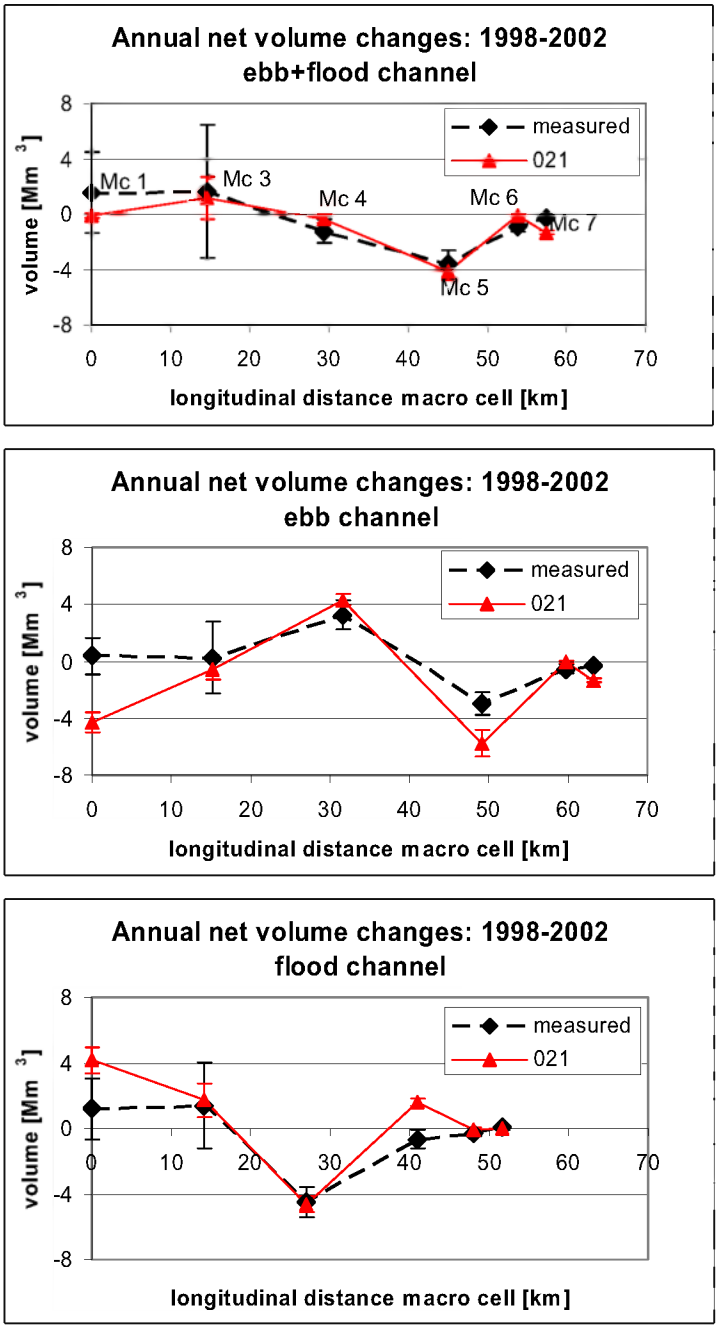

Figure 4.15: Annual net volume changes of sediment for the period 1998-2002 (4 years) for the macro cells (top panel), ebb channels (centre panel) and flood channels (lower panel). Macro cells are indicated by Mc 1 for macro cell 1, etc.

Figure 4.15 shows that the morphological model reproduces the magnitude and longitudinal variation of the observed net volume changes of the channels and macro cells, if averaged over a four year period. In the ebb channel of macro cell 1 (x ≈ 0 km) the model predicts significant net erosion, whereas a minor net deposition has been observed. In the flood channel of this macro cell deposition is overestimated by the model. In the ebb channel of macro cell 5 (x ≈ 50 km) erosion is overestimated. In the flood channel (x ≈ 40 km) the

model predicts net deposition, whereas the observation shows slight erosion. If the ebb and flood channels are aggregated per macro cell the computational results agree well with the observations.

If the observed and computed net volume changes of the ebb and flood channels of the macro cells are compared, the slope of the regression line (see Eq. 4.1) through the data points amounts to 1.29 with a regression coefficient r^2 of 0.63. This indicates, that computed yearly net volume changes are approximately 30% larger than observed changes.

Area changes per depth class

Area changes per depth class for the Western Scheldt are given in Figure 4.16. Qualitatively, the results are similar to those of the sensitivity runs 007-019: the areas for depths < -20 m NAP and > -5 m NAP become larger, and the area for depths in between becomes smaller, thus indicating a steepening of the bathymetry. The computed area changes, averaged over four years, are less than for the one year simulations and consequently differences with the observations reduce.

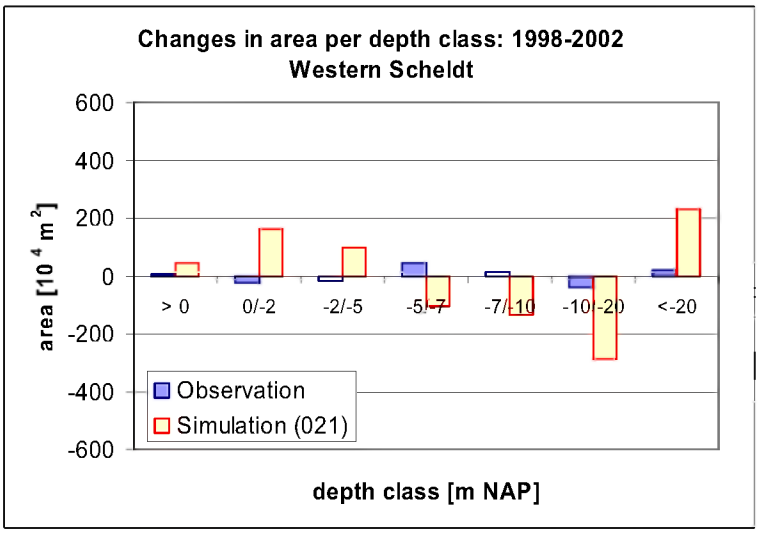

Figure 4.16: Observed and computed area changes for the Western Scheldt (ebb and flood channels). Averaged over the period 1998-2002.

The increase in the slope of the model bathymetry, relative to the measured bathymetry, can also be shown by plotting the wet area as a function of the water depth for the years 1998 and 2002. This is shown in Figure 4.17 for the whole Western Scheldt. These figures again illustrate that in the model the deeper channels erode too much while too much sedimentation occurs above approximately NAP-10 m.

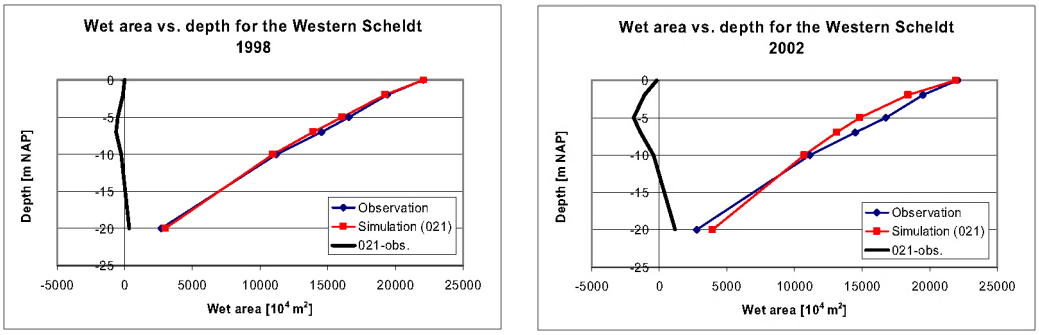

Figure 4.17: Measured and computed wet areas as a function of depth (below NAP) for 1998 and 2002.

Dredge volumes

Figure 4.18 compares the total measured and computed annual dredging volumes. Measured volumes are converted with a factor 0.9 to 'in situ cubic metre' to compare correctly with the model results.

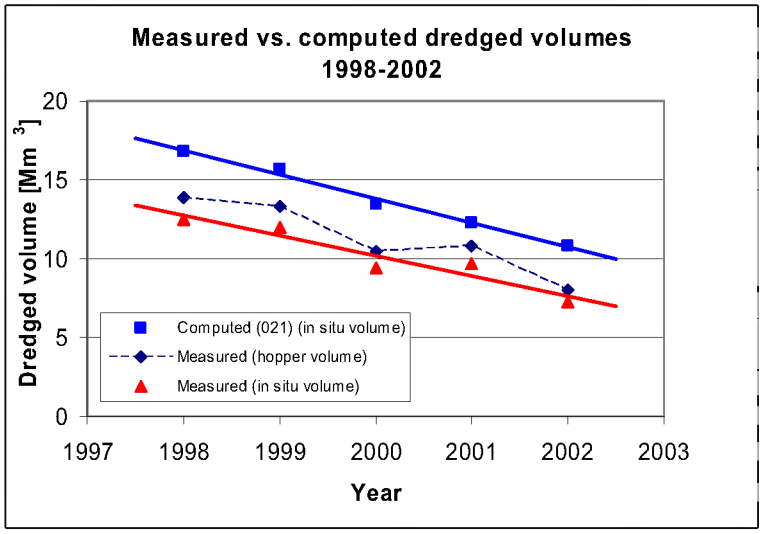

Figure 4.18: Measured and computed total dredge volumes for the period 1998-2002.

The figure shows that the model correctly predicts the decrease in dredging volume for the period 1998-2002, although the magnitude is 15-30% too large. Computed dredge volumes are 2.6 to 4.3 Mm^3 overestimated (on average 3.6 Mm^3), which is mainly due to the overestimation of the dredging at the Drempel van Hansweert.

Net sediment transport

Sediment transport is given by the model as the sediment volume per unit of time. In sand balance studies for the Western Scheldt the derived transports include the volume occupied by the pores. Therefore the computed net sediment transport by the model is converted by the multiplication of the computed transport with a factor *1/(1-n)*, where *n* is the porosity

(assumed to be 0.4). For all years the model predicts an annual net sediment *import*, which gradually decreases from 1.9 to 0.6 Mm^3 (excluding the pores) or 3.2 to 1.0 Mm^3 (including the pores) with an average import of 2.0 Mm^3 (including pores). From the sand balance for the period 1997-2001 a net annual sediment *export* from the Western Scheldt to the ebb tidal delta of 1.9 Mm^3 follows (including pores). In the latter case it is assumed, that the net sediment transport at the landward boundary is nil. If the model results are corrected such that no net transport is present at the landward boundary, then an average net import at the seaward boundary of 2.2 Mm^3 results (including pores).

Figure 4.19 presents the computed net sediment transport in all cross-sections in comparison with those from the sand balance studies (Nederbragt and Liek, 2004). Also indicated are the macro cell numbers, as enclosed by the cross-sections. The figure shows that, according to observations, the Western Scheldt is exporting in the seaward sections (1.9 Mm^3/year in the estuary mouth), whereas the transport is in landward direction in the eastern region. The model simulation results in a landward directed sediment transport for all sections with a magnitude that gradually decreases. Near the line Vlissingen-Breskens the net import amounts to 2.0 Mm^3/year.

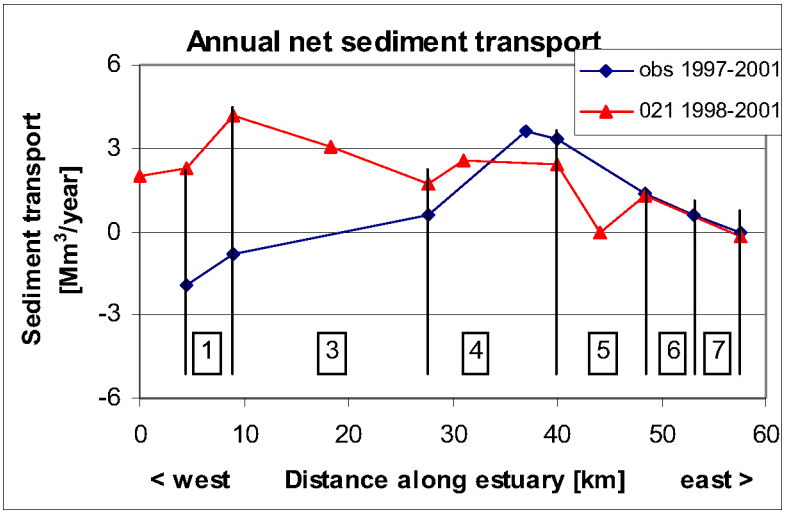

Figure 4.19: Annual-averaged net sediment transport along the Western Scheldt estuary for the period 1997-2001 (observations) and 1998-2001 (simulation) (landward = +; seaward = -). Computed transports are converted to volumes incl. pores, assuming a porosity of 0.4. Macro cells are indicated with numbers.

4.3.2 1960-1966

Sedimentation and erosion

The erosion and sedimentation pattern, as averaged over the period 1960-1966, is given in Figure 4.20. Similar to the first calibration period (1998-2002) the magnitude of erosion and sedimentation, as computed by the model, is too large. Similarities between observations and model results, in a qualitative sense, are erosion of the the ebb channels Pas van Rilland, Nauw van Bath, Overloop van Valkenisse, Bocht van Walsoorden/Zuidergat, Overloop van

Hansweert and of the flood channels Gat van Ossenisse and Everingen (see Figure 2.1 for names of the channels). A major discrepancy is again the computed large erosion of the ebb channel Honte, south of Vlissingen and the sedimentation in the adjacent area. The latter is probably the result of the aforementioned erosion of the Honte. Furthermore, in the dumping areas in the eastern region of the Western Scheldt significant deposition is shown by the model, which does not follow from observations. It indicates that the dredging-dumping functionality should be further optimised.

Net sediment volume changes

Net annual-averaged volume changes of the macro cells (ebb + flood channels) during period 1960-1966 are given in Figure 4.21. Compared to the period 1998-2002 macro cells 1 and 3 show a decrease of the sediment volume (net erosion) instead of an increase. This is correctly reproduced by the model (run 030). The ebb channel shows larger differences between observations and simulation, i.e. in macro cells 4 and 5 net erosion is predicted, whereas net deposition (macro cell 4) or no change (macro cell 5) follows from the observations. Jeuken (2000) found, that with a lower d_{50} the reproduction of the net volume changes of the ebb channel in macro cell 4 could be improved. For the flood channel erosion in macro cells 3 and 4 is underestimated and deposition in macro cell 5 is overestimated.

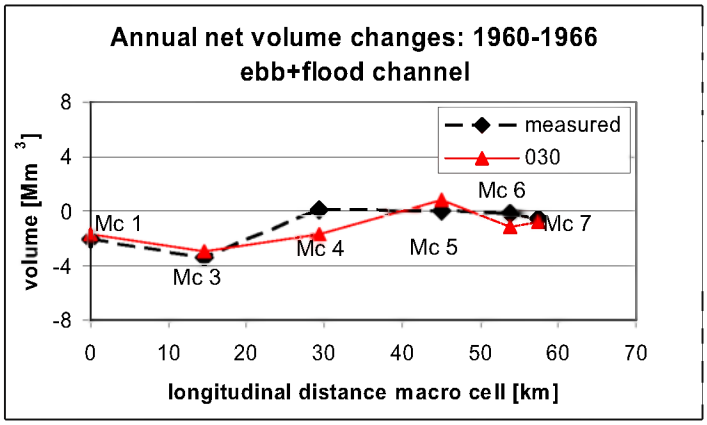

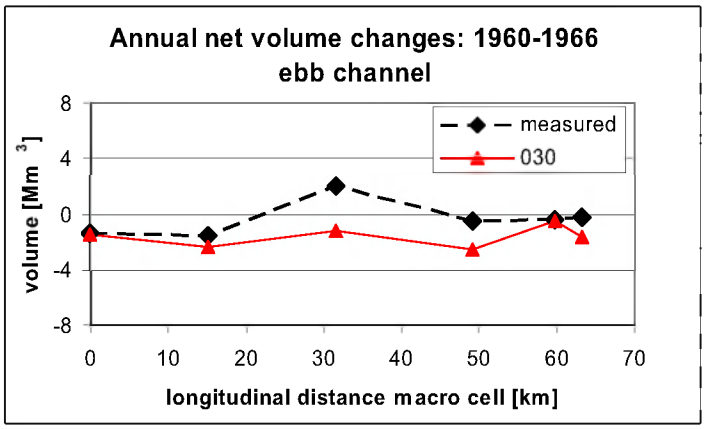

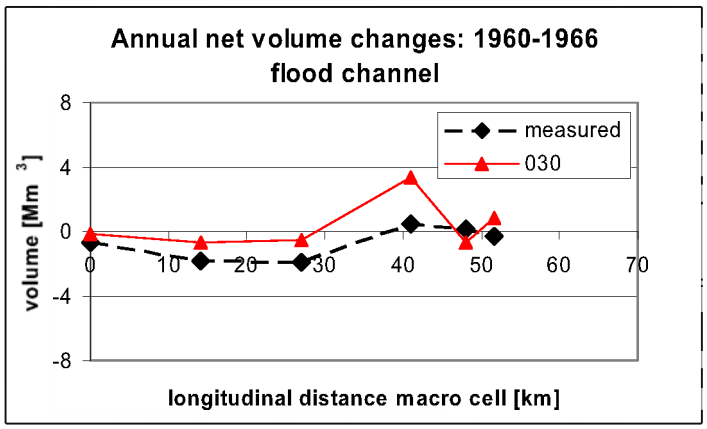

Figure 4.21: Annual net volume changes of sediment for the period 1960-1966 (6 years) for the macro cells (top panel), ebb channels (centre panel) and flood channels (lower panel). Macro cells are indicated by Mc 1 for macro cell 1, etc.

Area changes per depth class

In Figure 4.22 measured and computed areas for various depth classes in the Western Scheldt are compared. The depth classes, in metres relative to NAP, are: [> 0], [0, -2], [-2, -5], [-5, -7], [-7, -10], [-10, -20] and [<-20].

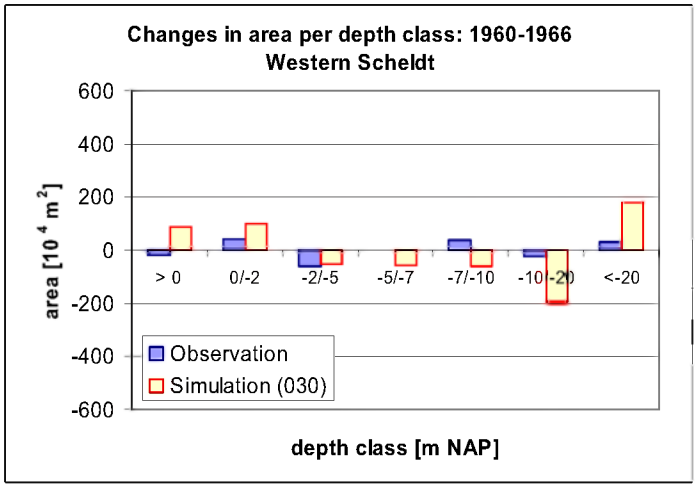

Figure 4.22: Average annual changes of areas per depth class during the period 1960-1966 (6 years) for the Western Scheldt.

The results of the simulation are, qualitatively, comparable with those for the period 1998-2002. The deepest channels (< -20 m NAP) increase in area to a larger extent than according to observations. This is also true for the depth classes > -5 m NAP, while for the intermediate depths, between -5 m NAP and -20 m NAP, the area decreases. The hypsometric curves (areas versus depths) are given in 4.23 for the years 1960 and 1966. Similar to the period 1998-2002 a steepening of the bathymetry is clearly visible.

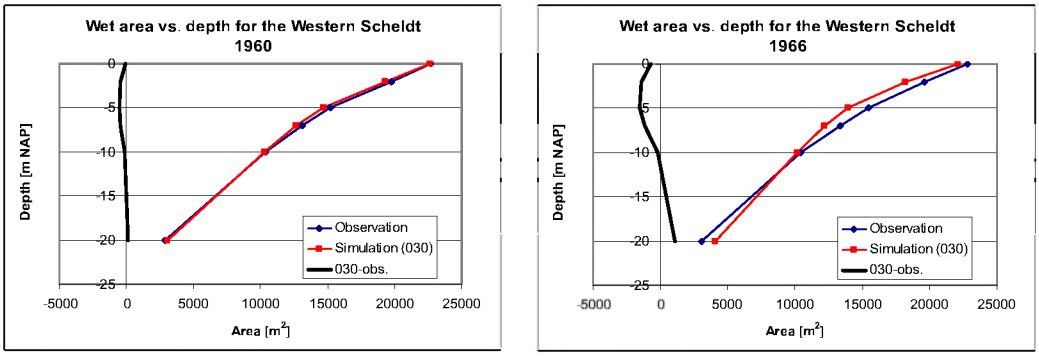

Figure 4.23: Measured and computed wet areas as a function of depth (below NAP) for 1960 and 1966.

Dredge volumes

Figure 4.24 compares the total measured and computed annual dredging volumes. Measured volumes are converted to in situ cubic metres to compare correctly with the model results.

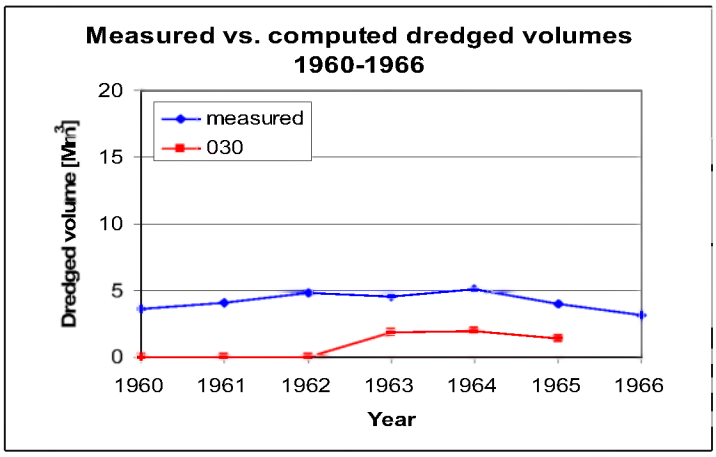

Figure 4.24: Measured and predicted total dredge volumes for the period 1960-1966.

Figure 4.24 shows that dredge volumes are underestimated by the model. Apparently, during 1960-1962 the bed level has not reached above the minimum required depth, so that no dredging is computed by the model.

Net sediment transport

The observed and computed residual sediment transport in a number of cross-sections is given in Figure 4.25.

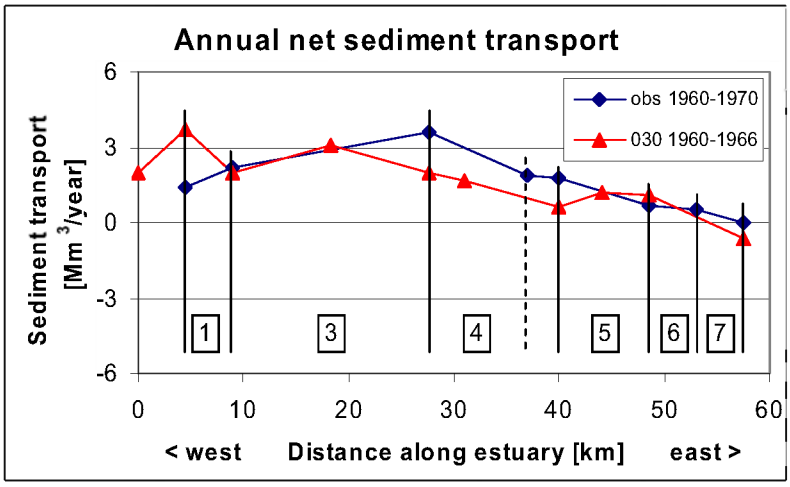

Figure 4.25: Annual-averaged net sediment transport along the Western Scheldt estuary for the period 1960-1970 (observations) and 1960-1966 (simulation) (landward = +; seaward = -). Computed transports are converted to volumes incl. pores, assuming a porosity of 0.4. Macro cells are indicated with numbers.

For all years the model predicts an annual net sediment *import* at the seaward boundary, which gradually decreases from 2.0 to 0.8 Mm^3 (excluding the pores) or 3.3 to 1.3 Mm^3 (including the pores), with an average import of 2.0 Mm^3 from the Voordelta and an average annual import of 0.7 Mm^3 at the Dutch-Belgium border (both including the pores). From the sand balance for the period 1960-1970, see Nederbragt and Liek (2004), a net annual sediment *import* of 1.4 Mm^3 follows (including the pores). In the latter case it is assumed, that the net sediment transport at the landward boundary is nil. If the model results are corrected so that there is no net transport at the landward boundary, then an average net import at the seaward boundary of 2.7 Mm^3 results, which is 1.3 Mm^3 larger than observed.

4.4 Improvement of 2D-morphology

Both calibration runs show, that the computed bathymetry has become steeper at the end of the simulation period. Apparently, the transverse sediment transport (i.e. perpendicular to the main flow direction) from the shallow areas to the channels is too small in the model. Possibly, some physical processes such as geotechnical instabilities and breaching play a role in nature. These processes are not accounted for by the model; however their effect can be investigated by enhancing the transverse bed slope coefficient. A first tentative run, similar to run 007 but with a transverse bed slope coefficient turned up from 1.5 to 50, has been carried out to assess the response of the system (run 023). Results are briefly discussed hereafter.

Net sediment volume changes

Computed net volume changes of run 023 are not very much different from the reference run 007. This is shown in Figure 4.26.

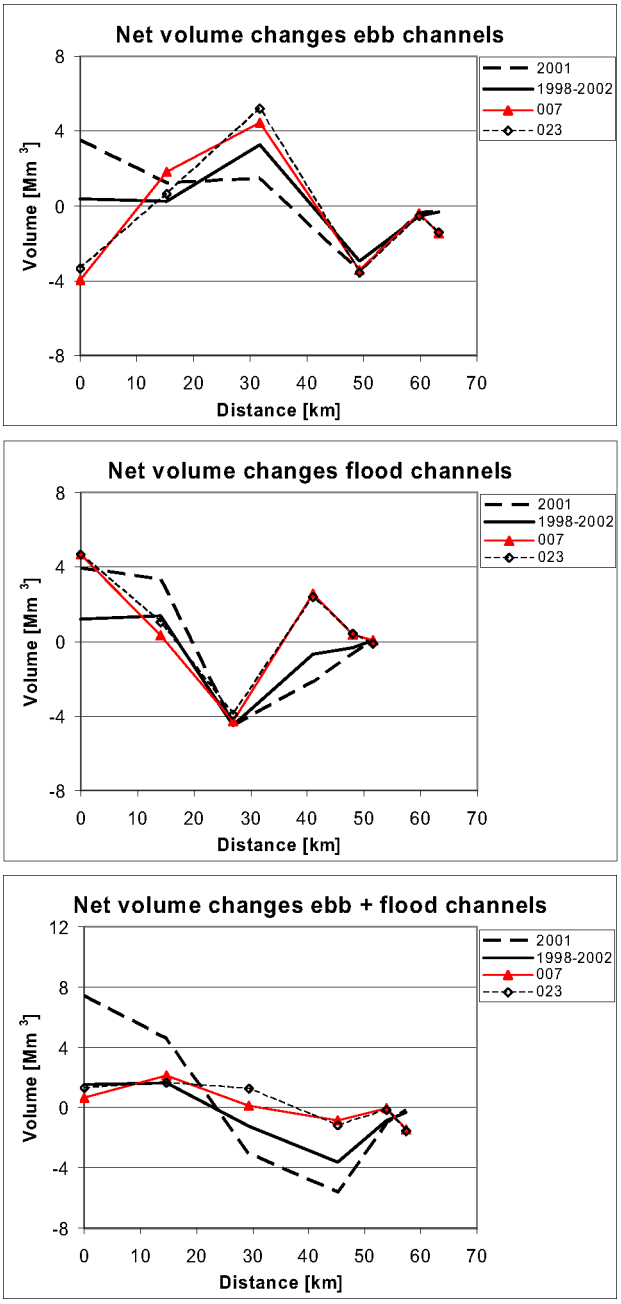

Figure 4.26: Computed and observed net volume changes of the ebb and flood channels of the macro cells. Run 023 versus run 007 and observations.

Area changes per depth class

The area changes for the seven depth classes are presented in Figure 4.27, showing that results improve. This is mainly achieved for the depth classes [-10, -20 m NAP] and [<-20 m NAP]. Results are also shown for some combined depth classes to investigate if results improve at a higher aggregation level. If only three depth classes are considered (> 0 m

NAP, < -10 m NAP and depths in between) model results qualitatively and quantitatively follow observed area changes.

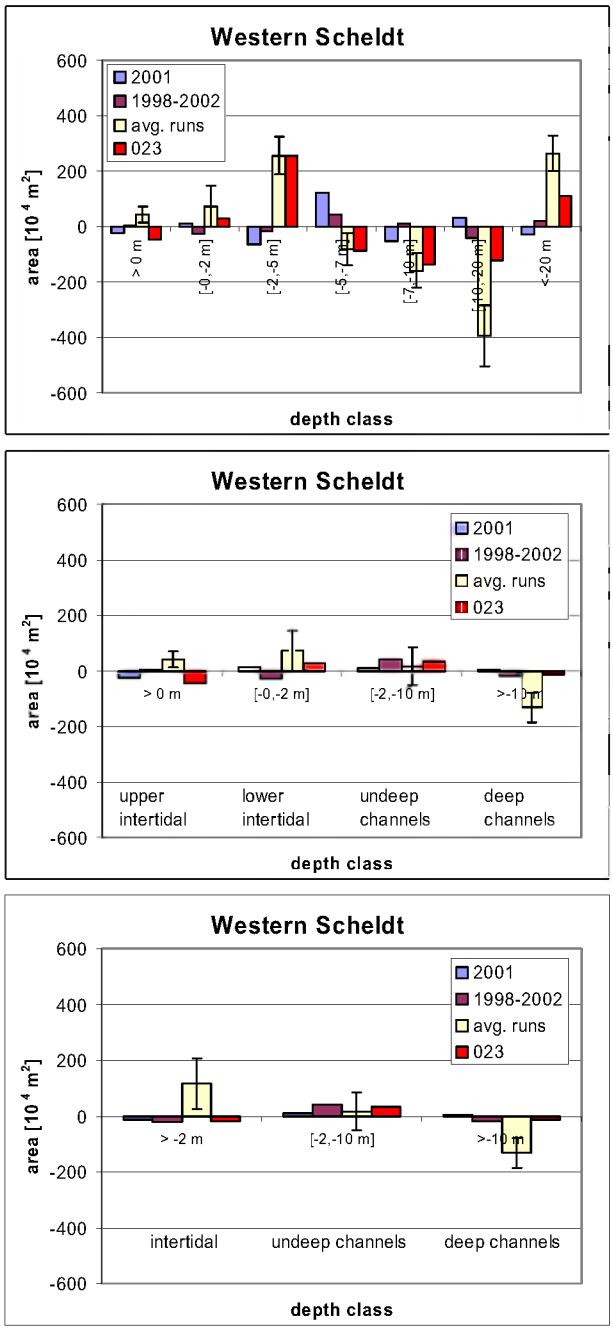

Figure 4.27: Average annual changes of areas per depth class for the Western Scheldt (Run 023).

Dredge volumes

The total dredge volume for 2001 amounts to 9.5 Mm^3, which is 10% less than for run 007 but still close to the observed value of 10.5 Mm^3.

Net sediment transport

The longitudinal variation of the net sediment transport is given in Figure 4.28, showing that the net sediment transport in the upper estuary is now reproduced rather good. In the western region differences between observations and simulation remain large, apparently due to a different sand balance for macro cell 3.

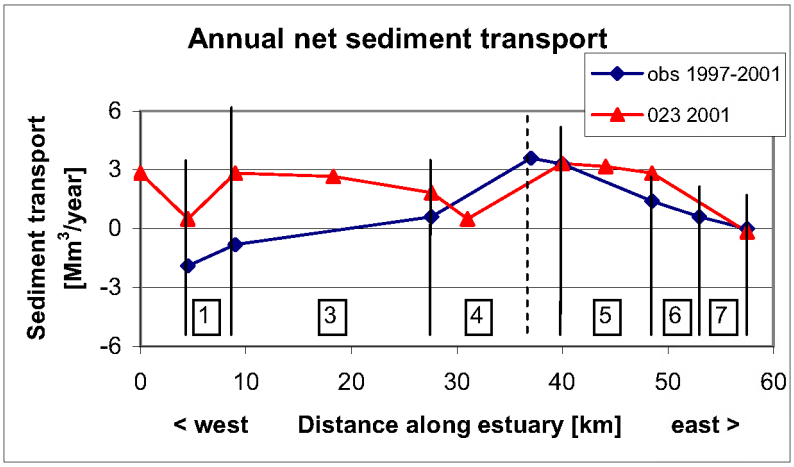

Figure 4.28: Annual-averaged net sediment transport along the Western Scheldt estuary for the period 1997-2001 (observations) and 2001 (simulation) (landward = +; seaward = -). Computed transports are converted to volumes incl. pores, assuming a porosity of 0.4. Macro cells are indicated with numbers.

Summarising, run 023, with an increased transverse bed slope coefficient, results in an improvement of the reproduction of the net area changes, while results for the other output parameters do not significantly change. The results for a four year run, as part of the sensitivity run for 1998-2002, will be discussed in the next section.

4.5 Sensitivity runs for 1998-2002

The purpose of the simulations, as discussed in this section, is to further investigate the sensitivity of the model results for different parameter settings of the model. This is done for the period 1998-2002 so that average observed changes and average computed changes are compared for the same period. In this way erratic fluctuations due to natural variation and measurement inaccuracies can be eliminated to some extent. The calibration run 021 is used as a reference with which the outcomes of the sensitivity runs are compared. These differences will be used in Chapter 5 to assess the broad range around model predictions. The sensitivity runs for 1998-2002 are summarised in Table 4.3, showing which parameter has been changed relative to run 021.

Run	Description
041	Phase shift of the quarterly tidal component (M_4) at the sea boundary.
042	Further increase of the transverse bed slope effect (= 100).
043	Decrease of the roughness parameter for the sediment transport.
044	Increase of the roughness parameter for the sediment transport.
045	Space-varying grain size diameter.
046	Application of the Bijker transport formula.

Table 4.3: Sensitivity runs for the period 1998-2002.

From the calibration of the hydrodynamic model (see Section 3.2) it followed, that a phase difference for the M_4 tidal component is present in the estuary compared to observations. Because it is believed, that the phase difference $2\varphi_2-\varphi_4$ between the semi-diurnal and quarterly-diurnal tidal component affects the morphology of the estuary, φ_4 is increased with 10 degrees (run 041). The transverse bed slope coefficient is increased from 1.5 (run 021) to 100 (run 042) to improve the reproduction of the area changes for the considered depth classes. The purpose of this significant increase is to account for processes such as bed instabilities and breaching, which are not represented by the model formulations. In run 021 the roughness parameter in the sediment transport formula is derived from the hydraulic roughness. It is possible to prescribe a roughness for the sediment transport, which is different from the hydraulic roughness. This is done with runs 043 and 044, with a roughness (k_s) value of 0.01 m and 0.20 m respectively. For run 045 a space-varying grain size diameter is applied, similar to run 011 as part of the sensitivity simulations (see Section 4.2). The grain size decreases from 200 μm in the western region to 150 μm in the east. From the sensitivity runs it further followed, that the type of sediment transport formula (van Rijn, Engelund Hansen, Ackers-White) largely determines the model results. Run 046 employs the Bijker transport formula. Results of the sensitivity runs are briefly discussed hereafter and will be further used in Chapter 5 for the broad range analysis.

Net sediment volume changes

Net volume changes, following from the sensitivity runs 041-046, are shown in Figure 4.29.

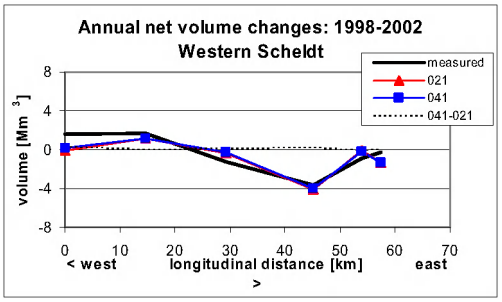

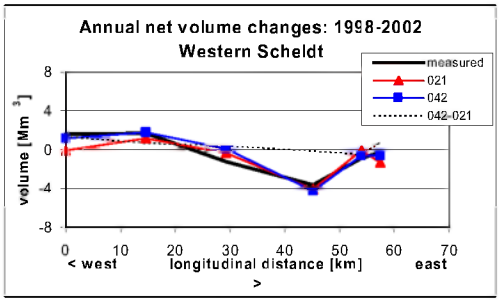

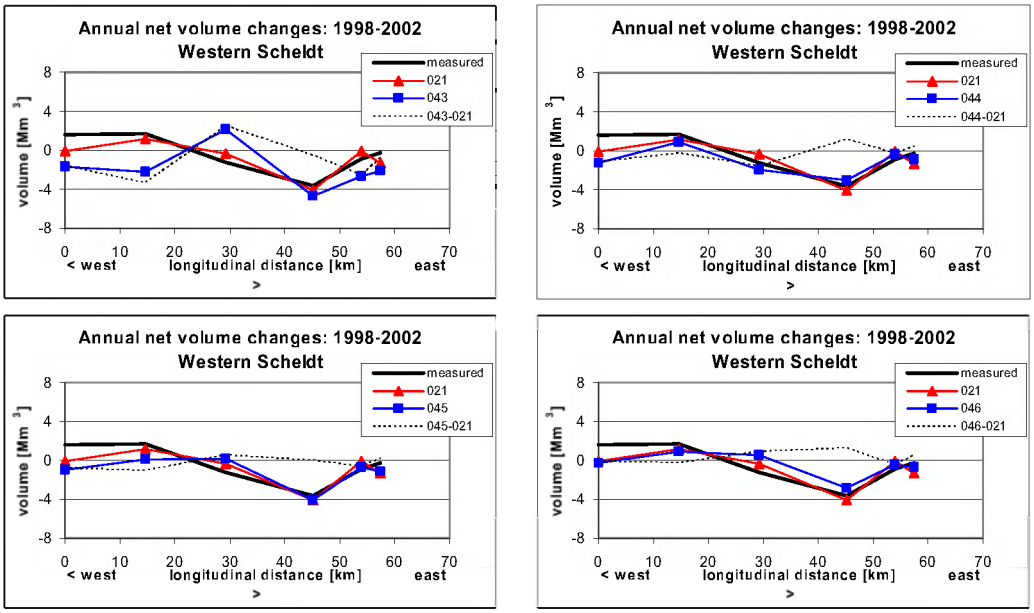

Figure 4.29: Computed and observed net volume changes of the macro cells. The dotted line indicates differences with reference run 021.

Apart from run 043 (decreased roughness) all sensitivity runs give comparable results with run 021. Comparison of the net volume changes of ebb and flood channels separately with observations according to Eq. (4.2) gives slopes and regression coefficients as presented in the table below.

Run	Slope b [-]	r^2 [-]
021 (ref.)	1.29	0.63
041	1.32	0.66
042	1.30	0.53
043	1.29	0.50
044	0.83	0.50
045	1.24	0.60
046	0.74	0.78

Table 4.4: Slope b of the regression line and regression coefficient of computed versus observed net volume changes (1998-2002) for the sensitivity runs.

Computed net volume changes of the ebb and flood channels, as denoted by the slope *b*, are 30% larger or smaller than observed. Regression coefficients vary between 0.5 and 0.8 with the largest value for the run with the Bijker transport formula.

Area changes per depth class

Results of the area changes per depth class are presented in Figure 4.30 showing that run 042 performs best for the depth classes [-10, -20 m NAP] and [< -20 m NAP]. For depth classes > -10 m NAP run 042 is comparable to or slightly better than the other sensitivity runs.

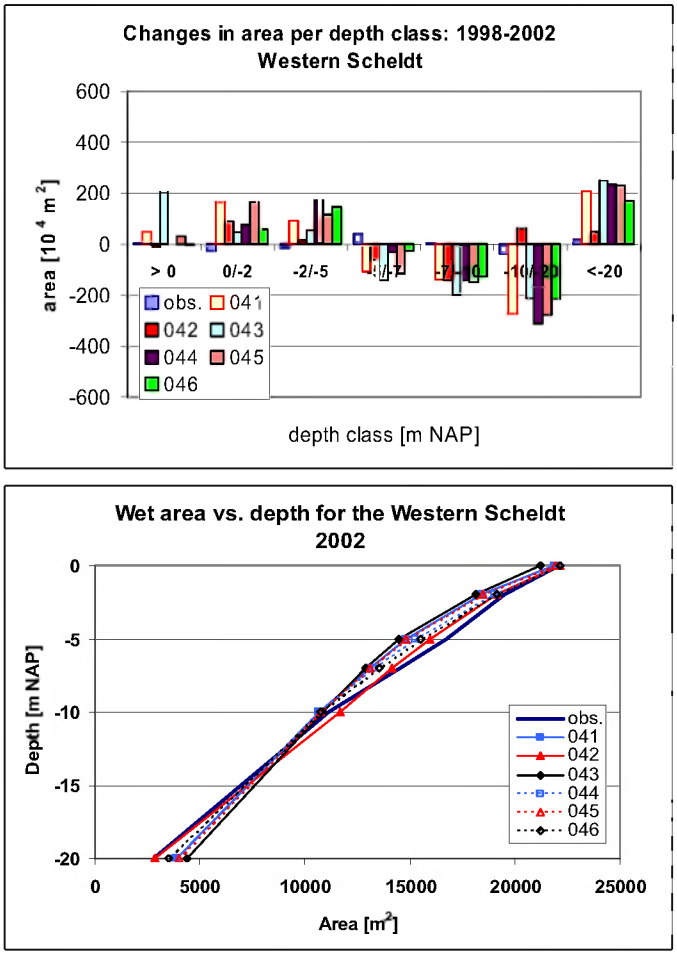

Figure 4.30: Average annual changes of areas per depth class during the period 1998-2002 (4 years) for the Western Scheldt (upper panel) and hypsometric curves (lower panel).

Dredge volumes

Computed total average dredge volumes for the period 1998-2002 are 20% lower or 50% higher than observed dredge volumes for runs 041, 042 and 044 to 046. For run 043 computed values are more than 100% larger than observed, see Figure 4.31.

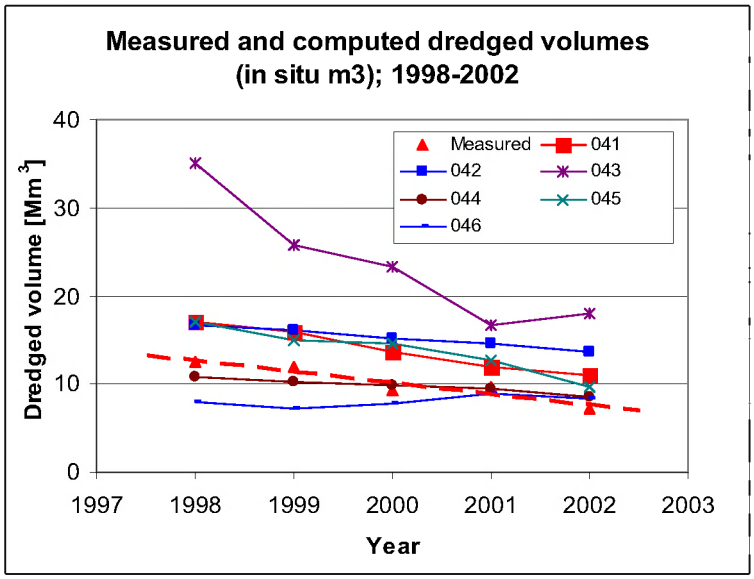

Figure 4.31: Measured and computed total dredge volumes for the period 1998-2002.

Net sediment transport

The net sediment transport through c.s. 1 (see Figure 4.12a) for the sensitivity runs 042-046 is given in Table 4.5, indicating that the computed net sediment import varies between 0.6 and 2.0 Mm^3/year.

run 042	run 043	run 044	run 045	run 046
0.6	1.7	1.4	2.0	0.7

Table 4.5: Net annual sediment transport [Mm^3/year] during 1998-2002 through cross-section 1 (see Figure 4.12a) for sensitivity runs 042-046.

4.6 Final calibration

Run 042, with the coefficient for the transverse bed slope effect increased to 100, appears to give better results regarding the area changes for the channels (deeper than -10 m NAP). As such it is decided that the parameter setting of run 042 represents the final calibration, which will be used for the verification run for the period 1970-1985 (see Chapter 6). The results of run 042, compared to observations and run 021, will be presented hereafter in more detail.

Sedimentation and erosion

The sedimentation and erosion pattern is shown in Figure 4.32. It resembles to a large extent the pattern of run 021, although locally differences can be observed.

Net sediment volume changes

Net volume changes of the macro cells are presented in Figure 4.33. The erosion of the ebb channel and the deposition of the flood channel of macro cell 3 have slightly increased. Net

deposition in the flood channel of macro cell 1 has also become larger. For the total of ebb and flood channels the result is almost similar to run 021.

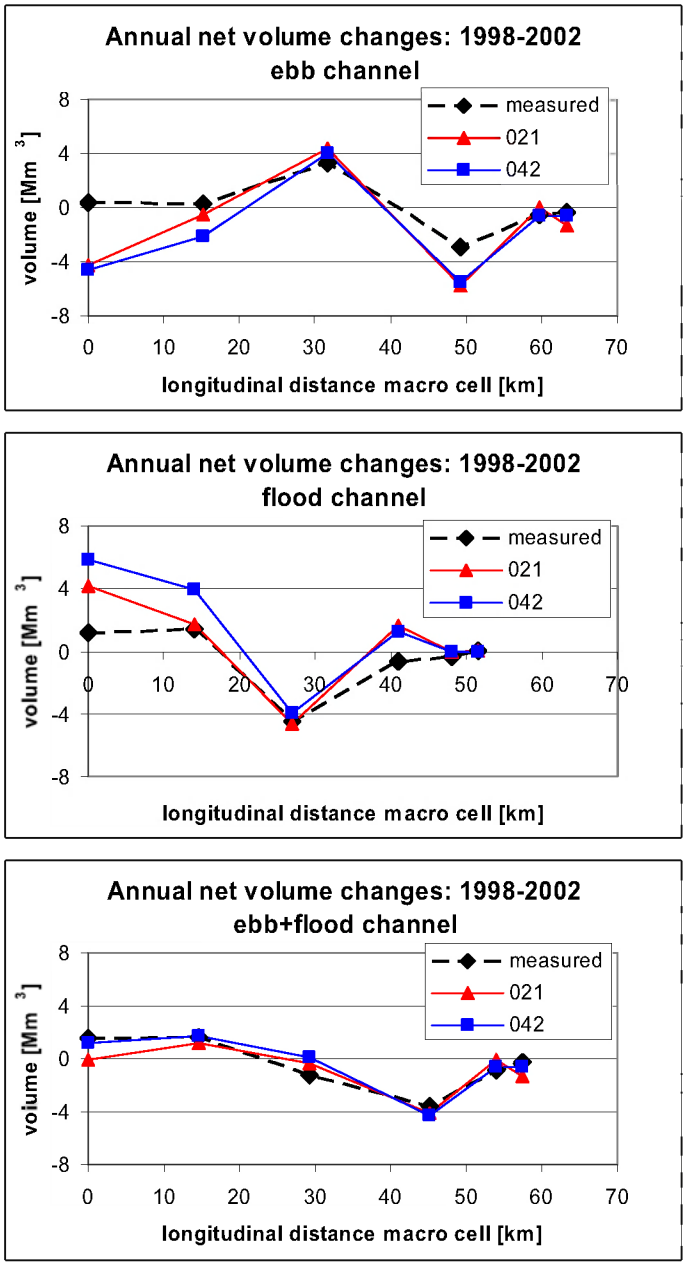

Figure 4.33: Computed and observed net volume changes of the ebb and flood channels of the macro cells. Run 042 versus run 021 and observations.

Computed yearly net volume changes are approximately 30% larger than the observed changes; see the slope of the regression line for run 042 in Table 4.4.

Area changes per depth class

Results for the area changes are shown in Figure 4.34 for the original seven depth classes as well as for some combined classes. In Figure 4.35 the hypsometric curves are presented for 1998 and 2002. Comparison with run 021 learns, that the 2D-morphology has improved, although further optimisation is required.

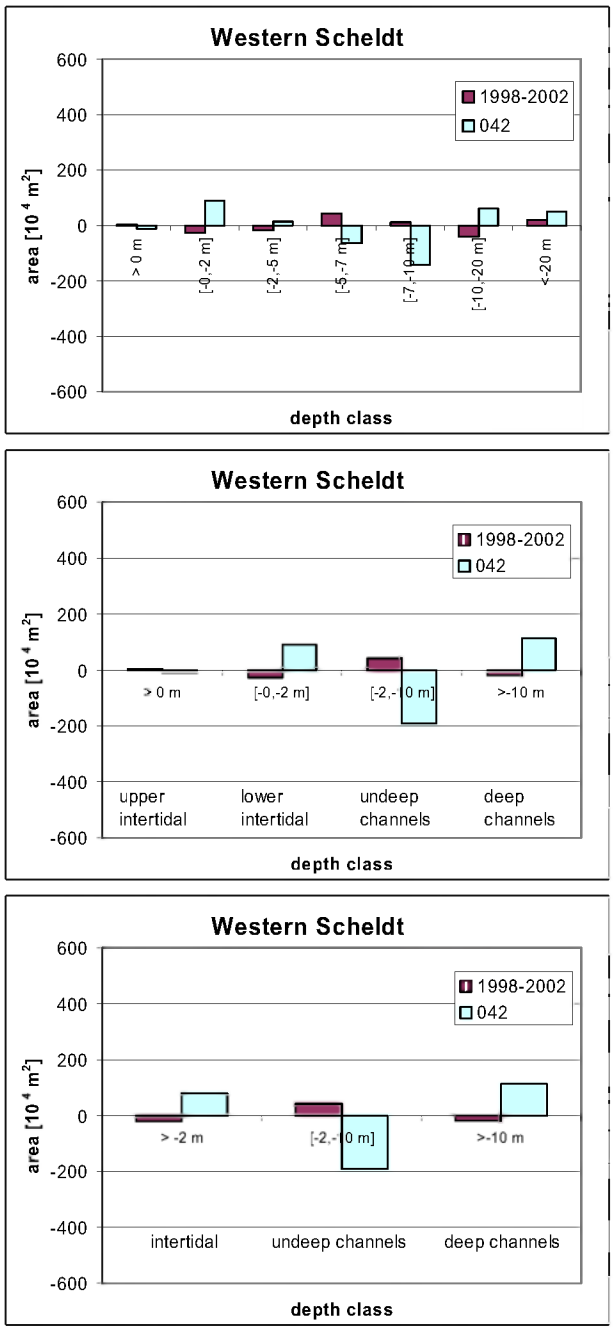

Figure 4.34: Average annual changes of areas per depth class during the period 1998-2002 (4 years) for the Western Scheldt for three combinations of depth classes.

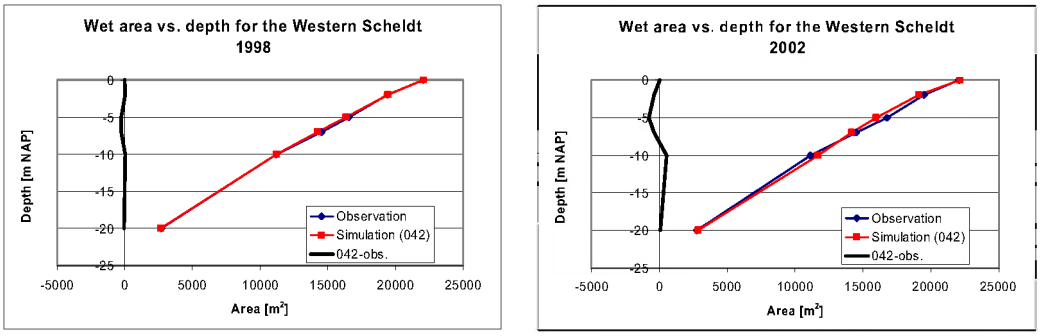

Figure 4.35: Measured and computed wet areas as a function of depth (below NAP) for 1998 and 2002.

Dredge volumes

The average total dredge volume of run 042 (15.2 Mm^3) is approximately 50% larger than observed (10.2 Mm^3) and 10% larger than for run 021 (13.8 Mm^3), see Figure 4.36.

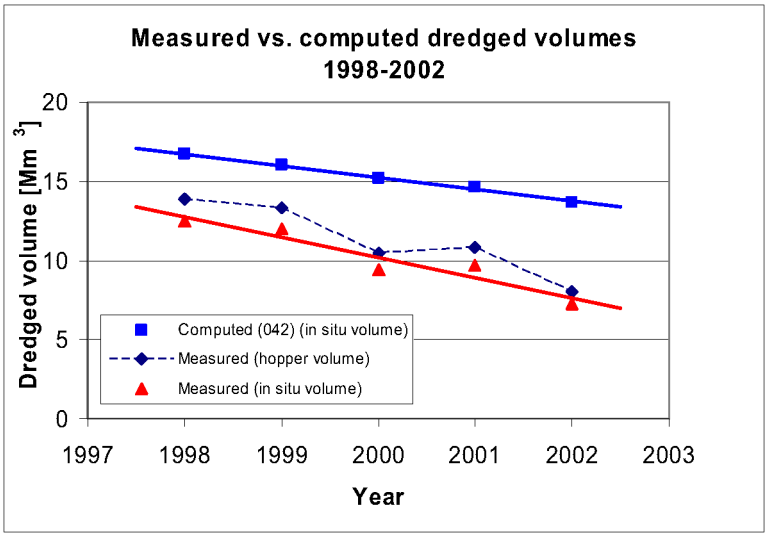

Figure 4.36: Measured and computed total dredge volumes (run 042) for the period 1998-2002.

Net sediment transport

The longitudinal variation of the net sediment transport is given in Figure 4.37. It is remarkable that, compared with the calibration run 021, the decrease in net sediment transport in macro cell 5 has now disappeared. The reproduction in macro cells 4, 5, 6 and 7 is good; large differences occur in macro cell 3, where the observed net sediment transport changes direction, whereas the computed transports are all in landward direction.

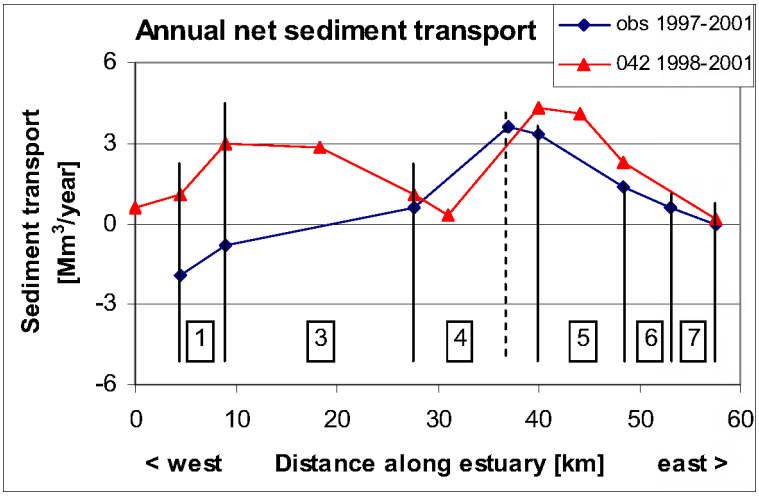

Figure 4.37: Annual-averaged net sediment transport along the Western Scheldt estuary for the period 1997-2001 (observations) and 1998-2001 (simulation) (landward = +; seaward = -). Computed transport is converted to volume incl. pores, assuming a porosity of 0.4. Macro cells are indicated with numbers.

The net sediment transport in the estuary mouth gradually decreases from an import of 2.0 Mm^3 in 1998 to a small export of 0.2 Mm^3 in 2001, see Table 4.6:

1998	1999	2000	2001	avg. 1998-2002
2.0 Mm^3/yr	0.7 Mm^3/yr	0.0 Mm^3/yr	-0.2 Mm^3/yr	0.6 Mm^3/yr

Table 4.6: Net sediment transport through the estuary mouth (+: landward, -: seaward).

4.7 3D-effects

To further investigate three-dimensional effects two additional, three-dimensional simulations are carried out:

1. A three-dimensional simulation *without* taking into account the effect of salinity gradients on the hydrodynamics;
2. A three-dimensional simulation *including* the effect of salinity gradients on the hydrodynamics.

Both 3D-simulations are carried out with 10 non-equidistant layers with the smallest layer thickness near the bed.

The objective of the aforementioned simulations is to assess: (i) the effect of 3D versus 2Dh (depth-averaged) modelling of the morphodynamics and (ii) the effect of density differences due to salinity gradients on the reproduction of the morphological changes of the Western Scheldt.

The transverse bed slope coefficient is set at 100 for both runs. The river discharge represents average conditions, so that the computed salinities (for the second simulation) follow a realistic distribution. The simulations require a number of additional computer runs:

- To obtain a salinity distribution which is in dynamic equilibrium with the tidal forcing and river discharge (spin-up of salinity modelling);
- To assess the proper dispersion coefficient in order to arrive at tidal salinity variations near Waarde between 18 and 22 ppt.

Two simulations (2Dh) over a period of 6 months are carried out to asses the dispersion coefficient D: run 060 with D = 50 m^2/s en run 061 with D = 250 m^2/s, both with a river discharge of 130 m^3/s. The latter results in a salinity variation between 17 and 25 ppt in 'Walsoorden', 'Baalhoek' and 'Schaar v.d. Noord', which is considered realistic for normal conditions. The salinity distribution for run 061 reaches a dynamic equilibrium after approximately 3 months; it is used as the initial condition for the salinity field of the subsequent 3D simulation (run 063). As part of run 063 four tides (in total 50 hours) are used for further adaptation of the salinity field. Following this 3D adaptation time, the morphological update of the bed is activated.

All other parameters are set equal to that of run 042. However, it appeared that neither the 3D run with salinity effects (inhomogeneous) nor the 3D run without salinity effects (homogeneous) could be run in combination with waves. The exact cause is yet unknown and should be further investigated. Therefore both run 063 and run 065 are performed without waves. In order to compare properly with a 2Dh simulation without waves, run 042 is repeated but without waves (run 066). Similar to run 042 the transverse bed slope coefficient is set at 100.

In a 3D-computation, the vertical exchange of momentum and matter (salinity/sand) is computed by the turbulence closure scheme. Various options exist ranging from relatively simple algebraic formulations to the more advanced k-ε model. This latter model solves 2 additional equations for the transport of turbulent kinetic energy (k) and turbulent energy dissipation (ε). In general, the salinity intrusion into an estuary is best modelled by applying the k-ε turbulence closure scheme. However, the Western Scheldt estuary is a well mixed estuary, whereas the benefits of the k-ε model mainly relate to (highly) stratified estuaries. The effect of the selected turbulence model, either algebraic or k-ε, is investigated by means of an additional simulation (run 063k) employing the k-ε turbulence model. For run 063 and run 065 the algebraic turbulence model is used.

All simulations are summarised in Table 4.7. It is noted that the 3D-simulations are only for a period of one year, i.e. 1998, to limit computing time. The year 1998 was selected for comparison of 3D with 2D results. In that case all simulations are preceded by one year for the spinning-up of the morphological model (run 066 is for the period 1998-2002, although results are presented only for the year 1998). The results of the simulations are described hereafter.

Run	Description
060	• 2Dh • 6 months for adaptation of the salinity distribution • D = 50 m^2/s
061	As run 060 with D = 250 m^2/s.
063	• 3D; 10 non-equidistant computational layers. • Inhomogeneous (i.e. *with* salt) with morphology • Initial salinity distribution of run 061 • Period: 1998 preceded by 1 year adaptation of morphology
063k	As run 063 with the k-ε turbulence model.
065	• 3D; 10 non-equidistant computational layers. • homogeneous (i.e. *without* salt) with morphology • Period: 1998 preceded by 1 year adaptation of morphology
066	• 2Dh, homogeneous with morphology • = run 042 without waves • Period: 1998-2002 preceded by 1 year adaptation of morphology

Table 4.7: Simulations with DELFT3D to investigate 3D-effects.

Sedimentation and erosion

The erosion-sedimentation patterns of the simulations for the year 1998 are given in Figure 4.38 for run 066 and run 065 and in Figure 4.39 for run 063 and 063k. Observations have been averaged for the period 1998-2002. The following observations are made:

- Both 3D-simulations show more pronounced (i.e. larger) erosion and sedimentation than the 2Dh-simulation.
- Individual 'patches' with erosion or sedimentation, as present for the 2Dh-simulation, connect to larger areas for the 3D-simulations. However, the overall pattern following from the 3D-simulations is not significantly different from the 2Dh-simulation.
- The 3D-simulations without and with salt show almost similar sedimentation and erosion.

Net sediment volume changes

In Figure 4.40 net volume changes of the macro cells (total of ebb and flood channels) are presented for run 066 (2Dh), run 065 (3D, homogeneous), run 063 (3D, inhomogeneous) and of run 063k (3D, inhomogeneous, k-ε turbulence model). Observed volume changes are averaged values for the period 1998-2002; computed volume changes are only for the year 1998.

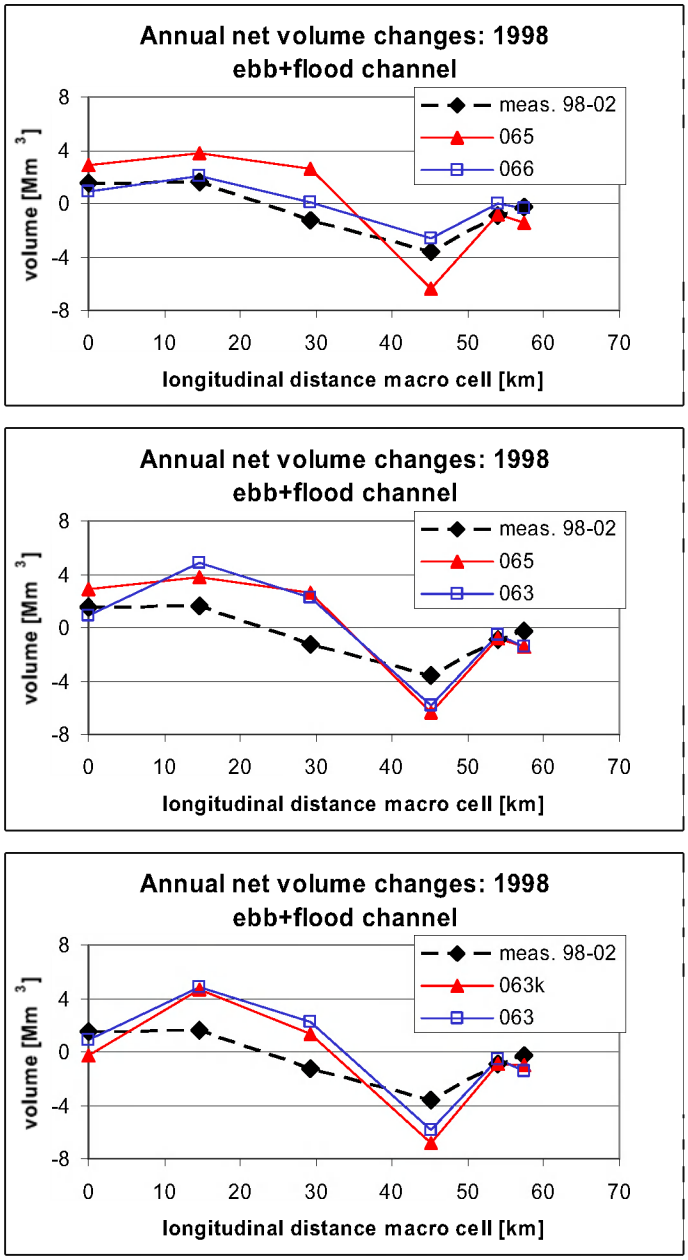

Figure 4.40: Computed and observed net volume changes of the ebb and flood channels of the macro cells for run 066, run 065, run063 and run 063k.

For the ebb and flood channels combined the 3D simulation (homogeneous: run 065) shows larger differences with the observations than the 2Dh-simulation (run 066). If the non-homogeneous 3D-simulation (run 063) is compared with the homogeneous 3D-simulation (run 065) it follows that differences between both runs are relatively small. This also holds for run 063 and run 063k.

Area changes per depth class

In Figure 4.41 computed changes in areas per depth class for the Western Scheldt are given for all simulations (run 66, run 065, run 063 and run063k). The computed results relate to changes over a one year period (1998). Observed area changes, averaged for the period 1998-2002, are also shown in Figure 4.41.

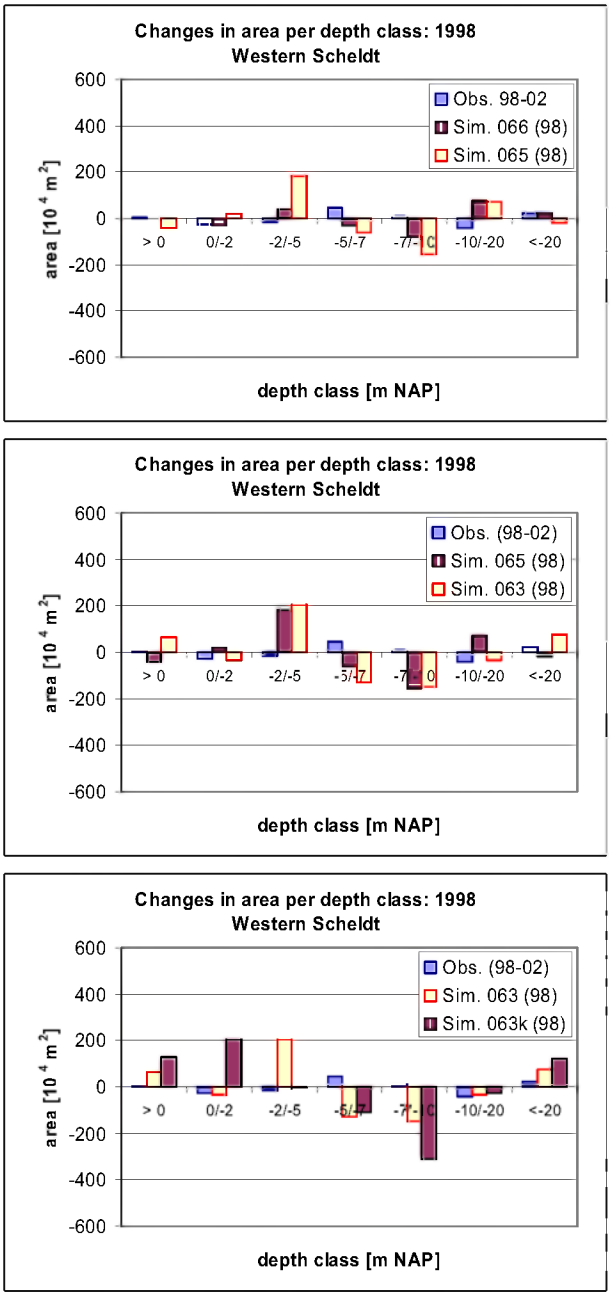

Figure 4.41: Average annual changes of areas per depth class during the period 1998-2002 (4 years) for run 066, run 065, run 063 and run 063k.

The area changes per depth class are affected by the number of spatial dimensions for the simulations (2Dh or 3D mode). For most depth classes differences between run 065 and observations are larger than between run 066 and observations. Comparison of both 3D runs (homogeneous and non-homogeneous) with observations indicates that for some depth classes run 065 performs better and in other cases run 063. Comparison of run 063 and run 063k with observations shows that generally run 063 performs better.

Dredge volumes

Computed total dredge volumes of the simulations are compared in Table 4.8.

Run	Total dredge volume [Mm^3]
Observations: 1998	13.9
Observations: averaged 1998-2002	9.7
066 (2Dh)	16.8 [1])
065 (3D, homogeneous)	21.0
063 (3D, inhomogeneous, algebraic turb. model)	24.7 [2])
063k (3D, inhomogeneous, k-ε turb. model)	30.4 [3])

Table 4.8: Measured and computed total dredge volumes.

[1]) For run 042 (= run 066 with waves) the total dredge volume for 1998 amounted to 16.7 Mm^3.

[2]) Dredge location 8 (Drempel van Hansweert): total dredge volume = 9.1 Mm^3 (observed: 3.4 Mm^3.

[3]) Dredge location 8 (Drempel van Hansweert): total dredge volume = 10.2 10^6 m^3.

The total dredge volume for run 066 (2Dh) is 21% larger than the total volume according to observations in 1998. The 3D-simulations result in a further increase of the total dredge volume with 50% (homogeneous), 80% (non-homogeneous) and 120% (k-ε).

Net sediment transport

The net sediment fluxes through a number of cross-sections are given in Figure 4.42. From the figures it follows that:

- The homogeneous 3D-simulation (run 065) results in net sediment fluxes in landward direction, which are approximately 1-1.5 Mm^3/year larger than for the 2Dh simulation (run 066).
- The non-homogeneous 3D-simulation (run 063) results in net sediment fluxes in landward direction, which are approximately 2-4 Mm^3/year larger than for the homogeneous 3D-simulation (run 065). This is induced by the estuarine circulation, resulting in a tide-averaged landward directed flow near the bed and a seaward directed flow near the water surface. In combination with the suspended sediment concentration profile, with highest concentrations near the bed, this results in an additional net sediment transport in landward direction.
- The application of the k-ε turbulence model instead of the algebraic turbulence model results in a further increase of the fluxes in the central and western region with 1-3 Mm^3/year (relative to run 063).

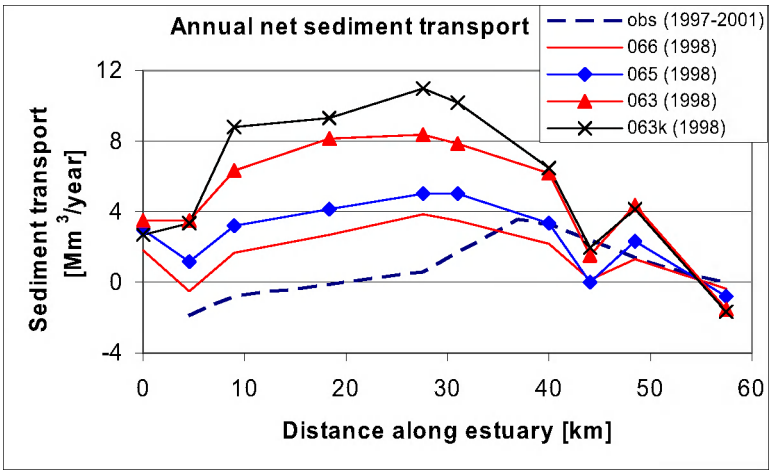

Figure 4.42: Annual-averaged net sediment transport along the Western Scheldt estuary for the period 1997-2001 (observations) and 1998 (simulations) (landward = +; seaward = -). Computed sediment transports are converted to volumes incl. pores, assuming a porosity of 0.4.

Conclusion regarding 3D-simulations and k-ε model

The overall conclusion of the 3D-simulations without and with k-ε model is that they do not improve results of morphological simulations for the Western Scheldt. Additional calibration of the 3D model appears to be necessary, before it can be applied to address specific managerial issues.

4.8 Conclusions

Sensitivity computations (002, 004 and 005)

1. The morphological simulation with (i) one single tide in combination with a morphological factor of 120 and (ii) a depth-averaged approach (one computational layer) shows good agreement with the simulation where a full spring-neap cycle is used (morphological factor of 24), combined with a three-dimensional approach (10 computational layers). This enables the morphological calibration with a depth-averaged approach (2Dh) and the application of one single tide in combination with a morphological factor of 120.
2. In case of a three-dimensional model, a non-equidistant vertical grid schematisation shows more correspondence with a depth-averaged approach than an equidistant grid.

Sensitivity simulations (007-019)

1. Both measurements and simulations indicate that no erosion/sedimentation occurs on the large shallow areas within the Western Scheldt estuary. Mainly the channels show morphological changes.
2. The amount of erosion/sedimentation, as computed by the model, is generally larger than the amount following from observations (approximately 0.3 to 0.5 m for the

sensitivity runs over the year 2001), indicating that transport gradients are overestimated. However the computed amounts of dredged material agree well with the information on the actual volumes of dredged material. This discrepancy is not yet understood and requires further study.

3. The model appears to reproduce the general tendency to deepen the channels. However, the computed erosion is larger than the observed erosion. The computed sedimentation on the channel edges is not in agreement with the measurements.
4. Although a large number of calibration computations have been executed, no major improvement with respect to the first calibration computation (run 007) could be obtained. The computed erosion/sedimentation patterns are all, more or less, comparable. The final calibration run therefore employs the parameter settings of run 007 but with the inclusion of waves (according to run 009), because they may be relevant to the morphology of the shallow areas in the western region of the Western Scheldt.

Calibration run 1998-2002 (021)

1. The calibration run over four years (1998-2002) also results in sedimentation and erosion, which are too large in comparison with measurements.
2. Annual-averaged net volume changes for the macro cells (totals of ebb and flood channel) are reproduced by the model. This also holds for the net volume changes for the individual ebb and flood channels of the macro cells, with the exception of the channels in macro cell 1. The model predicts erosion in the ebb channel, where a minor net deposition is observed, while erosion in the flood channel is overestimated.
3. Changes of areas for seven different depth classes, [> 0], [0, -2], [-2, -5], [-5, -7], [-7, -10], [-10, -20] and [<-20] (in m NAP), are not or at most, for some classes, qualitatively reproduced. In comparison with the observations, the model predicts a larger increase (or smaller decrease) of the areas for the depth classes [0, -2], [-2, -5] and [< -20] and a larger decrease (or smaller increase) of the areas for the depth classes [-5, -7], [-7, -10] and [-10, -20]. This implies that the model bathymetry of the ebb channels becomes steeper relative to observations.
4. The average total dredge volume amounts to 13.8 Mm^3 which is approximately 35% larger than observed (10.2 Mm^3). The observed decrease of the total dredging volume during the period 1998-2002 is reproduced by the model.
5. The model computes a net sediment import in the estuary mouth of 2 Mm^3/year, which differs from the observed net sediment export of 1.9 Mm3/year (averaged for the period 1997-2001).

Calibration run 1960-1966 (030)

1. Similar to the calibration run for 1998-2002, the erosion and sedimentation pattern, as computed by the model, is more pronounced than according to observations.
2. Net volume changes of the macro cells are reproduced by the model; differences with observations are comparable with those for the period 1998-2002.
3. Annual observed dredge volumes are underestimated by the model by approximately 3.5 Mm^3. The lower level of dredging volumes, relative to the period 1998-2002, is correctly predicted.

4. For the period 1960-1966 the model predicts an average import of sediment of 2.0 Mm^3/year, which agrees to a large extent with the observed import following from sand balance studies (= 1.4 Mm^3/year). At the Dutch-Belgian border the model computes a net import of 0.7 Mm^3/year, whereas in sand balance studies no net transport is assumed.

Final calibration run (042)

1. An improvement of the net area changes per depth class is obtained by an increase of the transverse bed slope effect. In this way the effect of processes, which are not included in the model (bed slope instabilities, breaching), are dealt with in a heuristic way. To some extent it reduces the overall steepening of the model bathymetry relative to the observed bathymetry.
2. Run 042 is considered as the final calibration run; parameter settings of this run will be used for the verification run for the period 1970-1985.
3. The average total dredge volume of run 042 (15.2 Mm^3) is approximately 50% larger than observed (10.2 Mm^3) and 10% larger than for run 021 (13.8 Mm^3).
4. The net sediment transport in the estuary mouth for the period 1998-2002 decreases from an *import* of 2.0 Mm^3 to an *export* of 0.2 Mm^3, with an average import of 0.6 Mm^3 for the period 1998-2002.

3D-effects (063, 065 and 063k)

1. None of the three-dimensional simulations, either with or without salt, gives an improvement of the reproduction of the morphological development of the Western Scheldt. Differences with observations are even larger than for the depth-averaged simulations.
2. The application of a k-ε turbulence model instead of an algebraic turbulence model does not improve the results of the morphological model.
3. The application of a 3D morphological model requires additional calibration of such a model.

5 Broad range analysis

5.1 Terminology

The background of broad range

In meteorological forecasts it is common practice to give a broad range around specific *predictions*. In morphodynamic forecasts this is not yet common practice. Often only one prediction is given. In complex dynamic morphodynamic systems, like the Western Scheldt estuary, broad ranges should actually also be part of the predictions. Another reason to work with broad ranges is related to the validation process of a morphodynamic model (*hindcast*). Model validation is the combined effort of model set-up, model calibration and model verification (Section 1.4). In the calibration process, the model is tuned in such a way that the output fits best with a set of measured data. In practice this means that several model runs are made, each with a different set of driving forces (input) and parameter setting. During the subsequent verification, the model is run for another set of measured data, with the "best-settings" as derived from the calibration (the so-called reference model run). To judge whether or not the model is capable of reproducing also the data set from the verification period, it is important to take into account a certain broad range around the model output. This is further explained below.

In the above context, broad range must not be considered a stochastic value. It has little to do with for instance a 90% reliability interval. It should be approached as the range in which the actual value of a certain parameter is most-likely to be found.

Two types of broad ranges

We distinguish two types of broad ranges.

Type 1 is related to natural variations. The morphology of the Scheldt estuary is subject to the hydrodynamic forcing, which can not be known beforehand as this depends on stochastic (meteorological determined) parameters like wind, waves and rainfall. The total amount of wave energy, for instance, differs from year to year as well as its predominant offshore direction. Another example is the yearly run-off and its distribution over the year of the Scheldt river. Tides on the other hand also change from year to year (induced for instance by the 18.6 year Saros-period), but they are deterministic. In theory, the hydraulic forcing of the morphology by tides can be predicted precisely. Type 1 broad range in this project is based on measured bathymetries (Section 5.2). This means that in addition to natural variations, also measuring inaccuracies and human interferences, like dredging and dredge disposal will automatically be included in the type 1 broad range.

Type 2 broad range is related to the limitations (and thus uncertainties) of the morphodynamic model and reflects the range in which the actual value of a certain model

output parameter is probably found. The hydraulic conditions for instance, were schematised into a few conditions which are supposed to represent the yearly set of conditions (input filtering). But also the modelling of sediment transport, in particular if different transport mechanisms are involved, has strong limitations. The accuracy of sediment transport formulas for instance, is still rather poor (in absolute sense reliable within factors rather than in percentages). Other possible explanations for model limitations are related to grid resolution, unknown morphodynamic feedback mechanisms, hardly any spatial variation in sediment particle sizes, etc. The situation in the Western Scheldt is further complicated by the dredging activities which were schematised to fit in the model operational possibilities. Finally, computer power is still hampering detailed computer simulations. All this and probably more, indicates that a morphodynamic model has its limitations. This is accounted for in the type 2 broad range, which is further worked out in Section 5.3.

Broad range parameters

The following output parameters are used in this study:

- Dredging volumes (in m^3);
- Changes in the areas between certain depth contours - per macro cell (ebb, flood, total) and for the combined area of all macro cells (in m^2 per considered time interval);
- Changes in the net sediment volume - per macro cell (ebb, flood, total) and for the combined area of all macro cells (in m^3 per considered time interval);
- Sediment exchange between sections of the estuary referred to as "1D sediment transport" (in m^3/y).

The broad range of these parameters is physically bounded. Dredging volumes for instance can not be negative. The broad ranges of other parameters may depend on each other. The hypsometry of the whole area or even sub-areas can not become too *weird*. This means that the subdivision in intertidal areas and deeper channel sections may fluctuate but can not change too extreme. We have not attempted to specify what still a reasonable hypsometry is and what is not, but this topic will be dealt with at a later stage when considering the total (type 2) broad range.

Application of broad range

In an ideal situation, a morphodynamic model is set up and calibrated against field data. Once a "best-model set-up" has been established and a reference run has been made, computations with the model are made to determine the type 2 broad range. In these "broad range computations", various parameters of the model are varied between "reasonable" boundaries. With "reasonable" we mean that the lower and upper values of the parameters are all possible settings. The result is a range of model output that can be considered as the broad range of possible model output. In the present project, most effort was put into a proper model calibration (Chapter 4). For the determination of the type 2 broad range we therefore used the model output of the calibration runs.

The application of both types of broad ranges depends on the use of the model.

If the model is used as a forecasting tool, then we need to distinguish between a prediction for a certain year (for instance the year 2011) and a prediction for the future on average (for instance per year in the period 2010-2015). In the first case we have to account for both

types of broad ranges. As natural variations and model limitations are independent, it is logical to add both types of broad ranges and to consider the combined broad range around the prediction of the reference computation. In the second case, we only need to consider the type 2 broad range as long as the natural variations are filtered out on the considered time interval.

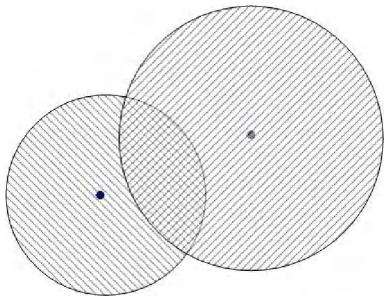

Figure 5.1: Schematisation of type 1 and type 2 broad ranges.

If the model is used in hindcasting mode, as is the case in the present project, then both types of broad range are used in a different way. This is illustrated with the two circles in Figure 5.1. One "dot" represents the "real" value of a morphologic parameter. The circle around it represents the broad range as this can be deduced from field data (type 1 broad range). The other "dot" represents the output value obtained from the verification computation. The circle around this dot represents the type 2 broad range of the model as this has been determined from the calibration runs. Only if both circles sufficiently overlap, one could argue that the model performs well. Here, the broad range is used as a method to judge the applicability of the model.

There are no general guidelines to indicate how much overlapping the circles must have before it can be concluded that the model performs well enough. Intuitively, this must at least be 30 -50 per cent of the measurement's "circle". The situation becomes a little more complicated if time is considered in the model output as well. Figure 5.2 shows on the vertical axis the value of a certain morphological parameter; on the horizontal axis stands time. One line represents the changes in the value of the parameter as this may follow from measurements. The 'true' value will be within a band around this line, as indicated in Figure 5.2.

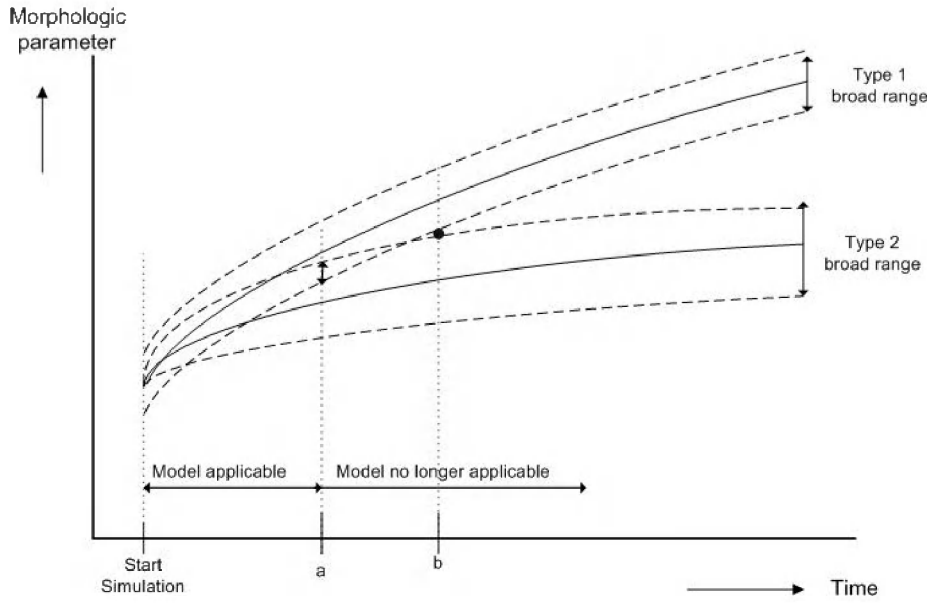

Figure 5.2: Type 1 and type 2 broad ranges for time varying morphological parameters.

Now suppose that the model computations lead to the other line. The starting points of both lines should ideally be the same as the model starts with the measured bottom. The band around the second line (the model line) is based on the type 2 broad range. At a time indicated with the letter b, both broad ranges do not overlap anymore. One could argue that at time "a", there is just enough overlap between both broad ranges. The conclusion that follows is that the model operates reasonably well until time a. For longer simulation periods the model is not applicable.

The above idealised examples illustrate how broad range can be used in model studies: either to indicate the range within which future developments are expected to occur, or to search for the boundaries of the model applicability. The latter is the case for the current project and is worked out in this Chapter.

5.2 Type 1 Broad Range

5.2.1 General approach

For the assessment of the type 1 broad range we have used available depth information. The data on the bathymetry have been processed to obtain a time series of the values of the four parameters mentioned in Section 5.1 (referred to as the broad range parameters). From year to year the various values of the broad range parameters fluctuate. This is the result of natural fluctuations, measuring inaccuracies and human intervention. Natural fluctuations are both triggered by meteorological fluctuations and the response on human interventions. Meteorological fluctuations are tide, river run-off, wind waves and set-up. The tide is exactly known and accommodates no broad range. The river run-off is dependent on stochastic rainfall and affects the longitudinal salinity distribution and stratification in the

estuary. The influence of wind waves is little within the estuary and set-up is an extreme event.

Different approaches can be followed to determine the broad range of a fluctuating time series. In this project we have used the time averaged envelope width as a measure for the type 1 broad range. The envelope width is determined by the absolute difference between the value at time t and the average of the values at t-1 and t+1, see Figure 5.3.

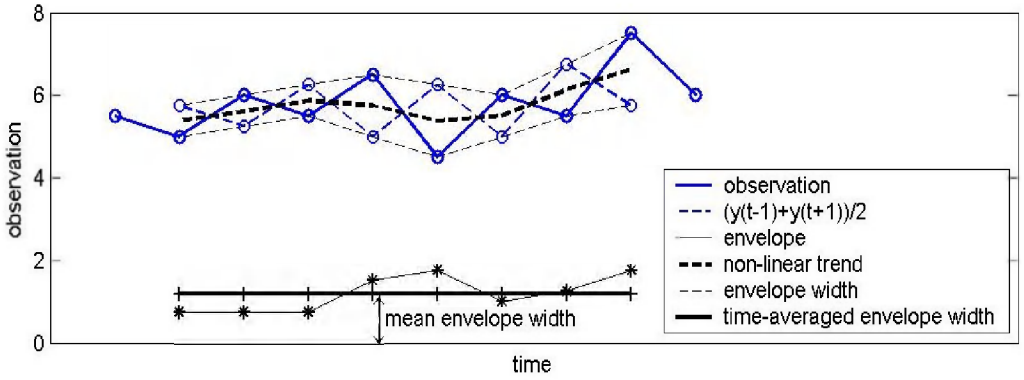

Figure 5.3: Time-averaged envelope for type 1 broad range.

The advantage of this method is that it can cope with any type of trend in the observed parameter. Further, positive and negative deviations of the envelope are equal in magnitude. Note that we have used the mean value of the envelope width as a measure for the broad range. We could also have used for instance the maximum width of the envelope width, which would lead to a larger broad range. The reason for this choice is that we have used the same approach also in the determination of the type 2 broad range. This may not be a very convincing argument, but there are simply no guidelines that can be followed on this matter.

5.2.2 Natural variations

The (measured) fluctuations depend on natural variations and on measurement inaccuracies. If we are interested in the natural variations only (as would be the case if we use the broad range in forecasts), then we should filter out the sounding inaccuracies. Sounding inaccuracies can be divided in: (a) stochastic inaccuracies, (b) systematic deviations and (c) variable systematic deviations. Marijs e.a. (2004) inventoried the various aspects that contribute to each of these sounding inaccuracies for the Western Scheldt.

Stochastic errors are determined for different intervals of time and different contributions, such as location errors, tide errors, sounding errors, bar check errors and heave/surf errors. Table 5.1 (from Marijs e.a., 2004) depicts an overview of stochastic errors. Note that the errors increase for older measurements and that they are relatively larger for slopes (defined as the areas with slope angles steeper than 1:15).

	Channel (57%)	shallows (36%)	slopes (7%)	total (100%)
2001-2004	0.11	0.11	0.11	0.11
2001	0.11	0.11	0.11	0.11
2001	0.25	0.25	0.59	0.28
1994-2000	0.25	0.25	0.59	0.28
1988-1993	0.29	0.27	1.14	0.34
1979-1987	0.38	0.37	1.16	0.43
1960-1977	0.39	0.38	2.14	0.51
1955-1959	0.43	0.41	2.14	0.54

Table 5.1: Inventory of stochastic errors [m].

A systematic error always points in the same direction and is caused for instance by a lack of squat-correction or by incorrect echo soundings at slopes. For squat one has to correct with +0.25 m for "deep areas" and "slopes" and with 0.15 m for shallow waters. Due to the echo soundings at slopes one has to impose a correction of 0.15 m until 1993 and 0.04 m after 1993 for slopes. Further, the use of hydro jet-engine driven sounding vessels introduced an error of approximately -0.10 m for specific years and areas.

Stochastic variable errors are caused by human errors and technical disturbances. These errors became smaller in the last years, but may have been significant in the older soundings.

In addition to measurement inaccuracies also human interventions, like dredging, will determine to a certain extent the measured bathymetry (see scheme below) Natural fluctuations can only be quantified in a totally natural driven estuary. Artificial interventions are partly determined by the human interpretation and response to natural fluctuations and partly by external factors (e.g. sand mining). It is impossible to filter either the natural or the artificial contribution to the measured fluctuations. As long as the human activities remain more or less the same, there is no need to understand the separate contributions. This may change if for example the dredging activities increase (in the future) or have fluctuated strongly (in the past).

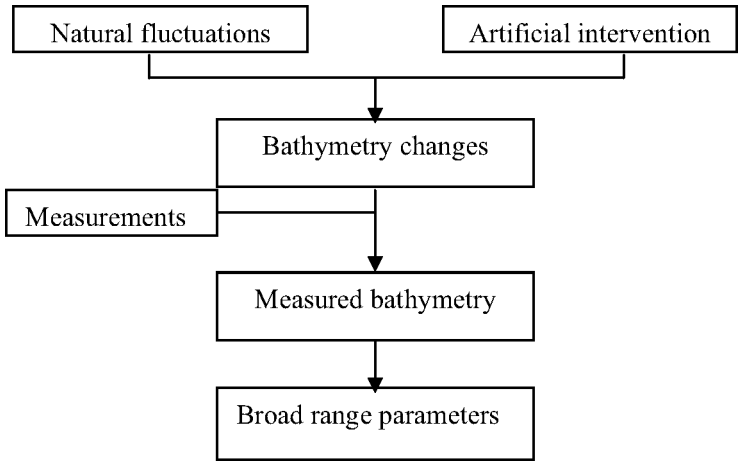

Based on the work of Marijs e.a. (2004) we determined the relevancy of the contribution of the above "disturbing factors" to the value of the broad range parameters (volumes and areas). The conclusions are as follows.

- Stochastic errors are balanced when considering a sounding compartment or a larger area and can be neglected.
- Systematic errors are cancelled to each other when considering volume chances if the errors are equal. Only when comparing measurements with different errors, a correction has to be applied. This is the case when considering the calibration period (1998-2002). Before 2002 no squat correction was used. When applying this to 85 km^2 of the considered 12 cells, this implies a volume correction of approximately 20 Mm^3 (for the whole estuary).
- Table 3.1 from Marijs e.a. (2004) gives figures on the variable systematic errors. They vary from 0.1 Mm^3 to 12.0 Mm^3 over a period of decades for a variety of smaller and larger areas. We did not attempt to account for this type of error, but it seems to be small for the most recent measurements (calibration period 1998-2002).

5.2.3 Results – dredging volumes

The total dredged volumes vary from year to year. This is due to both natural variations in local sedimentation and due to different dredging regimes. Analysing the years 1991 to 2001 with the described method results in a broad range of the total dredged volumes of approximately 1 Mm^3, giving a (symmetrical) broad range of [-0.5 Mm^3, +0.5 Mm^3]. This is illustrated in Figure 5.4.

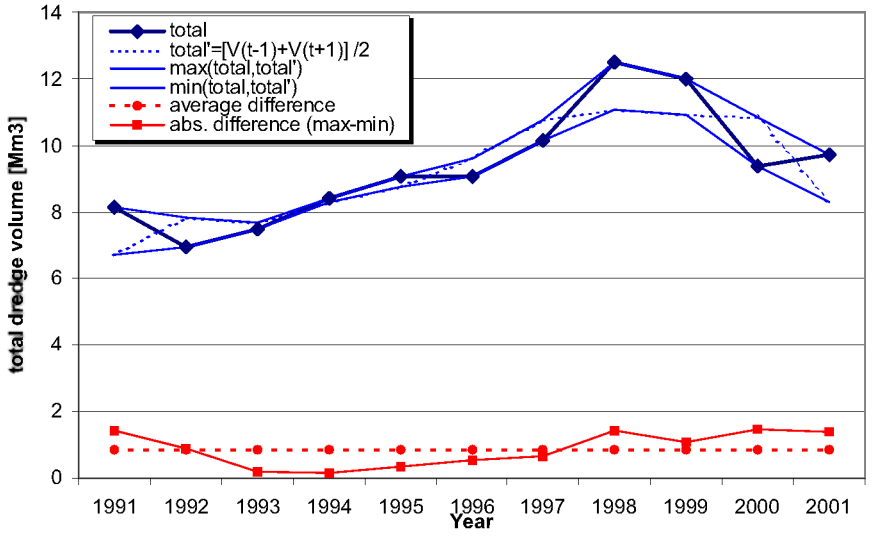

Figure 5.4: Assessment of the broad range for the total dredging volume (Mm^3).

Table 5.2 gives an overview of the broad ranges for a number of dredging areas. The figures are rounded off at 10^4 m^3 and translated into percentages (rounded off at 5 %). The applied method could not be used for the dredging areas 5, 6 10 and 11, due to a lack of continuation of the time series.

Dredge area	Mean Volume (Mm^3)	Mean envelope width	
		(Mm^3)	%
14	0.47	[-0.11,0.11]	[-25,25]
13	0.84	[-0.15,0.15]	[-15,15]
12	0.37	[-0.08,0.08]	[-25,25]
9	0.86	[-0.20,0.20]	[-25,25]
8	2.44	[-0.18,0.18]	[-5,5]
7	0.48	[-0.13,0.13]	[-25,25]
4	1.34	[-0.16,0.16]	[-10,10
3	1.31	[-0.16,0.16]	[-10,10]
Total	8.97	[-0.43,0.43]	[-5,5]

Table 5.2: Broad range dredging volumes for a number of dredging areas.

Table 5.2 shows that, relatively to the average dredging volume, area 14 (Drempel van Vlissingen), area 12 (Put van Terneuzen), area 9 (Overloop van Hansweert) and area 7 (Plaat van Walsoorden) have the largest broad range.

5.2.4 Results - changes in depths areas

The same depth areas as used in the previous chapters have been applied. These are:

- Areas with a depth above NAP 0 m;
- Areas with a depth between NAP –2 m and NAP 0 m;
- Areas with a depth between NAP –5 m and NAP –2 m;
- Areas with a depth between NAP –7 m and NAP –5 m;
- Areas with a depth between NAP –10 m and NAP –7 m;
- Areas with a depth between NAP –20 m and NAP –10 m;
- Areas below NAP –20 m.

Note that the areas presented in this report have been determined on the basis of the bathymetrical maps. This practical approach suits our present purpose where we are focusing on the changes of the depth areas and not so much on the absolute values. If one is interested in the absolute figures, the fluctuating water level and the spatial difference in tidal levels over the estuary should be accounted for.

The available data for the period 1998-2002 have been processed for each of the six ebb cells and flood cells, as well as for the total of both cells. Table 5.3 shows the broad range of the changes in the depth areas per depth class, for the ebb and flood cells separately. It is interesting to see that the flood channels are more dynamic than the ebb channels (in terms of changes in depth areas). Further it can be seen that the broad range increases from east to west (from 7 to 1).

Depth class	Ebb channels						Flood channels					
	1	3	4	5	6	7	1	3	4	5	6	7
>0	[-2, 2]	[-5, 5]	[-6, 6]	[-4, 4]	[-1, 1]	[-1, 1]	[-33,33]	[-17,17]	[-14,14]	[-10,10]	[-3, 3]	[-2, 2]
0/-2	[-23,23]	[-3, 3]	[-3, 3]	[-7, 7]	[-3, 3]	[-1, 1]	[-27,27]	[-11,11]	[-13,13]	[-9, 9]	[-5, 5]	[-3, 3]
-2/-5	[-25,25]	[-15,15]	[-8, 8]	[-4, 4]	[-1, 1]	[-1, 1]	[-7, 7]	[-59,59]	[-4, 4]	[-7, 7]	[-2, 2]	[-4, 4]
-5/-7	[-6, 6]	[-13,13]	[-10,10]	[-5, 5]	[-2, 2]	[-1, 1]	[-6, 6]	[-40,40]	[-3, 3]	[-10,10]	[-1, 1]	[-1, 1]
-7/-10	[-13,13]	[-16,16]	[-13,13]	[-7, 7]	[-1, 1]	[-1, 1]	[-28,28]	[-21,21]	[-7, 7]	[-10,10]	[-3, 3]	[-1, 1]
-10/-20	[-11,11]	[-18,18]	[-16,16]	[-7, 7]	[-2, 2]	[-2, 2]	[-26,26]	[-9, 9]	[-3, 3]	[-8, 8]	[-3, 3]	[0, 0]
<-20	[-3, 3]	[-8, 8]	[-1, 1]	[-10,10]	[-3, 3]	[-1, 1]	[-6, 6]	[-5, 5]	[-11,11]	[0, 0]	[0, 0]	[0, 0]

Table 5.3: Broad range depth areas ebb and flood channels (in 10^4 m^2).

If we combine the available data for all ebb cells and all flood cells and for the total of all cells, and use the same method to determine the broad range, then the figures in Table 5.4 are obtained. These figures are *not* the summation of the figures from Table 5.3, as fluctuations to a certain extent are compensated between the various cells. Similarly, the broad range for the ebb and flood channels combined (see Table 5.4) is not always the sum of the broad ranges of the individual channels.

Depth class	Ebb	Flood	Ebb+flood
>0	[-7, 7]	[-72,72]	[-79,79]
0/-2	[-21,21]	[-54,54]	[-75,75]
-2/-5	[-36,36]	[-69,69]	[-104,104]
-5/-7	[-11,11]	[-57,57]	[-56,56]
-7/-10	[-9, 9]	[-44,44]	[-38,38]
-10/-20	[-30,30]	[-15,15]	[-16,16]
<-20	[-1, 1]	[-14,14]	[-14,14]

Table 5.4: Broad range depth areas total of ebb and flood channels (in 10^4 m^2).

5.2.5 Results - changes in sediment volumes

The changes in the net sediment volume for each of the six ebb and flood cells are given in Table 5.5. These figures are based on the available data for the period 1998-2002, so only a four years period. A longer period is not possible since yearly observations are only available for the mentioned period. The relatively short period may be one of the reasons why the type 1 broad range is restricted to an average value of ± 1 Mm^3.

macro cell	Ebb channels	Flood channels	Ebb+flood channels
1	[-0.2,0.2]	[-0.1,0.1]	[-0.3,0.3]
3	[-0.1,0.1]	[-1.4,1.4]	[-1.5,1.5]
4	[-1.1,1.1]	[-0.1,0.1]	[-1.2,1.2]
5	[-1.5,1.5]	[-1.8,1.8]	[-0.3,0.3]
6	[-2.1,2.1]	[-1.3,1.3]	[-2.4,2.4]
7	[-1,1]	[-0.2,0.2]	[-1.1,1.1]
Average	[-1,1]	[-0.8,0.8]	[-1.1,1.1]

Table 5.5: Broad range sediment volume of ebb and flood channels (in Mm^3).

5.2.6 Results - 1D sediment transport

The parameter referred to as "1D-sediment transport" is related to the large scale sediment exchange between sections of the Western Scheldt. Nederbragt and Liek (2004) studied this in detail based on the available bathymetrical maps. They have calculated the sediment volume changes in areas that largely cover the (six) macro cells inside the estuary as well as

an area covering the outer delta. The approach to obtain sediment exchange between the various areas is rather straightforward and assumes no sediment exchange between the most eastern sub area and the Scheldt river further upstream. If for example, from the data it follows that the sediment volume of the most eastern sub area increases with 1 Mm^3, and there was no dredging, dumping and sand mining in the area, then there must have been a sediment transport in eastern direction from the neighbouring sub area. In the case of dredging, dumping and sand mining this is included in the sand balance and also the net transport from the neighbouring follows. Going from east to west, this leads to an estimate of the sediment exchange between the various sub areas.

Here we only focus on the sediment exchange between the outer delta and the estuary. The borderline between two areas is approximately at the line Vlissingen-Breskens. The sediment exchange trough this cross-section is a measure for the question whether or not the estuary is importing or exporting sediment.

Based on Figure 3.2 from Nederbragt and Liek (2004) we determined the type 1 broad range for the 1D sediment transport through the estuary mouth. From the natural changes in sediment volume of the Western Scheldt (i.e. net volume changes corrected with dredging, dumping and sand mining) the yearly net sediment transport was derived for the period 1991-2002; see the upper panel of Figure 5.5.

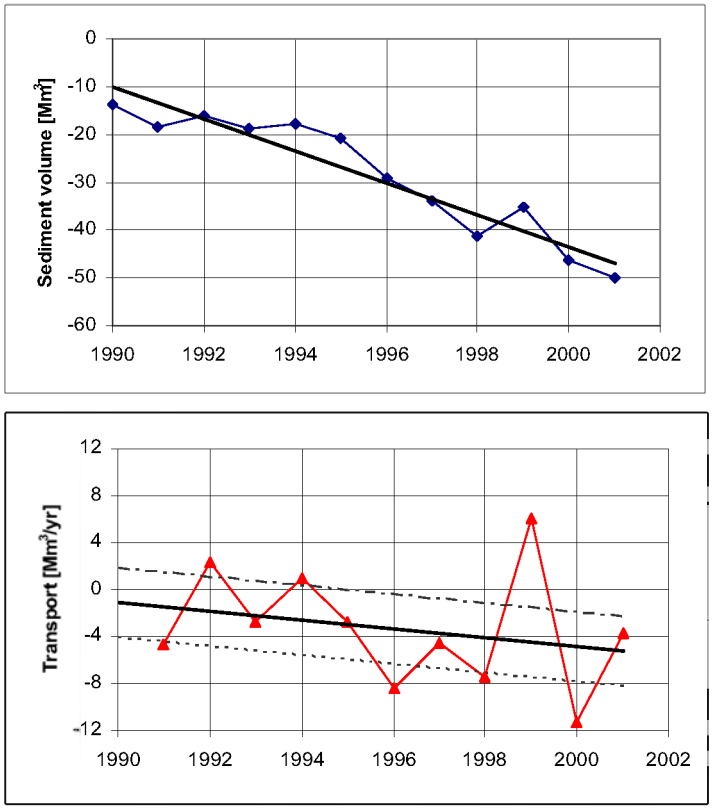

Figure 5.5: Natural volume changes for the Western Scheldt (upper panel) and derived net yearly sediment transport through the estuary mouth (lower panel).

A linear trend could be drawn through the measuring "points", from which the type 1 broad range was estimated to be in the order of [-3, +3] Mm^3, see the lower panel of Figure 5.5 The relatively large net sediment fluxes for the years 1999 (+6 Mm^3/year) and 2000 (-11 Mm^3/year) have been omitted for the computation of the broad range.

5.3 Type 2 Broad Range

5.3.1 General approach

The second type of broad range originates from limitations of the numerical model. Different computations, all with "reasonable" input and parameter settings, will give a range of possible model results. All the computer simulations that were made for the calibration have been used. A distinction can be made between simulations for the one-year period 1998-1999 and simulations for the four-year period 1998-2002.

Compared to the determination of type one broad range, there is not only variation in time, but also variation between different simulations. For each of the simulations we have determined the difference of the specific model output relative to the output of the reference-simulation. For the one-year simulations this is simulation with the code 007; for the four years period this is the simulation with the code 021. The broad range can now be determined in a similar way as for the type 1 broad range, by considering the deviations of the model output relative to the output of the reference simulation(s). For the four-year simulations we have determined the time-averaged envelope width similar as what has been done for the type 1 broad range (Section 5.2.1).

Table 5.6 below summarises the available model simulations. They have been grouped together to show which parameter is actually tested.

run	Simulation characteristics
Transport formulation	
012	Engelund Hansen
013	Ackers-White
046	Bijker
Bottom roughness schematisation	
008	Chézy =60 $m^{1/2}/s$
043	Bottom roughness = 0.01
044	Bottom roughness = 0.20
Grain diameter	
010	d=200μm instead of d=150μm
011	Variable grain size distribution, 2001
045	Variable grain size distribution, 1998-2002
Physical parameters	
014	Hor. dispersion coeff. $50m^2/s$ instead of $1m^2/s$
017	Hor. dispersion coeff. $0m^2/s$ instead of $1m^2/s$
019	Horizontal viscosity = 25 m^2/s instead of 2 m^2/s
016	Enhanced bottom shear stress
042	Increased transverse bed slope effects
Schematisation (2D,3D,waves)	
040	3D, including salinity
041	Phase postponement M4 component
063	3D, inhomogeneous, algebraic
063k	3D, inhomogeneous, k-ε
065	3D, homogeneous
066	2Dh, homogeneous
009	007 with waves
018	Channel near Hansweert non-erodible

Table 5.6: Overview of available model simulations for the determination of type 2 broad range.

The maximum and minimum deviations from the reference simulation are the basis for the considered broad range. More combinations of settings are possible than the number of performed simulations. The range of possible model results is larger, but since none of the settings is fully independent of other settings, the deviations may not be added.

In the following Sections the results are presented for each of the four broad range parameters. This is done by first presenting the results as these follow directly from the various model output. Next, we discuss these results, leading finally to a proposed type 2 broad range.

5.3.2 Results – dredging volumes

Results from model output

When considering the total (computed) dredge volumes, yearly quantities vary between 5.5 Mm^3 and 35 Mm^3. Differences compared to the two calibration runs (007 for one year and 021 for four year simulation) vary from –6.5 Mm^3 to +10.7 Mm^3, see Table 5.7 and Figures 5.6 and 5.7.

run	Simulation characteristics	Dredge volume [Mm^3]	Difference with 007/021 [Mm^3]
007	**Reference run, 1 year, 2001**	**10.6**	**0.0**
008	Like 007, Chézy = 60 $m^{1/2}/s$	8.2	-2.4
009	Like 007, with waves	11.6	1.0
010	Like 007, d = 200 μm instead of d= 150 μm	12.0	1.4
011	Variable grain size distribution	11.0	0.4
012	Engelund Hansen	8.9	-1.7
013	Ackers-White	5.4	-5.2
014	Hor. dispersion coeff. 50 m^2/s instead of 1 m^2/s	8.2	-2.4
016	Enhanced bottom shear stress	10.6	0.0
017	Hor. dispersion coeff. 50 m^2/s instead of 1 m^2/s	11.1	0.5
018	Channel near Hansweert non-erodible	10.2	-0.4
019	Horizontal viscosity = 25 m^2/s instead of 2 m^2/s	5.5	-5.1
021	**Reference run, 4 years**	**14.5**	**0.0**
040	3D, including salinity	19.8	3.0
041	Phase postponement M4 component	15.1	0.6
042	Increased transverse bed slope effects	15.6	1.1
043	Bottom roughness = 0.01 m	25.2	***10.7***
044	Bottom roughness = 0.20 m	10.1	-4.4
045	Variable grain size distribution	14.8	0.3
046	Bijker	8.0	***-6.5***
066	**2Dh, homogeneous (reference run for 3D)**	**16.8**	**0.0**
063	3D, inhomogeneous	24.7	7.9
065	3D, homogeneous	21.0	4.2

Table 5.7: Computed dredge volumes and deviations with the reference simulations.

Based on the maximum and minimum deviation, the time average broad range would be [-6.5, 10.7], determined by the Bijker transport formulation (run 046) and the low bottom roughness (run 043).

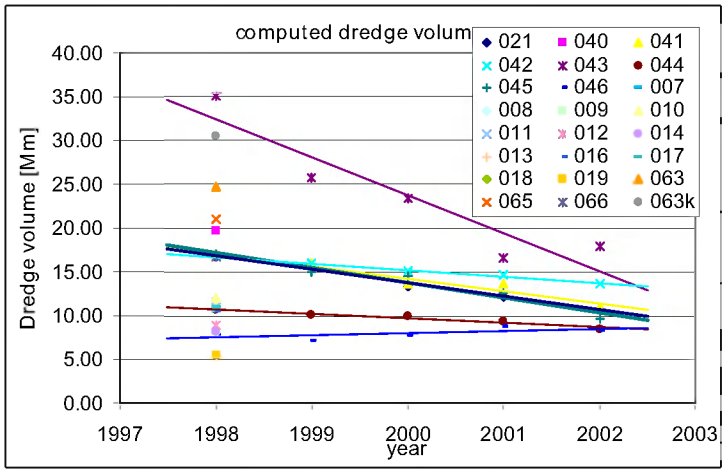

Figure 5.6: Computed dredge volumes for the various simulations (total of all dredge areas).

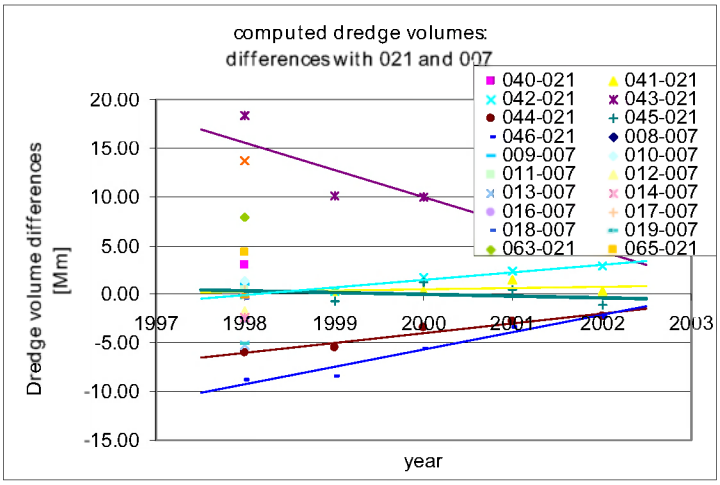

Figure 5.7: Computed dredge volumes: differences with reference simulations.

Interpretation

The two above Figures clearly show how the 4-years model runs all converge to more or less the same (total) dredge volumes. This suggests that the broad range decreases for longer simulation periods, which does not fit in the general perception that the broad range should increase on longer time horizons.

Lower limit of the broad range

The lower limit of the broad range is caused by simulation 046 (the Bijker formula). It is a well-known feature of the Bijker formula to compute too low transport capacities in tide-driven channels. Since the deposition in the dredge areas depend on the sediment transport in the channels, it is not surprising that the computed dredge volumes are so small (compared to the output of the reference simulation). If we disregard run 046 for the lower limit for this reason, then run 013 becomes decisive (Ackers White). Again the transport formula determines the lower limit of the broad range. The other near-decisive run is run 019 (horizontal viscosity). This simulation, however, does not have a "reasonable" parameter setting which is required for the assessment of the broad range (run 019 was meant as a sensitivity run).

Upper limit of the broad range

The upper limit is completely determined by run 043 (bottom roughness). It can be argued that the chosen parameter setting (1 cm bottom roughness for the whole area) is beyond reasonable limits. Comparison with run 044 shows however, the large dependency of the computed dredge volumes on the bottom roughness.

Concluding type 2 broad range

Based on the above considerations and the results from Table 5.7, we propose to use the following broad range for the total dredge volumes: [-4, +7] Mm^3. Decisive for this large broad range is the uncertainty due to the bottom roughness and the transport formula.

5.3.3 Results - changes in depths areas

Results from model output

The maximum and minimum deviations from the reference run(s) for the areas per depth sector are given in Table 5.8 below. The results for the ebb cells are given in Table 5.8a; for the flood cells in Table 5.8b and finally for the two combined in Table 5.8c.

Depth class	Ebb channels					
	1	3	4	5	6	7
> 0	[-9,8]	[-28,10]	[-15,36]	[-14,11]	[-2,8]	[-10,4]
0/-2	[-33,0]	[-38,41]	[-21,32]	[-40,61]	[-12,7]	[-31,4]
-2/-5	[-44,36]	[-95,78]	[-58,50]	[-15,57]	[-16,21]	[-42,9]
-5/-7	[-11,38]	[-43,61]	[-52,36]	[-22,35]	[-10,26]	[-14,24]
-7/-10	[-49,13]	[-61,27]	[-90,70]	[-64,15]	[-19,12]	[-30,47]
-10/-20	[-19,49]	[-127,89]	[-78,105]	[-140,178]	[-29,46]	[-18,39]
<-20	[-40,46]	[-30,65]	[-80,59]	[-116,89]	[-22,23]	[-18,20]

Table 5.8a: Maximum and minimum deviations in area changes per depth class– ebb channels (in 10^4 m^2).

Depth class	Flood channels					
	1	3	4	5	6	7
> 0	[-55,55]	[-23,30]	[-43,99]	[-13,46]	[-10,24]	[-14,2]
0/-2	[-64,79]	[-39,147]	[-76,15]	[-18,23]	[-22,10]	[-67,8]
-2/-5	[-94,109]	[-180,140]	[-18,43]	[-22,46]	[-29,17]	[-32,41]
-5/-7	[-125,43]	[-221,73]	[-30,22]	[-53,40]	[-10,30]	[-32,35]
-7/-10	[-107,124]	[-49,71]	[-54,19]	[-92,86]	[-25,12]	[-8,35]
-10/-20	[-51,53]	[-144,111]	[-161,213]	[-95,56]	[-18,13]	[-3,174]
<-20	[-25,41]	[-74,148]	[-175,126]	[0,2]	[0,0]	[-135,0]

Table 5.8b: Maximum and minimum deviations in area changes per depth class– flood channels (in 10^4 m^2).

Depth class	Ebb	Flood	Ebb+flood
> 0	[-26,42]	[-100,116]	[-112,159]
0/-2	[-115,75]	[-122,185]	[-192,260]
-2/-5	[-167,190]	[-209,307]	[-360,449]
-5/-7	[-37,149]	[-368,119]	[-321,151]
-7/-10	[-183,72]	[-94,136]	[-207,152]
-10/-20	[-339,347]	[-335,331]	[-674,625]
<-20	[-182,212]	[-192,216]	[-371,428]

Table 5.8c: Maximum and minimum deviations in area changes per depth class– ebb+flood channels (in 10^4 m^2).

Interpretation

A detailed analysis of the maximum and minimum deviations shows that in particular run 014 (extremely large horizontal dispersion coefficient) and runs 063/063k (3D inhomogeneous) determine to a large extent the results. As indicated before, these

computations were mainly meant to investigate the sensitivity of the model. If we disregard these three simulations, we obtain a smaller broad range as indicated in the tables below.

Concluding type 2 broad range

Based on the above results and leaving out the results from runs 014, 063 and 063k, the following figures are proposed for the broad ranges (figures have been rounded off):

Depth class	Ebb channels					
	1	3	4	5	6	7
> 0	[-10,10]	[-30,10]	[-20,40]	[-10,10]	[0,10]	[-10,0]
0/-2	[-30,0]	[-40,40]	[-20,20]	[-40,20]	[-10,10]	[-30,0]
-2/-5	[-30,40]	[-80,70]	[-60,50]	[-10,60]	[-10,20]	[-40,10]
-5/-7	[-10,40]	[-10,60]	[-30,40]	[-10,40]	[-10,10]	[-10,20]
-7/-10	[-50,10]	[-60,10]	[-90,60]	[-60,10]	[-20,10]	[-30,50]
-10/-20	[-20,50]	[-100,70]	[-70,40]	[-140,180]	[-10,50]	[-20,40]
<-20	[-40,30]	[-30,40]	[-70,60]	[-120,90]	[-20,10]	[-20,20]

Table 5.9a: Proposed type 2 broad range for area changes per depth class– ebb channels (in 10^4 m^2).

Depth class	Flood channels					
	1	3	4	5	6	7
> 0	[-60,60]	[-20,30]	[-40,100]	[-10,50]	[-10,20]	[-10,0]
0/-2	[-60,70]	[-40,70]	[-80,20]	[-20,20]	[-20,10]	[-70,10]
-2/-5	[-90,110]	[-40,140]	[-20,40]	[-20,30]	[-30,10]	[-30,40]
-5/-7	[-130,40]	[-220,70]	[-30,40]	[-50,10]	[-10,30]	[-30,30]
-7/-10	[-110,120]	[-50,70]	[-30,20]	[-50,90]	[-20,10]	[-10,30]
-10/-20	[-40,50]	[-60,100]	[-160,210]	[-100,60]	[-20,10]	[0,170]
<-20	[-30,40]	[-70,70]	[-180,130]	[0,0]	[0,0]	[-130,0]

Table 5.9b: Proposed type 2 broad range for area changes per depth class– flood channels (in 10^4 m^2).

Depth class	Ebb	Flood	Ebb+flood
> 0	[-30,40]	[-100,120]	[-110,160]
0/-2	[-120,30]	[-120,100]	[-190,160]
-2/-5	[-170,190]	[-150,310]	[-310,450]
-5/-7	[-10,150]	[-370,120]	[-280,150]
-7/-10	[-180,70]	[-60,140]	[-210,150]
-10/-20	[-260,350]	[-280,330]	[-500,630]
<-20	[-180,190]	[-190,180]	[-370,340]

Table 5.9c: Proposed type 2 broad range for area changes per depth class– ebb+flood channels (in 10^4 m^2).

5.3.4 Results – changes in sediment volumes

Results from model output

Table 5.10 shows the computed net sediment volume changes, compared to the reference simulations. The minimum and maximum deviation from the reference computations is given in the lowest two rows. We have used grey shades to indicate which computer simulations determine the two limits of the broad range.

run	Ebb channels						Flood channels						Ebb + flood channels					
	1	3	4	5	6	7	1	3	4	5	6	7	1	3	4	5	6	7
008-007	1.6	2.7	-4.1	-4.5	-0.8	0.4	1.7	2.6	-1.7	0.7	1.0	0.0	-0.4	2.4	-2.7	-0.5	0.6	0.0
009-007	5.0	2.9	-3.5	-3.1	-0.4	0.5	-0.9	-0.1	0.6	-0.2	0.0	0.0	0.4	0.0	0.1	0.1	0.1	0.1
010-007	3.3	2.6	-5.2	-2.8	-0.9	0.5	0.2	1.6	1.0	-0.3	0.1	0.0	-0.2	1.4	-1.1	0.2	-0.3	0.1
011-007	3.7	3.1	-3.3	-2.7	-0.9	0.5	-0.4	-0.1	0.0	0.0	0.1	0.0	-0.3	0.2	-0.2	0.7	-0.4	0.0
012-007	1.3	3.4	-3.7	-3.9	-0.4	-0.2	6.3	-1.0	-9.4	5.5	0.9	0.9	0.5	1.7	-2.4	0.2	0.9	-0.7
013-007	0.9	4.0	-1.0	-4.7	-0.8	-0.4	3.1	-0.1	-2.7	1.7	0.6	0.0	0.3	1.1	-0.6	0.3	0.3	-0.9
014-007	4.3	5.9	-2.6	-3.7	-0.6	-0.4	-1.1	0.1	-2.8	0.9	1.2	-0.1	-0.5	3.2	-2.3	0.5	1.0	-1.0
016-007	3.6	2.8	-3.7	-3.5	-0.5	0.5	-0.2	0.0	0.3	-0.2	0.0	0.0	-0.3	0.0	-0.3	-0.3	0.0	0.0
017-007	3.7	2.9	-3.1	-3.3	-0.5	0.5	-0.1	0.0	0.0	0.0	0.0	0.0	-0.1	0.1	0.0	0.0	0.0	0.0
018-007	3.6	2.9	-2.9	-3.8	-0.5	0.4	0.0	0.1	-1.0	1.2	0.0	0.0	-0.1	0.1	-0.7	0.8	0.0	0.0
019-007	1.2	2.9	-2.7	-5.2	-1.0	-0.5	2.1	2.1	-1.4	1.3	0.5	0.2	-0.4	2.1	-1.0	-0.5	0.0	-0.7
063-007	0.5	2.7	-3.5	1.2	0.8	-0.5	-1.1	-3.3	1.0	-1.1	-0.1	0.3	-0.6	-0.6	-2.4	0.2	0.6	-0.2
63k-021	3.7	5.6	-3.4	2.1	1.4	-0.6	-3.1	-5.9	1.9	-0.9	-0.5	0.1	0.6	-0.4	-1.5	1.2	1.0	-0.6
065-021	-2.9	1.1	-2.7	0.8	0.7	-0.6	0.3	-0.6	0.0	0.0	0.2	0.5	-2.6	0.5	-2.8	0.8	0.8	-0.1
066-021	-3.5	2.7	3.8	-4.6	-0.2	-1.3	2.9	-0.5	-4.0	1.6	0.3	0.1	-0.6	2.3	-0.2	-3.0	0.1	-1.2
040-021	0.6	0.8	1.6	-0.2	0.5	0.4	-3.1	-0.2	-1.2	0.9	0.0	0.0	-2.5	0.6	0.5	0.7	0.5	0.4
041-021	0.3	0.3	0.3	0.1	0.0	0.0	-0.1	-0.3	-0.2	0.1	-0.1	0.0	0.3	0.0	0.1	0.2	-0.1	0.0
042-021	-0.4	-1.6	-0.3	0.2	-0.6	0.7	1.7	2.2	0.7	-0.4	0.1	-0.1	1.3	0.6	0.4	-0.2	-0.5	0.7
043-021	0.9	-3.3	1.4	-0.8	-3.0	-0.5	-2.5	-0.1	1.1	0.2	0.3	-0.3	-1.6	-3.4	2.5	-0.6	-2.6	-0.8
044-021	0.3	0.3	-2.6	1.8	-0.5	0.3	-1.5	-0.6	1.0	-0.7	0.3	0.1	-1.2	-0.2	-1.6	1.1	-0.2	0.4
045-021	0.0	-1.2	0.2	0.1	-0.7	0.2	-0.8	0.1	0.4	-0.1	0.0	0.0	-0.8	-1.1	0.5	0.0	-0.6	0.2
046-021	3.3	1.6	-1.1	2.5	-0.5	0.6	-3.4	-1.8	2.0	-1.2	0.1	0.0	-0.1	-0.3	0.9	1.3	-0.4	0.6
Broad range	-3.5	-3.3	-5.2	-5.2	-3.0	-1.3	-3.4	-5.9	-9.4	-1.2	-0.5	-0.3	-2.6	-3.4	-2.8	-3.0	-2.6	-1.2
	5.0	5.9	3.8	2.5	1.4	0.7	6.3	2.6	2.0	5.5	1.2	0.9	1.3	3.2	2.5	1.3	1.0	0.7

Table 5.10: Net sediment volume changes, deviation with reference simulations (in Mm^3).

Interpretation

The computed broad range decreases for all of the ebb and flood cells from west to east. Note that the broad range of the combined ebb and flood cells is less than what would follow from a summation of the ebb and flood cells separately. This can be explained by the fact that most of the sediment is exchanged with the neighbouring macro cell.

There is not a single simulation that determines the broad range for all of the cells. Only run 043 (extreme low bottom roughness), runs 012 and 046 (Engelund-Hansen and Bijker transport formulas) and run 066 seems to dominate a little. If we disregard these simulations then we obtain smaller broad ranges (see Table 5.11 below). This can be motivated by accepting that the mentioned computer runs were sensitivity computations rather then realistic broad range computations.

Concluding type 2 broad range

Based on Table 5.10, the above considerations and the notice that not one simulation should dominate the limits of the broad range, we propose the following broad ranges (rounded off at Mm^3):

Macro cell	Ebb	Flood	Ebb+flood
1	[-3 , 5]	[-3 , 3]	[-3 , 1]
3	[-2 , 5]	[-3 , 3]	[-1 , 2]
4	[-5 , 2]	[-3 , 1]	[-3 , 1]
5	[-5 , 2]	[-1 , 2]	[-1 , 1]
6	[-1 , 1]	[-1 , 1]	[-1 , 1]
7	[-1 , 1]	[0 , 1]	[-1 , 1]

Table 5.11: Proposed type 2 broad range for the sediment volume changes (in Mm^3).

5.3.5 Results – 1D sediment transport

Results from model output

Although the numerical model gives the opportunity to give the transport rates across as many cross-estuary boundaries as we would like, we focus here on the transport rates across the entrance of the estuary. That figure can be compared with the one based on observations as presented in Section 5.2.6. The sediment import or export of the whole estuary is computed directly from the computed transport fields. They are not based on volumetric changes as was the case in Section 5.2.6.

Table 5.12 gives the deviations of the computed transport rates for each of the simulations. It is noted that all simulations give a net landward sediment transport (in the order of 0.5 to 2 Mm^3/y from west to east), which implies that according to the simulations the estuary is importing sediment.

Run	Transport [Mm^3/y]	Deviation [Mm^3/y]
007 (2001)	**1.8**	**0**
008	1.5	-0.3
009	2	0.2
012	0.7	-1.1
013	0.6	-1.2
014	0.8	-1
016	1.8	0
017	1.8	0
018	1.8	0
019	1.9	0.1
021 (1998-2002)	**1.2**	**0**
042	0.6	-0.6
043	1.7	0.5
044	1.4	0.2
045	2.0	0.8
046	0.7	-0.5
021 (1998)	**1.9**	**0**
063	2.1	0.2
63k	1.6	-0.3
065	1.8	-0.1
066	1.1	-0.8

Positive: landward transport (from west to east).

Table 5.12: Computed transport rates across the line Vlissingen-Breskens (c.s. 1, see Figure 4.12a).

Interpretation

There is not a single run that really dominates the range. We therefore see no reason to narrow the broad range.

Concluding type 2 broad range

The proposed type 2 broad range for the import and export of sediment in the Western Scheldt estuary is [-1.2 , +0.8] Mm^3. For comparison with results from sand balances the figures should be multiplied with 1.7 to account for the volume occupied by the pores. In that case the type 2 broad range becomes [-2.0 , +1.3] Mm^3.

6 Verification of the morphodynamic model

Verification of the model is done for the 15-year period 1970-1985. All model parameters have been taken from run 042 without any adjustments and consequently the transverse bed slope coefficient is set at 100. Boundary conditions for the sea and river boundary have been generated using the astronomical components. Dredging, dumping and sand mining are included in the model using the average polygons defining these locations. For each of the dredge locations a critical depth is specified. If, during the simulation, the bed level becomes higher than the critical depth, sand is removed from the dredge location and brought to one or more dump locations. The distribution of removed sediment over the dredge locations (if more than one) is based on available data. In sand mining locations, a volume of sand is removed from the system in accordance with observed quantities. The simulation covered the period during which the first deepening of the navigation channel was executed, see Figure 6.1. According to Kornman et al. (2003) periods for the actual deepening varied per location: Drempel van Borssele between 1973 and 1976, Drempel van Hansweert between 1973 and 1979, Drempel van Valkenisse between 1973 and 1978 and Drempel van Bath between 1967 and 1978.

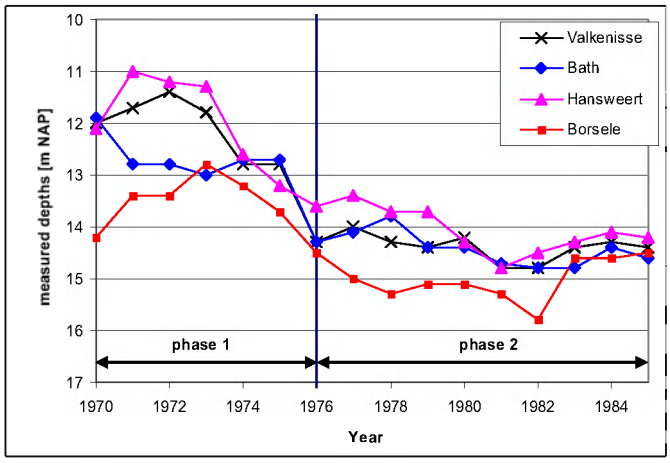

Figure 6.1: Dredge depths during the period 1970-1985 (data derived from Kornman et al., 2003).

The total average dredging for 1970-1985 amounts to 8.0 Mm^3/year (in situ). During this period a volume of 2.6 Mm^3/year was extracted from the estuary due to sand mining.

Because the model employs average polygons, dredging depths and quantities for sand mining the period 1970-1985 is subdivided into two consecutive periods: 1970-1976 (phase 1: run 050) and 1976-1985 (phase 2: run 051). During the second period dredging depths are increased to account for the local deepening of the bathymetry. The top level of the first non-erodible layer is included in the model schematisation and as such the thickness of the erodible bed is known.

Results of the simulation are given hereafter and compared with observations. The ranges of possible outcomes of the model results are also indicated, if model parameters are changed

within the bounds as applied during the sensitivity simulations (see Section 5.3). In addition the broad ranges for the observations are shown, reflecting variations due to natural fluctuations and measurement accuracies (see Section 5.2).

Sedimentation and erosion

The computed and observed yearly-average erosion and sedimentation for the period 1970-1985 is given in Figure 6.2. Regarding the reproduction of the observed sedimentation and erosion there is a major difference between the western and eastern region of the Western Scheldt.

West of Terneuzen many differences between observations and model results are clearly visible. The model fails to reproduce the erosion south of Vlissingen (near the Schaar van Spijkerplaat). Elsewhere minor morphological changes occur according to observations, whereas the model predicts, for instance, erosion south of Vlissingen along the margins of the estuary, deposition in the Honte and Everingen and deposition as well as erosion in the Pas van Terneuzen.

East of Terneuzen observed changes are reproduced much better by the model, i.e. erosion of the Schaar van de Noord, Overloop van Valkenisse, Zuidergat Overloop van Hansweert and deposition in the Middelgat. In a number of dump locations in the model the effect of dumping is clearly visible (net deposition), whereas this does not follow from observations.

Net sediment volume changes

Net volume changes are given in Figure 6.3 for the ebb channel, flood channel and the ebb and flood channel combined.

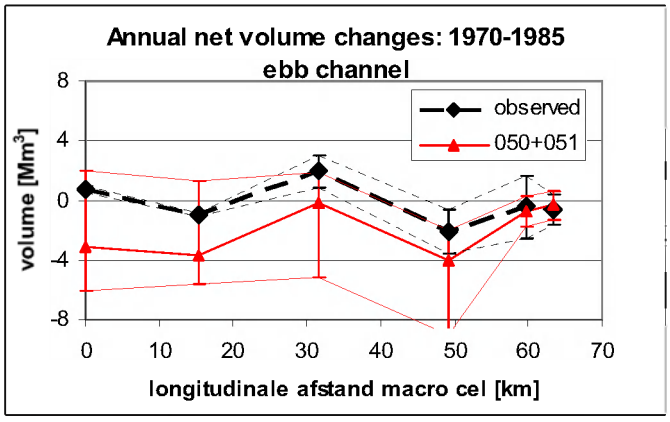

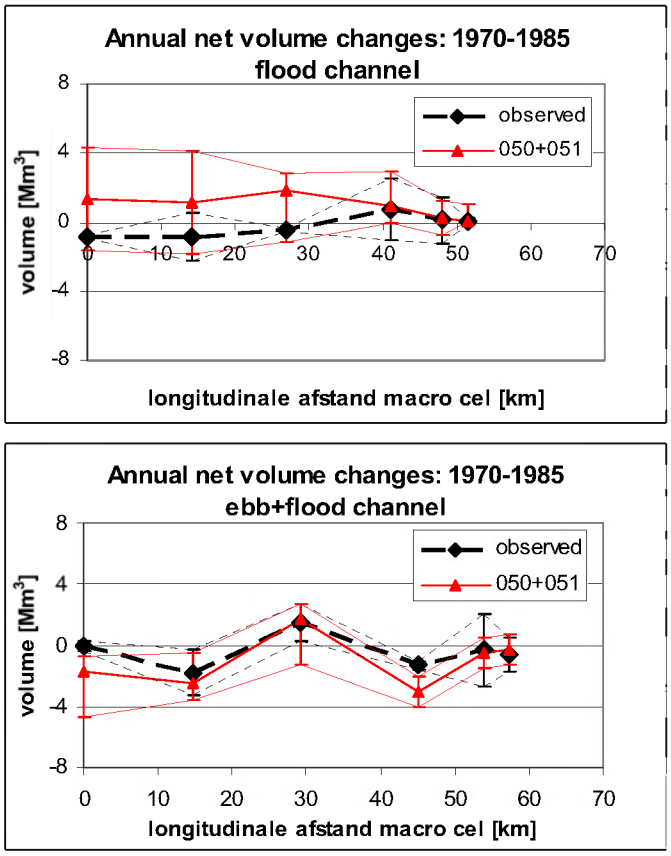

Figure 6.3: Computed and observed net volume changes of the ebb and flood channels of the macro cells for the verification period 1970-1985.

Both for the ebb and flood channel separately the broad ranges for the observations and simulations overlap each other to a large extent (at least 50%). For the ebb and flood channel combined macro cells 1 and 5 show a distinct behaviour (no overlap of the type 1 and type 2 broad ranges), i.e. too much erosion is predicted by the model. In these macro cells the model results appear to deviate systematically from the observed changes.

Area changes per depth class

The yearly-averaged area changes during 1970-1985 are given in Figure 6.4. The broad ranges of the observations and computational results, as derived in Chapter 5, are also shown. It is noted, that at the start of the simulation for period 1976-1985 the bathymetry showed differences with the bathymetry at the end of the simulation for the period 1970-1976[2]. This occurred mainly at shallow depths. Therefore, the net area changes for the individual depth classes are computed for the periods 1970-1976 and 1976-1985 separately. The net average area changes for the whole simulation period follows then from the weighted averages (ratio 6:9) of the first period (6 years) and second period (9 years).

[2] *Resulting from re-interpolation of the computed bed levels necessary for the restart of the simulation.*

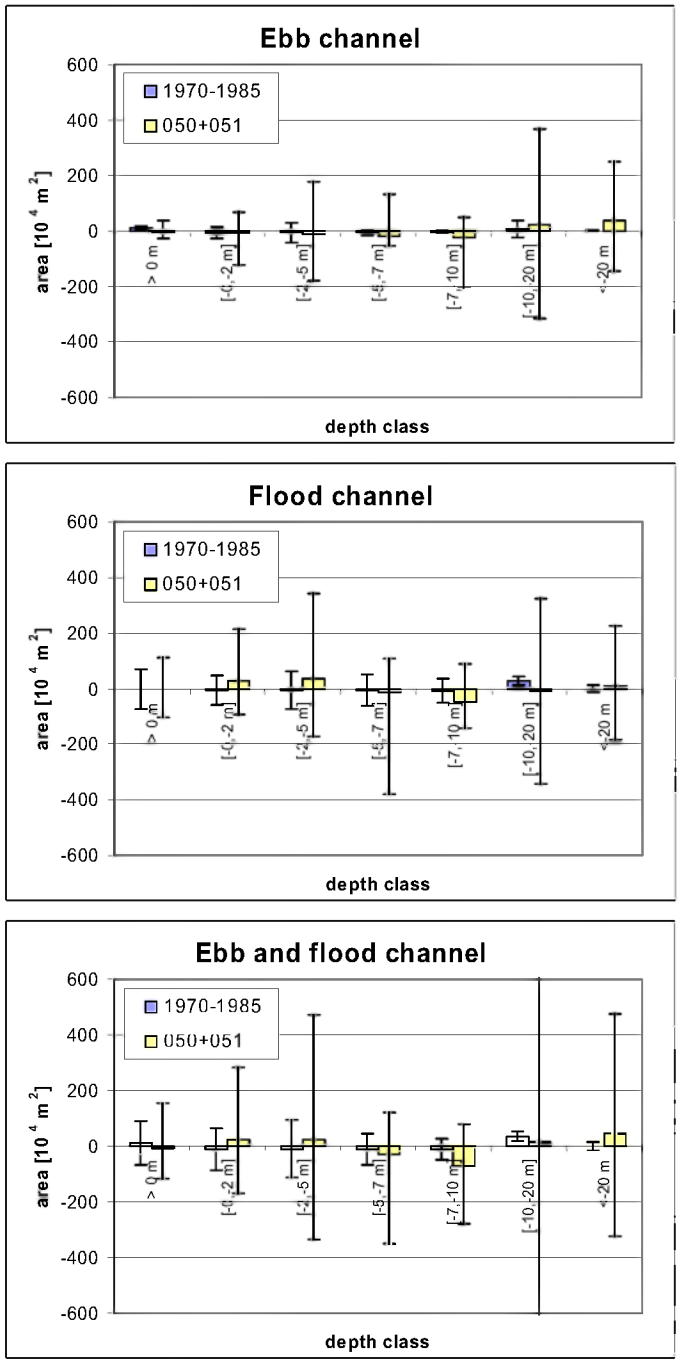

Figure 6.4: Average annual changes of areas per depth class during the verification period 1970-1985 (15 years).

If the broad ranges for the model simulation are neglected, it follows that for most of the depth classes (ebb and flood channel separately and combined) the computed area changes are within the bounds for the observations. Only for some of the classes representing intervals at larger depth, model results are beyond the broad ranges as set by the observations. The broad ranges for the model results reflect possible outcomes due to realistic variation of the model parameters. If these are considered as well it follows that *for each separate depth class* there may be complete agreement between observations and

computational results for one specific set of model parameters. The question remains however if this will also be the case for all other depth classes.

Dredge volumes

Computed and observed dredge volumes are compared in Figure 6.5. Also the broad range for the model simulation is shown, i.e. computed values minus 4 Mm^3 and plus 7 Mm^3. For the observations the broad range is $\pm$ 0.5 Mm^3 (not indicated in the figure). All observed dredge volumes are within the range as obtained from the model results. The observed dredge volumes already show an increase in 1974, whereas the computed volumes do not. The reason is, that the deepening of the navigation channel already started in 1974, while in the model the dredging depths remain constant in time until 1976. The sudden increase of the computed dredge volumes in 1976 is thus explained by the sudden increase of the dredging depths in 1976.

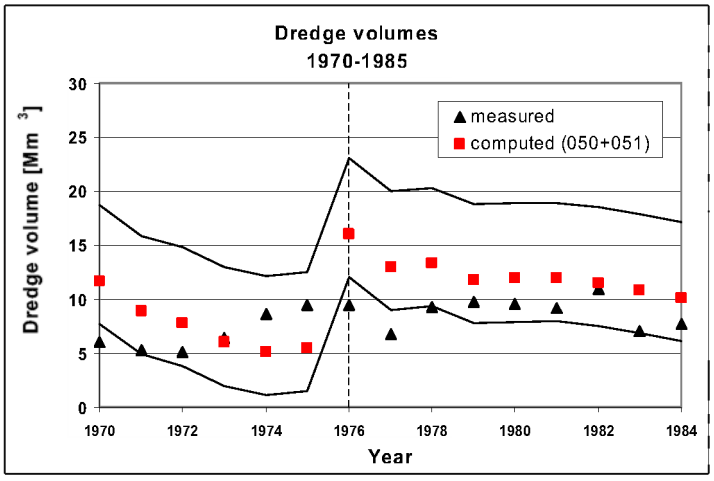

Figure 6.5: Measured and computed total dredge volumes (run 050 and 051) for the period 1970-1985.

Observed and computed total dredge volumes are given in Table 6.1. For the total period, 1970-1985, the computed volume is 2.3 Mm^3 larger than the observed volume, which is well within the range [-4, +7] Mm^3 as derived in Section 5.3.2.

	Observed annual-averaged dredge volume [Mm^3/year]	Computed annual-averaged dredge volume [Mm^3/year]
1970-1976	6.8	7.5
1976-1985	8.8	12.3
1970-1985	8.0	10.3

Table 6.1: Observed and computed dredge volumes for the period 1970-1985.

Net sediment transport

The computed annual net sediment transport for a number of cross-sections, averaged over the period 1970-1985, is given in Figure 6.6a. Also indicated is the observed net transport for the periods 1970-1981 and 1981-1990 following from sand balances for these periods

(see Nederbragt and Liek, 2004). Computed transports are given by the model in volumes of sediment per unit of time. To compare correctly with field data, they are multiplied by the factor *1/(1-n)* (*n* is the porosity [-], which is assumed to be 0.4).

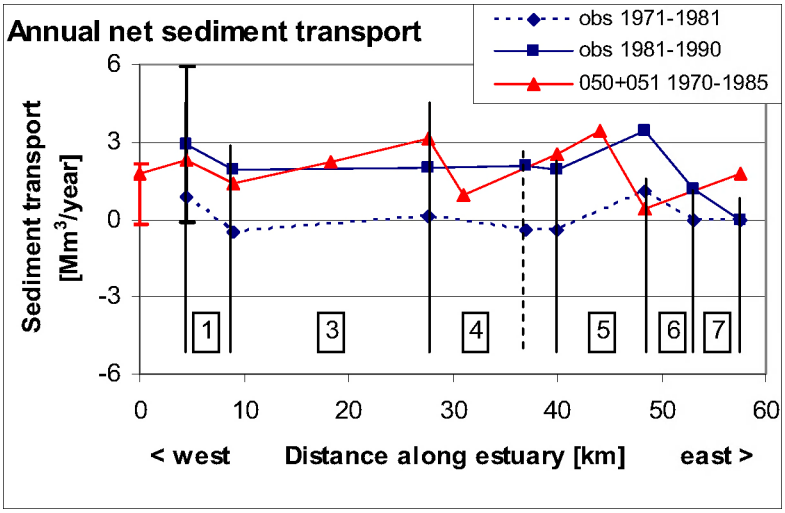

Figure 6.6a: Annual-averaged net sediment transport along the Western Scheldt estuary for the periods 1971-1981 and 1981-1990 (observations) and 1970-1985 (simulation) (landward = +; seaward = -). Computed transport is converted to volume incl. pores, assuming a porosity of 0.4. Macro cells are indicated with numbers.

The figure shows, that the results from the model simulation compares well with the observations for the period 1981-1990, but not with the observations for 1971-1981. Observed net sediment transports for the latter period are systematically lower than for 1971-1981 and almost nil. The broad range for the net transport through the estuary mouth is indicated with bars. The broad range for the computed transport lies completely within the range for the observations (only indicated for the period 1981-1990).

It is noted, that for the sand balances no sediment transport is assumed at the Dutch-Belgian border. If the computed transports are corrected with the eastward directed transport at the border (i.e. 1.8 Mm^3/year), all computed net transports are reduced with the same amount. The results are shown in Figure 6.6b.

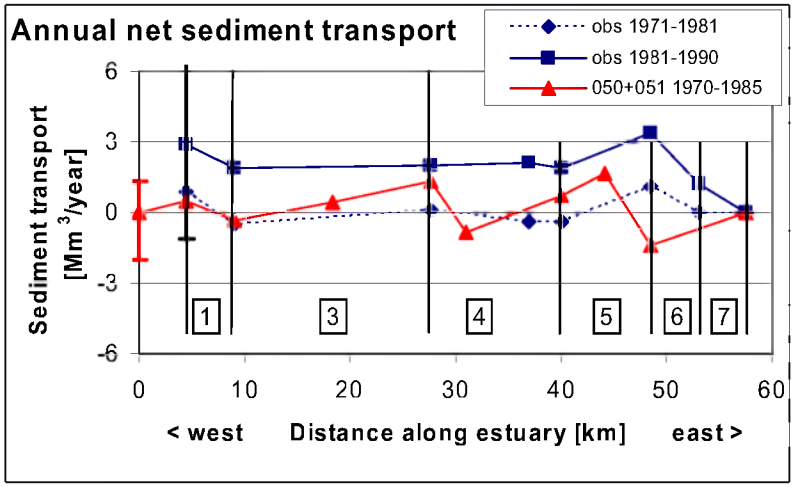

Figure 6.6b: Annual-averaged net sediment transport along the Western Scheldt estuary for the periods 1971-1981 and 1981-1990 (observations) and 1970-1985 (simulation). Model results have been corrected, so that the net transport at the eastern boundary is nil.

Computed results now show a better agreement with the observations for 1971-1981. Largest differences occur in the cross section between macro cells 5 and 6.

7 Applicability of the model to management issues

Methodology

In this chapter we will discuss to what extent the validated model can be applied to help resolve the management issues listed in Section 1.2 of this report. The purpose of this exercise is not to actually answer the management issues, but to assess the applicability of the morphological model. References to the text are included, where the model performance with respect to the governing processes have been presented (if possible). Apart from giving a brief discussion per aspect we have tried to give a simple ranking from 1 to 5 according to the table below.

Applicability ranking	Description
5	Model has been shown to be applicable in an absolute sense (e.g. to predict the autonomous development of the estuary).
4	Model has been shown to be applicable in a relative sense (i.e. to investigate and compare various alternatives/scenario's).
3	Model could be applied, but needs to be further calibrated on this aspect.
2	Model could be applied in principle, but needs to be improved and validated on this aspect.
1	Model is fundamentally not applicable to assess this aspect.

We must stress that this ranking has subjective elements, and mainly reflects our opinion on the status of the model; in a relative sense it may give a quick overview of where more attention is needed most or where the model is best applicable.

Detailed discussion

A. Optimum sand mining strategy:	• *What is the effect of sand mining activities on sediment import into or sediment export out of the estuary?* Sand mining takes place on a large enough scale to be represented in the model. The accuracy of the local response to the sand mining is similar to that of the erosion-sedimentation pattern. The model is able to predict trends in the import / export although the absolute net number is difficult to model (and measure) as it is so small. *Applicability ranking: 2-3* Reference: sections on net sediment transport in Chapter 4 and Chapter 6.
B. Optimum dredging and dumping strategy:	• *Can the Western Scheldt and the sub-tidal delta be considered as one overall system, sharing the total amount of available sand?* On short time-scales the cells act independently of each other, but on larger time-scales the whole system will react to major changes. Within the estuary it is obvious that any change in the morphology leads to other changes, so the amount of sand is indeed shared. For the sub-tidal delta there is a large exchange with the North Sea and adjacent coastlines, so that the effect of changes does not have to be within the estuary only, but may lead to changes in neighbouring areas. The model should be able to resolve this type of questions, though refinement is needed if adjacent coastal sand transports are to be resolved. *Applicability ranking: 3* Reference: sections on net volume changes and net sediment transport in Chapter 4 and Chapter 6.
	• *What is the effect of the dumping strategy on the tidal asymmetry?* The model is very well capable of representing tidal asymmetry, expressed in various parameters, and is sensitive to changes of the order of the present and expected dumping practice. *Applicability ranking: 5* Reference: sections on tidal asymmetry in Chapter 3.

	• *To what extent can the Western Scheldt be considered as a closed (sand conserving) system?* The model results and the data so far show that net import /export of the system is small compared to gross changes and, for instance, dredging and dumping volumes. With further validation for long periods, the model can be used to assess whether the estuary is likely to respond by trying to return to equilibrium with minimum import/export or by degenerating into an increasingly exporting system. *Applicability ranking: 3* Reference: sections on net sediment transport in Chapter 4 and Chapter 6.
	• *What is the natural fluctuation of the various components of the sand balance of the estuary?* The model appears to represent temporal trends in volumes at cell level, as well as net transports, even with the applied constant forcing. This indicates that much of the natural fluctuation comes from the morphological behaviour: a certain state of the morphology leads to a next state and so forth, in a quasi-cyclic pattern. We are confident that the model will help in understanding the natural behaviour, and the planned long hindcasts will help in assessing this skill. *Applicability ranking: 3* Reference: sections on net volume changes and net sediment transport in Chapter 4 and Chapter 6.
	<u>Following dumping of sediment:</u> • *How long should the dumping capacity of a channel be exceeded, to transfer a two-channel system into a single channel system?* In principle, this could be resolved by running a series of scenarios (long-term simulations) with increasing dumping volumes, for a particular channel or for a number of channels. *Applicability ranking: 3*
	• *Along which trajectories net transport of sediment occurs?* The comparison of measured and computed sedimentation / erosion patterns shows that there is some skill but also considerable discrepancies. Further validation of current

	patterns and detailed hindcasts of dumping tests will improve the skill on this point, especially in areas where there is no clear net transport direction. *Applicability ranking: 3* Reference: sections on sedimentation and erosion in Chapter 4 and Chapter 6.
	• *Under which conditions is this transport initiated?* So far, most model runs have been carried out using a single morphological tide or a spring-neap cycle, with constant wind/wave forcing. Further simulations can be carried out to assess the variation within the spring-neap cycle or the effect of more extreme wind, wave or discharge conditions. *Applicability ranking: 3* Reference: sections on sedimentation and erosion in Chapter 4 and Chapter 6.
	• *What is the variation in time?* We believe the variation in time will have a pulsating character due to the spring-neap cycle, as well as a propagating and damping character. The model is capable of representing the first type of behaviour only for a morphological factor of one, i.e. for short time-scales; the second type can be followed longer under a schematised set of conditions *Applicability ranking: 3* Reference: sections on sedimentation and erosion in Chapter 4 and Chapter 6.
	• *And to what extent do these temporal aspects differ from the situation without dumping?* As long as all of the dumping takes place under water (in the model this must be improved) and the very short-term aspects of the dumping process are not considered, the situation is very similar. *Applicability ranking: 3* Reference: sections on sedimentation and erosion in Chapter 4 and Chapter 6.

C. Effects of the deepening/widening of the navigation channel on the morphology:	• *How can the sand export from the Western Scheldt be related to the deepening/widening of the navigation channel in the 1970's and 1990's* When a satisfactory representation of the main trends in the net transport in the Western Scheldt has been provided, systematic runs over a period of decades, with different scenarios of deepening and widening, can isolate the impact of the deepening/widening from the natural evolution. *Applicability ranking: 2-3* Reference: sections on dredge volumes and net sediment transport in Chapter 4 and Chapter 6.
	• *What will be the consequences of a sand-exporting system on the physical and ecological characteristics?* The present rate of sand export is small for the size of the estuary (bottom changes order 8 mm/yr) and comparable to for instance sea level rise of order 2-8 mm/yr. Longer-term runs may indicate if there is an accelerating trend towards export. *Applicability ranking: 2-3* Reference: sections on area changes per depth class and net sediment transport in Chapter 4 and Chapter 6.
	• *Is the decrease of the maintenance dredging volume since the 48'/43' widening caused by either the widening or the deepening or is it the result of the increased sand export from the Western Scheldt?* The effect of widening or deepening can be investigated by systematic scenario runs; the dredging volumes are represented reasonably well in the present model. It seems possible, that an increased sand export leads to less dredging. *Applicability ranking: 3-4* Reference: sections on dredge volumes and net sediment transport in Chapter 4 and Chapter 6.
	• *What mechanisms govern the development of sills and how can they be modelled morphologically? How are they affected by dredging and dumping?* The main mechanism appears to be the centrifugal force (advective terms) that cause the ebb and flood currents to choose different paths where the channel crosses over. This

	essentially 2DH process is modified by 3D divergences of the flow profile from a logarithmic distribution. Also flood flow over shoals seaward of a sill may contribute. The present model is capable in broad terms, though not in all detail, of representing these mechanisms. Possibly, dumping sand right next to the navigation channel may lead to narrower and deeper sill areas. *Applicability ranking: 3*
	• *What can be the explanation that the total intertidal and shallow water area has developed differently from what was predicted in the MOVE-project after the 48'/43' widening and deepening?* This requires a more thorough analysis of observed and modelled changes at macro-cell level. We have seen that the model, with certain settings, is able to capture some important trends in shallow areas, but much more work is needed here. *Applicability ranking: 2-3*
D. Effects of future large-scale interventions on the morphology:	• *How can the relations between the physical processes and an intervention be described in a conceptual model?* The model can help quantifying parameters in a more conceptual model and can serve as a test bed for more simplified approaches. *Applicability ranking: 4*
	• *Can sand, originating from a further deepening, be dumped in the sub-tidal delta (Voordelta), so that it will remain available for the Western Scheldt?* The dynamic link between the sub-tidal delta and the estuary is probably much less active than the connections within the estuary, and there are likely to be losses to the North Sea, so that the effectiveness of this strategy seems questionable. Model exercises may clarify this. *Applicability ranking: 2-3* Reference: sections on dredge volumes and net sediment transport in Chapter 4 and Chapter 6.
	• *What will be the effect of a further deepening of the Wielingen/Scheur on the morphology of the Voordelta and the adjacent coastal areas of South-west Walcheren and Zeeuws Vlaanderen?* This depends on what is done with the dredged material; if it

	is dumped locally, effects may be local and relatively small. Further validation of the model is needed with respect to the Voordelta. *Applicability ranking: 3*
	• *What (innovative) large-scale morphological measures can be undertaken to mitigate the steepening of the coast of South-west Walcheren?* Various measures such as long dams (comparable to Eijerland), massive nourishments, permanent bypass schemes, can be examined using a finer version of the model (e.g. at SCALWEST resolution). *Applicability ranking: 3-4*
E. Effects of future large-scale interventions on the ecology:	• *What are the effects of dredging and dumping on the intertidal and shallow water areas (of importance for the ecosystem), such as level, duration of drying, hydrodynamics, morphodynamics and sediment composition?* Some first results for these areas have been generated in terms of areas of certain depth zones, even considering just sand. Reasonable estimates may be given for parameters following from the morphology; sediment composition has not been considered yet and requires both model improvement and validation. *Applicability ranking: 2* Reference: sections on dredge volumes and area changes per depth class in Chapter 4 and Chapter 6.
	• *What are the effects of deepening of the navigation channel on the development of the intertidal and shallow water areas?* Direct effects on the tidal propagation can be assessed readily, but shallow area processes are still represented crudely. *Applicability ranking: 2* Reference: sections on dredge volumes and net sediment transport in Chapter 4 and Chapter 6.
	• *How will the steepness of the tidal flats be affected after morphological interventions?* The processes and parameters governing the steepness of the tidal flats are not known yet.

	Applicability ranking: 1-2
	• Which interventions influence the development of salt marshes? First approaches are being developed in the framework of biogeomorphology research and applications in Venice lagoon; simple heuristic methods may provide first-order answers. *Applicability ranking: 2*

Summary

In the table below we have summarised the rankings for key aspects regarding the applicability of the model to Western Scheldt management problems. Clearly, much progress has been made in representing the large-scale behaviour and the effects of dredging and dumping, while the overall sediment balance and shallow areas need much more attention.

Type of problems/aspects	**Applicability ranking**
Effects on overall hydrodynamic parameters (e.g. asymmetry).	5
Dredging volumes, effects of management, support of conceptual models.	4
Behaviour of large-scale system and effects of strategies. Behaviour of sills. Spatial and temporal variations in transport patterns.	3
Overall import/export: effects of management strategies.	2-3
Tidal flats: effects of deepening, dumping.	2
Salt marshes and effects on them.	1-2

8 Recommendations for further research

Validation of the morphological model has been done for three different periods: 1998-2002 en 1960-1966 (both part of the calibration process) and 1970-1985 (verification). Results were compared with observations during these periods for a number of quantities: patterns of erosion and sedimentation, net volume changes of the ebb and flood channels of the macro cells, net area changes for various depth classes, dredge volumes and residual sediment transport. Although the confrontation of the hindcast simulations with field data shows, that the model is able to reproduce qualitatively, and for some aspects also quantitatively, various morphological features, it also points out that further improvement is needed. With the following recommendations it is expected, that such an improvement can be accomplished.

1. The tendency of the model to steepen the bathymetry may be due to an underestimation of down slope processes, such as geotechnical failure and breaching processes, which are not included in the model. This especially affects reliable predictions with respect to the morphological development of intertidal and sub tidal areas, which is important for e.g. the assessment of human interventions on the ecological functioning of the estuary. Pragmatically, an improvement has been achieved by artificially increasing the transverse bed slope effect. However, further knowledge on the basic processes is required.

2. The large scale activities with respect to dredging, dumping and sand mining in the Western Scheldt is suspected to have a major impact on the morphological development. The model employs a dredging/dumping algorithm, which reproduces in detail the artificial relocation of sediments; however further improvement is needed. Dump locations should make use of a dump capacity to prevent, that more sediment is locally dumped than what is actually realised (normally dumping is done up to a bed level of NAP-5 m). This is essential for long-term simulations over several years to decades.

3. The sediment grain size has been varied as part of the sensitivity simulations between 150 and 200 μm. The effect on the morphological changes appeared to be small. Closer inspection of available data reveals that grain sizes up to 300 μm can be found in the channels. It is recommended to perform simulations with an initial distribution of the grain size, which resembles more closely field conditions. As such, east-west variation as well differences for shallow areas and channels need to be accounted for.

4. The calibration run for 1998-2002 shows significant erosion south of Vlissingen. It is known, that locally a non-erodible shell layer is present, but the horizontal extent of this layer may be larger than included in the model. It is recommended to study the available field data in more detail and to perform a sensitivity analysis.

5. The present model deals with morphological changes as governed by the transport of non-cohesive sediment. Although the movement of sand contributes most to these changes, cohesive sediments can affect the transport processes along the margins of the estuary and on the intertidal flats. It may be necessary to incorporate cohesive sediment

transport processes in the model to arrive at reliable predictions regarding the morphological behaviour of intertidal and sub tidal areas. It is recommended to investigate the feasibility of such an extension of the present model.

6. The morphological simulations have shown that the type of sediment transport formula (van Rijn, Engelund Hansen, Ackers-White and Bijker) largely affects the results. Further optimization seems to be possible, which is illustrated with the erosion-sedimentation pattern according to Figure 8.1 (run 070). This simulation is similar to the final calibration run for 1998-2002 (run 042) but with sediment transports reduced to 30% of the original value. The results show, that the reproduction of the erosion-sedimentation pattern has improved significantly. Although also other output quantities should be addressed for an overall assessment, the result suggests that the performance of the model can be further improved. The challenge here is to find a set of model parameters and process formulations giving optimal results for all aspects. The attention should thus also focus on the optimization procedure. During the present study the erosion and sedimentation *pattern* was evaluated visually, which brings about a high degree of subjectivity. It is recommended to investigate the feasibility of (statistical) techniques to evaluate these patterns.

7. The present simulations cover a time span up to 15 years. It is recommended to simulate a longer period (decades) to examine the model behaviour on the long-term.

8. The adopted wave climate suffices for the calibration of the model; the net effect of waves on a yearly basis is probably limited in the Western Scheldt. A more detailed analysis of the dynamics of intertidal areas requires a more elaborate schematisation of the wave climate (including set-up). In that case extreme conditions may be of more importance. Especially for the ebb tidal delta the effect of waves will be larger than for the Western Scheldt. It is recommended to study these aspects in more detail.

9. One of the few ways of obtaining synoptic patterns of (bed load) sediment transport in the field is the analysis of bed forms as measured from multi-beam soundings. Erkens (2003) presents a data analysis of such soundings for the Oostgat, where based on the asymmetry of the large-scale bed forms a complex pattern of bed load transport directions is inferred. Even though the grid of the present model is relatively coarse, it is interesting to compare the 'observed' pattern with the tide-averaged bed load transport pattern from the present model.

10. Conventional sediment transport formulae adopt constant roughness heights representing average conditions. It is known that at large flow velocities (say > 1.3 m/s) bed forms gradually disappear so that finally a plane bed is obtained. The roughness decreases and consequently the sediment transport. However, this process is not included in available sediment transport formulae and thus at larger flow velocities transports are overestimated. Presently, a roughness predictor is being developed, which will be included in DELFT3D in 2004. It is recommended to study in future the effect of such a roughness predictor on computed sediment transports in and resulting morphological changes of the Western Scheldt.

11. The 3D-simulations, carried out within the present project as sensitivity computations, did not show an improvement (but rather a deterioration) of the reproduction of the

morphological processes. It indicates, that the transition from 2D to 3D morphological modelling (with and without density effects) and the application of a k-ε turbulence model require supplementary calibration. It is recommended to investigate the actual causes for these differences between 2D and 3D results (with or without k-ε) and to calibrate a 3D morphological model for the Western Scheldt, if such a model is required for future studies.

References

Claessens, L., H. Belmans, 1984, Overzicht van de getijwaarnemingen in de Zeescheldebekken gedurende de periode 1971-1980. *Tijdschrift van de Openbare Werken van België*, nr. 3 (in Dutch).

Dyer, K.R., 1997, Estuaries: a physical introduction, John Wiley and Sons Ltd., 2nd edition.

Eck, G.Th.M. van, 1999, De ScheldeAtlas, een beeld van een estuarium, Schelde InformatieCentrum (in Dutch).

Erkens, G. 2003,. Analyse Multibeam data Oostgat. Geomorfologische analyse op basis van multibeam data uit 2002. Werkdocument RIKZ/OS/2003.168x (in Dutch).

Gruijters, S.H.L.L., J. Schokker, J.G. Veldkamp, 2004, Kartering moeilijk erodeerbare lagen in het Schelde estuarium, Netherlands Organisation for Applied Scientific Research (TNO), report NITG 03-213-B1208 (in Dutch).

Haring, J., 1949, Inhouds- en diepteveranderingen Westerschelde 1878-1931. Directie Benedenrivieren, Studiedienst, Report B335 (in Dutch)

Haring, J., 1955, Inhouds- en diepteveranderingen Westerschelde 1931-1952. Directie Benedenrivieren, Studiedienst, Report D164 (in Dutch)

Jeuken, M.C.J.L. 2000. On the morphologic behaviour of tidal channels in the Westerschelde estuary. Phd. thesis, Utrecht University.

Jeuken et al., 2003a, Evaluatie van het beleid voor vaargeulonderhoud en zandwinning sinds de tweede vaargeulverdieping op basis van veldwaarnemingen en het verbeterde Cellenconcept Westerschelde, WL | Delft Hydraulics, Rapportnr. Z3467 (in Dutch).

Jeuken et al., 2003b 'Morphological response of estuaries to nodal tide variation' International Conference of Estuaries and Coasts, Hangzhou, China.

Jeuken, M.C.J.L., Z.B. Wang, T. Van der Kaaij, M. Van Helvert, M. Van Ormondt, R. Bruinsma, I. Tanczos, 2004, Morfologische ontwikkelingen in het Schelde estuarium bij voortzetting van het huidige beleid en effecten van een verdere verdieping van de vaargeul en uitpolderingen langs de Westerschelde, Deelovereenkomst 2 en 3 Morfologie, Arcadis/Technum/WL|Delft Hydraulics (in Dutch).

Kornman, B.A., G.A. Liek, H. Schippers, 2003, Baggeren en storten in de Westerschelde – een nieuwe kijk op het onderhoudsbaggerwerk, Werkocument RIKZ/AB/840x, RIKZ.

Lesser, G.R., J.A. Roelvink, J.A.T.M. van Kester, G.S. Stelling, 2004, Development and validation of a three-dimensional morphological model, Coastal Engineering 51, pp. 883-915.

Marijs, K., E. Parée, 2004, Nauwkeurigheid vaklodingen Westerschelde en –monding: "de praktijk", Notitie nr. ZLMD-04.N.004, Meetinformatiedienst Zeeland (in Dutch).

Nederbragt, G., G.A. Liek, 2004, Beschrijving zandbalans Westerschelde en monding. RIKZ, Rapport RIKZ/2004.020 (in Dutch).

Peters, B.G.T.M., G.A. Liek, J.W.M. Wijsman, M.W.M. Kuijper, G.Th. van Eck, 2003, Monitoring van de effecten van de verruiming 48'/43', een verruimde blik op waargenomen ontwikkelingen. MOVE Evaluatierapport. Rapport RIKZ/2003.027; deel A: Samenvatting en deel B: Hoofdrapport (in Dutch).

RWS & MVG, 2001, Langetermijnvisie Schelde Estuarium, RWS Directie Zeeland en het Ministerie van de Vlaamse Gemeenschap (in Dutch).

Verlaan, P.A.J., 1998, Mixing of marine and fluvial particles in the Scheldt estuary, Ph.D., Delft University of Technology.

Wang Z.B., M.C.J.L. Jeuken, H. Gerritsen, H.J. de Vriend en B.A. Kornman, 2002, Morphology and asymmetry of the vertical tide in the Westerschelde estuary, Journal of Continental Shelf Research, Vol. 22

Winterwerp, J.C., C. Kuijper, 2002, Morfologisch model Westerschelde: verkennende studie naar operationalisering, report Z3222, WL | Delft Hydraulics (in Dutch).

Winterwerp, J.C., M.C.J.L. Jeuken, 2004, Samenvatting van het morfologisch onderzoek in het kader van de strategische milieueffectenrapportage en de ontwikkelingsschets 2010, Morfologische ontwikkelingen in het Schelde estuarium bij voortzetting van het huidig beleid voor vaargeulonderhoud en zandwinning en effecten van een verdere verdieping van de vaargeul en uitpolderingen langs de Westerschelde, Arcadis/Technum/WL|Delft Hydraulics, rapport Z3561 (in Dutch).

A Model description

Overzicht model karakteristieken	
A. Waterbeweging	
Volgorde in modellenketen	*1.*
Programmatuur/versie nr., datum release/standaard/debugs	*Delft3D-Flow versie 3.33; Nov 6 2003 Release version.*
Voor dit project aangebrachte wijzigingen in de source	*None.*
Bodemschematisatie /versienr, datum, datum bodem /bijzonderheden	*Bathymetry corresponds with 2001; Based upon Scalwest bathymetry.*
rooster rechtlijnig , Δx, Δy of kromlijnig $\Delta\xi_{min}$, $\Delta\xi_{max}$, $\Delta\eta_{min}$, $\Delta\eta_{max}$	*Curvi-linear; Δx = 60 m – 900 m; Δy = 50 m – 1400 m.*
mmax, nmax, aantal domeinen	*mmax = 129; nmax = 239; 1 single domain.*
per domein : aantal lagen, laagverdeling (1-k in %)	*100 %.*
Modelparameters (bodemwrijving, etc etc)	*Friction: space varying manning roughness originating from Scalwest schematization.*
Afwijkende modelparameters	
In studie gevarieerde parameters:	*Method of specifying bed friction.*
Randvoorwaarden : soort, plaats, representatie, bijzonderheden	*Open sea boundaries: Astronomical forcing (25 tidal constituents); Boundary signal: Riemann invariant; Boundaries originating from Scalwest model.*
	Open river boundary: Astronomical forcing (21 tidal constituents); Boundary signal: Discharges; Boundary conditions originate from time series computed with Scalwest.
Rekentijdstap, uitvoertijdstappen	*Δt = 1 min; history: 10 minutes.*
1e calibratie periode	*2000, 2001, 2002.*
Calibratie data	*Water levels, discharge measurements and velocity measurements.*
Nauwkeurigheid calibratie	---
Validatie periode	*1972.*
Validatie data	*Water levels, discharge measurements.*
Nauwkeurigheid validatie	---
Gekoppeld met : via:	
Teruggekoppeld met : via:	
Terugkoppelingsinterval	

Overzicht model karakteristieken	
B. Morfologie	
Volgorde in modellenketen	*2.*
Programmatuur/versie nr., datum release/standaard/debugs	*Delft3D-Flow versie 3.33; Nov 6 2003 Release version.*
Voor dit project aangebrachte wijzigingen in de source	*Dredging and dumping and sand mining included.*
Hydrodynamische randvoorwaarden	*One single tidal day resulting in sedimentation erosion patterns comparable with actual tidal forcing.*
Sediment eigenschappen	*Sand, D_{50} = 200 um.*
Transportformule	*van Rijn 1993.*
Morfologische versnellingsfactor	*120.*
In studie gevarieerde parameters:	*Type of hydrodynamic forcing, 2D vs. 3D; Transport formula applied; D_{50} of the bed material; Horizontal dispersion; Horizontal grid layout.*
1^{e} calibratie periode	*1998 - 2002.*
Calibratie data	*Erosion sedimentation patterns; Dredged volumes; Sand balance; Volumes per macro cell; Areas per macro cell and depth class.*
Nauwkeurigheid calibratie	---
2^{e} calibratie periode	*1960 - 1966.*
Calibratie data	*Erosion sedimentation patterns; Dredged volumes; Sand balance; Volumes per macro cell; Areas per macro cell and depth class.*
Nauwkeurigheid validatie	---